ENTRAINMENT IN AN AIR/WATER SYSTEM INSIDE A SIEVE TRAY COLUMN

by

Ehbenezer Chris Uys

Thesis presented for the Degree

of

MASTER OF SCIENCE IN ENGINEERING

(CHEMICAL ENGINEERING)

in the Department of Process Engineering

at the University of Stellenbosch

Supervised by

Prof. J.H. Knoetze and Prof. A.J. Burger

STELLENBOSCH

MARCH 2010

Declaration

I, the undersigned, hereby declare that the work contained in this thesis is my own original work and that I have not previously in its entirety or in part submitted it at any university for a degree.

…….. ……

Signature Date

Abstract

Mass transfer efficiency in distillation, absorption and stripping depends on both thermodynamic efficiency and hydrodynamic behaviour. Thermodynamic efficiency is dependent on the system kinetics while hydrodynamics is the study of fluid flow behaviour. The focus of this thesis is the hydrodynamic behaviour in tray columns, which affects entrainment. In order to isolate hydrodynamic behaviour from the thermodynamic behaviour that occurs inside sieve tray columns, investigations are conducted under conditions of zero mass transfer. When the gas velocity is sufficiently high to transport liquid droplets to the tray above, entrainment occurs. The onset of entrainment is one of the operating limits that determines the design of the column and thus impacts on the capital cost. By improving the understanding of the parameters that affect entrainment, the design of the tray and column can be improved which will ultimately increase the operability and capacity while reducing capital costs.

Existing correlations predicting entrainment in sieve tray columns are based on data generated mainly from an air/water system. Previous publications recommend that more testing should be performed over larger ranges of gas and liquid physical properties. An experimental setup was therefore designed and constructed to test the influence of the following parameters on entrainment:

1. gas and liquid physical properties
2. gas and liquid flow rates
3. tray spacing

The experimental setup can also measure weeping rates for a continuation of this project.

The hydrodynamic performance of a sieve tray was tested with air and water over a wide range of gas and liquid flow rates and at different downcomer escape areas. It was found that the downcomer escape area should be sized so that the liquid escaping the downcomer always exceeds a velocity of approximately 0.23 m/s in order to create a sufficient liquid seal in the downcomer. For liquid velocities between 0.23 and 0.6 m/s the area of escape did not have an effect on the percentage of liquid entrained. It was also established that entrainment increases with increasing gas velocity. The rate at which entrainment increases as the gas velocity increase depends on the liquid flow rate. As soon as the liquid flow rate exceeded 74 m^3/(h.m) a significant increase in entrainment was noted and the gas velocity had to be reduced to maintain a constant entrainment rate. This is because the increased liquid load requires a longer flow path length for the froth to fully develop. The undeveloped froth, caused by the short (455 mm) flow path, then creates a non-uniform froth that is pushed up against the column wall above the downcomer. Consequently, the

froth layer is closer to the tray above resulting in most of the droplets ejected from the froth reaching the tray above and increasing entrainment. By reducing the gas velocity, the froth height and ejecting droplet velocity is reduced, resulting in a decrease in entrainment.

The results from the experiments followed similar trends to most of the entrainment prediction correlations found in literature, except for the change noted in liquid flow rates above 74 m^3/(h.m). There was, however, a significant difference between the experimental results and the correlations developed by Hunt *et al.* (1955) and Kister and Haas (1988). Although the gas velocities used during the air/water experiments were beyond the suggested range of application developed by Bennett *et al.* (1995) their air/water correlation followed the results very well.

The entrainment prediction correlation developed by Bennett *et al.* (1995) for non-air/water systems was compared with the experimental air/water results to test for system uniformity. A significant difference was noted between their non-air/water prediction correlation and the air/water results, which motivates the need for a general entrainment prediction correlation over a wider range of gas and liquid physical properties.

Based on the shortcomings found in the literature and the observations made during the experiments it is suggested that the influence of liquid flow path length should be investigated so that the effect on entrainment can be quantified. No single correlation was found in the literature, which accurately predicts entrainment for a large range of liquid loads (17 – 112 m^3/(h.m)), high superficial gas velocities (3 – 4.6 m/s) and different gas and liquid physical properties. It is therefore recommended that more work be done, as an extension of this project, to investigate the influence of gas and liquid physical properties on entrainment (under zero mass transfer conditions) for a large range of liquid (5 – 74 m^3/(h.m)) and gas (2 – 4.6 m/s) flow rates. In order to understand the effect of droplet drag on entrainment, tray spacing should be varied and increased to the extent where droplet ejection velocity is no longer the mechanism for entrainment and droplet drag is responsible for droplet transport to the tray above.

Since it is difficult and in most cases impossible to measure exact gas and liquid loads in commercial columns, another method is required to measure or determine entrainment. Since liquid hold-up was found to be directly related to the entrainment rate (Hunt *et al.* (1955), Payne and Prince (1977) and Van Sinderen *et al.* (2003) to name but a few), it is suggested that a correlation should be developed between the dynamic pressure drop (liquid hold-up) and entrainment. This will contribute significantly to commercial column operation from a hydrodynamic point of view.

Acknowledgements

I would like to convey my sincere gratitude towards my supervisors Prof. J.H. Knoetze, Prof. A.J. Burger and Dr. C.E. Schwarz for their continuous encouragement, patience, support and critique.

Without the financial support from Sasol Pty (Ltd), the South African Department of Trade and Industry through THRIP and Koch-Glitsch this project would not have been made possible.

To my father, Dirk Uys, I want to extend my heartfelt and most sincere gratitude for teaching me how to endure even at times when the answers don't seem to come. You taught me that giving up is not part of the equation to success. It is because you exposed me to the mechanical side of engineering that I could develop the experimental setup required for this work.

To my mother, Martie Uys, I will never forget your love and continuous motivation. Through you I realised that even if you reached the pinnacle of success, without love life would have no meaning.

To my close friend, Sarel Lamprecht, without your daily support, memorable moments and reasoning through problems at times when the going was tough, I want to extent many thanks. You are indeed a friend for life.

The Process Engineering workshop, Jannie Barnard, Anton Cordier and Howard Koopman, should take the glory for helping with the construction of a versatile and brilliant experimental setup.

Table of contents

Glossary

Bubbling area

Measured as column area minus two downcomer areas.

Clear liquid height

The liquid inventory (hold-up) on and above the tray expressed as the height the liquid will occupy when it is not a frothy gas liquid mixture. This can also be seen as the pressure drop across the froth above (space between the trays) the tray.

Downcomer Escape Area

Clearance area under the downcomer apron (see Figure 1.2).

Dry tray pressure drop

The pressure drop across the tray without the presence (or effect) of liquid.

Entrainment

Entrainment occurs when the gas velocity is sufficiently high to transport liquid as droplets to the tray above.

Gas Superficial velocity

Gas velocity based on the column net area (total column area minus one downcomer area for single pass trays)

Fractional hole area

Fractional hole area is defined as the ratio of the total hole area over the area covered by the holes.

Froth height

Height of the froth above the tray deck (see Figure 1.2).

Froth Regime

In the froth regime vapour passes through the liquid continuous layer in the form of jets or a series of bubbles. The froth regime is formed by moderate to high liquid flow rates and low to moderate vapour flow rates.

Liquid flow path length

The section of the tray where the liquid exits the downcomer and crosses the tray, measured from the downcomer exit to the exit weir (see Figure 1.2).

Liquid hold-up

See the definition for clear liquid height.

Perforated area

Area of the tray covered with holes/perforations (see Figure 1.2).

Residual pressure drop

The total tray pressure drop minus dry tray pressure drop minus the equivalent liquid head. This was defined by Hunt *et al.* (1955) which used a constant head tank (no liquid cross flow) to manipulate and measure the liquid height above the tray.

Spray Regime

In the spray regime vapour is continuously jetting through the holes creating liquid droplets. This regime is characterized by high vapour flow rates and low liquid flow rates resulting in low liquid depths (hold-up) on the tray.

Weeping

Weeping occurs when the gas velocity is sufficiently low so that the liquid in the tray is "dumped" through the tray perforations to the tray below.

Abbreviations

AW – Air/water

PLC – Programmable logic controller used as the main controller on the pilot plant.

NAW – Non air/water

MEK – Methyl ethyl ketone

Nomenclature

Symbol	Description	Units
A_b	Bubbling Area (A_c-2A_d)	m^2
A_c	Column area	m^2
A_d	Downcomer area	m^2
A_p	Perforated (Active) area, including blank areas	m^2
A_{ap}	Clearance area under downcomer apron (Downcomer Escape Area)	m^2
A_h	Total hole area	m^2
A_h*	Total hole area	ft^2
A_n	Net area available for vapour-liquid disengagement (A_c-A_d)	m^2
A_f	Fractional hole area (A_h/ A_p) or tray free area	-
B	Weir length per unit bubbling area	m^{-1}
C_b	Capacity factor based on A_b, $C_b = u_b\sqrt{\rho_g/(\rho_L-\rho_g)}$	m/s
C_D	Venturi discharge coefficient	
C_p	Capacity factor based on A_p, $C_p = u_p\sqrt{\rho_g/(\rho_L-\rho_g)}$	m/s
C_s	Capacity factor based on A_n, $C_s = u_s\sqrt{\rho_g/(\rho_L-\rho_g)}$	m/s
C_f	Flooding factor, Souders and Brown flooding constant	m/s
D_H	Hole diameter	m
d_H	Hole diameter	mm

d_H*	Hole diameter	in
E	Entrainment (mass liquid/mass vapour)	-
E_f	Entrainment in the froth regime (kg liquid/kg vapour)	-
E_s	Entrainment in the spray regime (kg liquid/kg vapour)	-
E_w	Entrainment measured while weeping occurs simultaneously (kg liquid/kg vapour)	-
F_S	F-factor, $F = u_s\sqrt{\rho_g}$	$(kg/m)^{1/2}/s$
F*	F-factor, $F = u_b\sqrt{\rho_g}$	$(lb/ft)^{1/2}s$
F_P	F-factor, $F = u_p\sqrt{\rho_g}$	$(kg/m)^{1/2}/s$
F_P*	F-factor, $F = u_p\sqrt{\rho_g}$	$(lb/ft)^{1/2}s$
G	Gas/Vapour mass flow	kg/s
g	Gravitational constant, 9.81	m/s^2
g_c	Gravitational constant, 32.2	$lbm/(lbf.s^2)$
H_b	Bed height	m
h_b	Bed height	mm
H_d	Dynamic pressure drop	m, water
h_d	Dynamic pressure drop	mm, water
h_d*	Dynamic pressure drop	in, water
H_{DP}*	Dry tray pressure drop	ft, vapour
H_F	Froth height	m

H_{Fe}	Effective froth height (Developed by Bennett *et al.* (1995))	m
h_F	Froth height	mm
h_f*	Froth height	in
$H_{f,t}$	Froth/Dispersion height at the froth to spray transition	m
H_L	Clear liquid height	m
$H_{L,tr}$	Clear liquid height at the low – to – high-liquid layer transition, see Van Sinderen *et al.* (2003)	m
h_L	Clear liquid height	mm
$h_{L,f}$	Clear liquid height in froth regime	mm
$h_{L,t}$	Clear liquid height at the froth to spray transition	mm
$h_{L,t}$*	Clear liquid height at the froth to spray transition	in
h_M	Momentum heads	mm, water
H_R	Residual pressure drop	m, water
H_t	Total tray pressure drop	m, water
h_t*	Total tray pressure drop	in, water
H_w	Weir height	m
h_w	Weir height	mm
L	Liquid mass flow (Entering the tray from the downcomer)	kg/s
L’	Entrained liquid mass flow	kg/s
l	Weir length	m
q_L	Liquid flow per weir length	$m^3/(s.m)$

P	Hole pitch	m
p	Hole pitch	mm
Q_L	Liquid flow per weir length	$m^3/(h.m)$
Q_L*	Liquid flow per weir length	(US)gpm/ft
Q_L^+	Liquid flow per weir length	(Imp)gpm/ft
Q_v	Gas volumetric flow rate	m^3/s
R	Gas constant	J/(kg.K)
S	Tray spacing	m
s	Tray spacing	mm
S*	Tray spacing	in
u_c	Gas velocity based on column area	m/s
u_{D0}	Droplet ecjection velocity	m/s
u_b	Gas/vapour velocity based on A_b	m/s
u_h	Gas/vapour hole velocity based on A_h	m/s
u_h*	Gas/vapour hole velocity based on A_h*	ft/s
u_L	Liquid escape velocity, based on A_{ap}	m/s
u_p	Gas/vapour velocity based on A_p	m/s
u_p*	Gas/vapour velocity based on A_p	ft/s
u_s	Superficial vapour velocity based on A_n	m/s
u_t	Droplet terminal velocity	m/s
u_t*	Droplet terminal velocity	ft/s

V_g	Gas volumetric flow rate	m^3/s
V_l	Liquid volumetric flow rate	m^3/s

Greek Symbols

ε	Froth density as clear liquid fraction	-
ρ_g	Gas/vapour density	kg/m^3
ρ_L	Liquid density	kg/m^3
σ	Liquid surface tension	mN/m
μ	Liquid viscosity	mPa.s
ζ	Correction term for Eq. 2.38 defined by Eq. 2.39	

List of figures

List of tables

1 Introduction

The most common method available to separate liquid mixtures with different volatilities is distillation. Distillation is a physical separation method conducted by boiling a liquid mixture and using energy as a separation agent. As the temperature of the mixture increases the more volatile component will reach boiling point first and escape from the liquid mixture as a vapour while the less volatile component remains a liquid. Distillation is used commercially for numerous applications. Crude oil is separated into components which are used for transport, power generation, heating and packaging to name but a few. Old desalination plants used distillation to separate water from salt. To produce nitrogen, oxygen and argon on industrial scale, air is distilled at very low temperature.

In order to purify a gas/vapour stream with constituents that can dissolve in an absorbent, an absorption process is used. The gas is brought into contact with the liquid absorbent where the constituents in the gas dissolve in the liquid to varying extents based on their solubilities. Commercially, carbon dioxide is separated from combustion products by absorption with aqueous solutions of ethanolamine.

Stripping is the inverse of absorption during which a liquid mixture is purified with a gas or vapour stripping agent. The objective is to create a favourable environment for the component in the liquid phase to transfer to the vapour phase and hence stripping is conducted at elevated temperatures and atmospheric, or lower, pressure. Steam stripping is generally used to remove volatile organic components (which are partially soluble in water) from waste water.

1.1 Background

Distillation, absorption and stripping are of the largest and most widely used separation processes in the separations industry. In distillation both thermodynamic and hydrodynamic behaviour determine the degree of separation (the separation efficiency) that can be achieved between two or more components. Thermodynamic behaviour focuses on the mass transfer efficiency and kinetics while hydrodynamics is the study of the fluids in motion. This thesis addresses the hydrodynamic behaviour occurring inside sieve tray columns.

Distillation is commonly used when liquid mixtures with different relative volatilities that are thermally stable, with little or no corrosive properties have to be separated on a large scale. Inside distillation columns contacting devices are used to create a mass transfer interface

between the less dense and more dense phases. These devices are divided into three main groups known as structured packing, random packing and trays. Each group of contacting devices has a unique application based on system parameters, operating conditions and column geometry. Random packing is generally used in smaller diameter columns when working with corrosive liquids where plastic or ceramic materials are preferred over metals. Packed columns are preferred over tray columns in applications where foaming may be severe and when the pressure drop must be low. Tray columns can be designed, scaled up with more reliability, and are less expensive than packed columns (Seader and Henley 1998). Columns with random packing are generally used when liquid velocities are high while tray columns are used for low to medium liquid velocities (Seader and Henley, 1998).

1.2 Introduction to hydrodynamics in tray columns

A tray column is a vertical, cylindrical vessel in which vapour and liquid are contacted on a series of trays (plates). The vapour and liquid flow counter-currently inside the column, as shown in Figure 1.1 and Figure 1.2. The liquid flows across each tray, exiting over an outlet weir into a downcomer which transfers the liquid by gravity to the tray below. The amount of liquid on and above the tray is defined as the liquid hold-up and expressed as the clear liquid height. The clear liquid height is therefore the pressure drop across the liquid froth, measured in vertical meters (hydrostatic pressure) of the specific liquid.

A great deal of work has been done on hydrodynamics in tray columns, including:

1. Tray pressure drop (Hunt *et al.* 1955, Thomas & Ogboja (1978)).
2. Froth density and height (Thomas & Ogboja (1978), Hofhuis and Zuiderweg (1979), Bennett *et al.* (1995), Jaćimović and Genić (2000)).
3. Flow regime definitions (Zuiderweg (1982), Kister and Haas (1988), Bennett *et al.* (1995)).
4. Entrainment (Hunt *et al.* 1955, Thomas & Ogboja (1978), Kister and Haas (1988), Bennett *et al.* (1995)).
5. Downcomer flooding (Zuiderweg (1982)).
6. The influences of fractional hole area (free area) of the tray on the hydrodynamic behaviour (Thomas & Ogboja (1978)).
7. The influence of weir height (Van Sinderen *et al.* (2003))
8. The influence of tray spacing (Hunt *et al.* 1955, Thomas & Ogboja (1978))

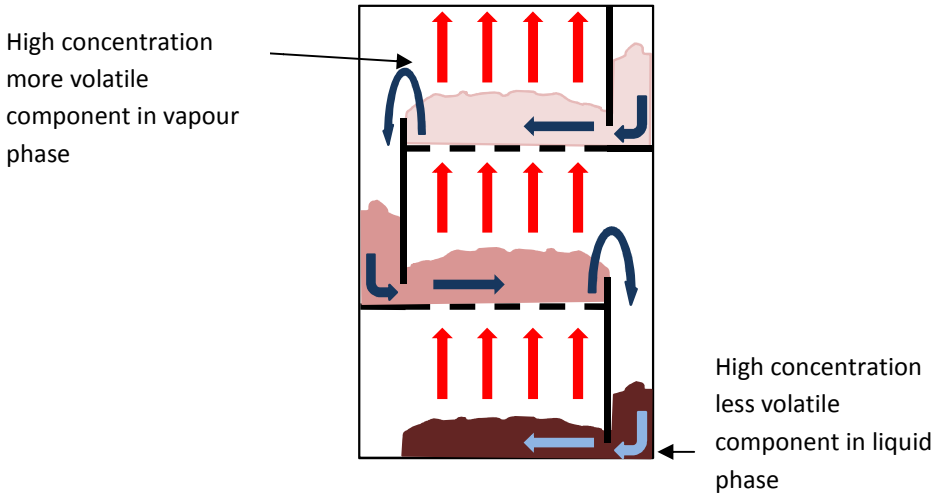

Figure 1.1 Illustration of vapour and liquid flow paths in a tray column.

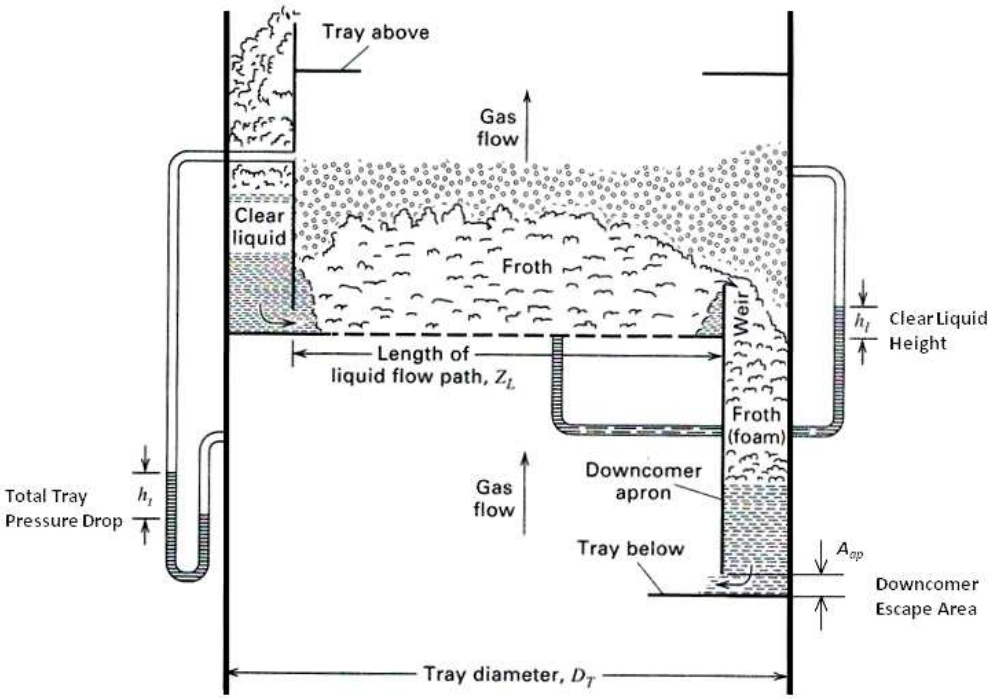

Figure 1.2 Contacting inside a tray column. [Adapted with permission from: Separation Process Principles; J.D. Seader and Ernest J. Henley; Copyright © 1998 John Wiley & Sons, Inc.].

Tray Geometry:

Vapour rises upward through both the openings in the tray and the liquid on the tray. Openings in the tray can range between perforation (commonly referred to as sieve), valves, or bubble caps (see Figure 1.3). The simplest and most common type is the sieve tray. The sieve tray is also the least expensive of all the tray types. The vapour passes through perforations, or holes (3.2 – 25.4mm diameter), made in sheet metal.

Valve trays have larger openings, 38 – 51mm in diameter, than the sieve tray. Two types of valve trays are commonly used, namely fixed valve and floating valve type trays. The floating valve is a cap that overlaps the hole in the tray deck, with legs that limit the vertical rise of the cap while the same horizontal position is maintained. Thus at zero to low gas velocities the valve will cover the hole and at increased gas velocities the valve will rise. A fixed valve is similar to a floating valve but is fixed at a certain elevation above the tray deck. A bubble cap tray has fixed caps, usually 76 – 152mm in diameter, with rectangular or triangular slots cut around the sides for vapour passage. The caps are placed over and above a riser, 50 – 76mm in diameter.

Figure 1.3 compares the different tray types based on economic and operational differences.

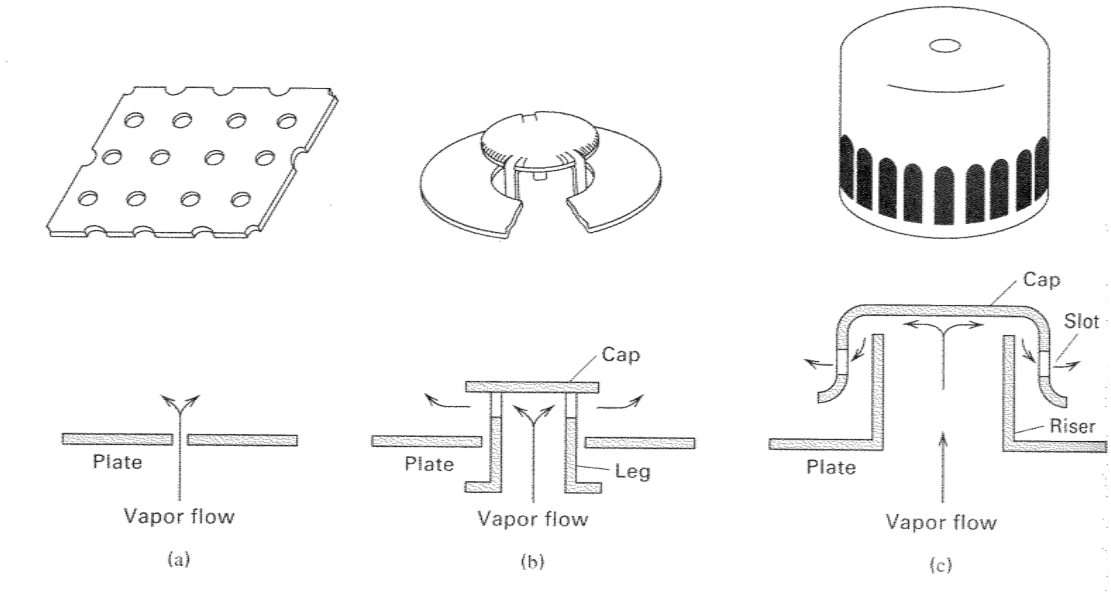

Figure 1.3 The three tray opening types for liquid and vapour contacting: (a) sieve or perforation; (b) floating valve; (c) bubble cap. [Reprinted with permission of John Wiley & Sons Inc., Separation Process Principles; J.D. Seader and Ernest J. Henley; Copyright © 1998 John Wiley & Sons, Inc.].

Table 1.1 Comparing the different tray types (Seader and Henley 1998).

Description	Sieve Trays	Valve Trays	Bubble Cap Trays
Relative Cost	1.0	1.2	2.0
Pressure Drop	Low	Intermediate	High

Table 1.1 Comparing the different tray types (Seader and Henley 1998).

Description	Sieve Trays	Valve Trays	Bubble Cap Trays
Efficiency	Low	High	High
Vapour Capacity	High	High	High
Turndown Ratio	2	4	5

The turndown ratio is the ratio of the gas flow rate at the onset of entrainment to the minimum gas rate when the liquid weeps through the perforations. Since the sieve tray is the simplest tray design, this thesis will focus on entrainment in sieve tray columns.

Tray hydraulics:

In the case where the tray openings are holes, different two-phase-flow regimes can be encountered. Hofhuis and Zuiderweg (1979) defined four (see Figure 1.4) flow regimes namely the spray regime, the mixed froth regime, the free bubbling regime, and the emulsified flow regime. They suggest that the spray regime is significant for applications operating under vacuum while the emulsion flow regime applies to high pressure distillation and high liquid load absorption. From the flow regime diagram (Figure 1.4) it can be seen that gas and liquid density will influence the operating flow regime. They suggest that viscosity and surface tension have little or no effect on the flow regime.

Most of the work done in literature focuses on the spray regime, mixed regime (transition from emulsified to spray regime) and the froth regime (which represents the emulsified regime). Each author defines and determines the regimes differently. According to Seader and Henley (1998) the most favoured regime is the froth regime in which the vapour passes through the liquid continuous layer in the form of jets or a series of bubbles. The mixed froth regime is formed by moderate to high liquid flow rates and low to moderate vapour flow rates. In the spray regime the vapour is continuously jetting through the holes, creating liquid droplets. This regime is characterized by high vapour flow rates and low liquid flow rates resulting in low liquid depths (hold-up) on the tray.

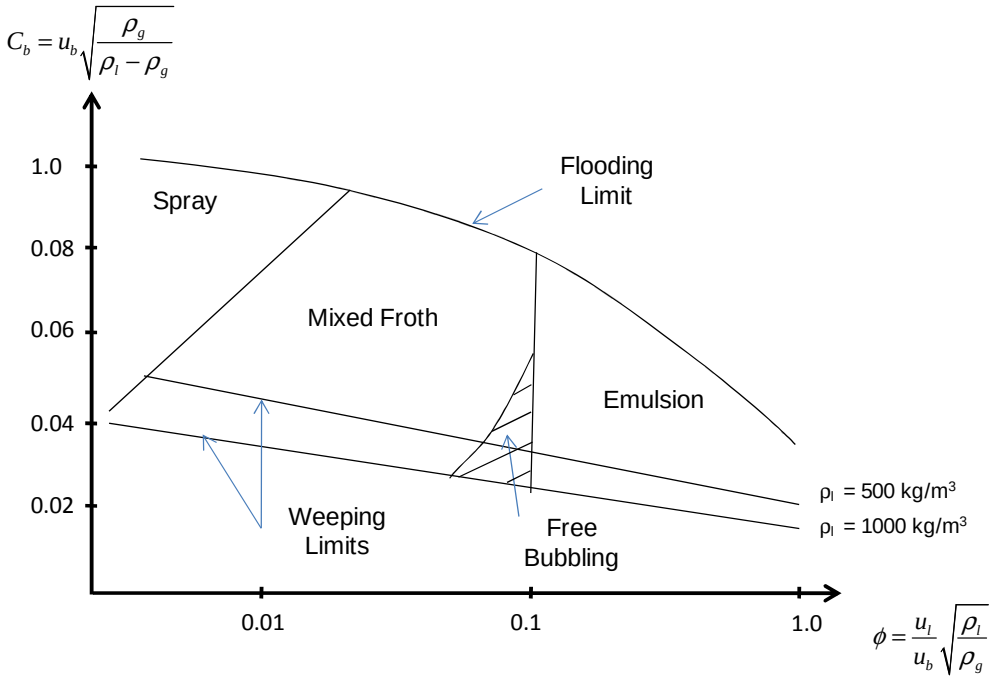

Figure 1.4 The flow regime diagram redrawn from Hofhuis and Zuiderweg (1979).

At low vapour flow rates and moderate liquid flow rates the bubble regime occurs where bubbles rise through the quiescent liquid layer. At high liquid and low to moderate vapour rates the emulsion (froth) flow regime can occur. In the emulsion regime small gas bubbles can be undesirably suspended in the liquid.

In order to express and correlate hydrodynamic behaviour dimensionless numbers or modified (from the known/common groupings) dimensionless numbers are used. The most common dimensionless numbers used to characterise hydrodynamic behaviour in tray columns are:

1. The Froude number ($Fr = \frac{u_{D0}^2}{gH_F}$) or ($Fr = \frac{u_b}{\sqrt{gH_L}}$) where u_{D0} is the droplet ejection velocity, g is gravitational acceleration, H_F is the froth height, u_b is the gas velocity based on the tray bubbling area and H_L is the clear liquid height.
2. The Bond number ($Bo = \frac{\rho g L^2}{\sigma}$) where ρ is the density or the density difference of the fluid/s, g is gravitational acceleration, L is a characteristic length (normally droplet diameter or hole diameter) and σ is the liquid surface tension.

3. The Weber number ($We = \frac{\rho v^2 l}{\sigma}$) where ρ is the density of the fluid, v its velocity, l is a characteristic length and σ is the liquid surface tension.

The Froude number compares the inertia forces with the gravitational force acting on an object and is based on a speed over length ratio. The Bond number is the ratio of gravitational (or body forces) to surface tension forces. To compare the inertia of a fluid with its surface tension the Weber number is used. The Weber number is useful in analysing the flow behaviour of thin films and the formation of droplets and bubbles.

Entrainment:

When the velocity of the gas is sufficiently high to transport liquid droplets to the tray above, liquid entrainment occurs. This influences the mass transfer separation efficiency, as shown in Figure 1.5, since the entrained liquid contains a higher fraction of the less volatile component than the liquid on the tray above. This increases the concentration of the less volatile component on the tray above. The onset of entrainment is one of the operating parameters which constrain the mass transfer separation efficiency. The maximum allowable entrainment is achieved when the separation efficiency on each tray is reduced to the point where the overall required separation cannot be obtained with the number of trays available in the column. Therefore the onset of entrainment is a vital parameter in the design of the column and thus directly impacts the cost.

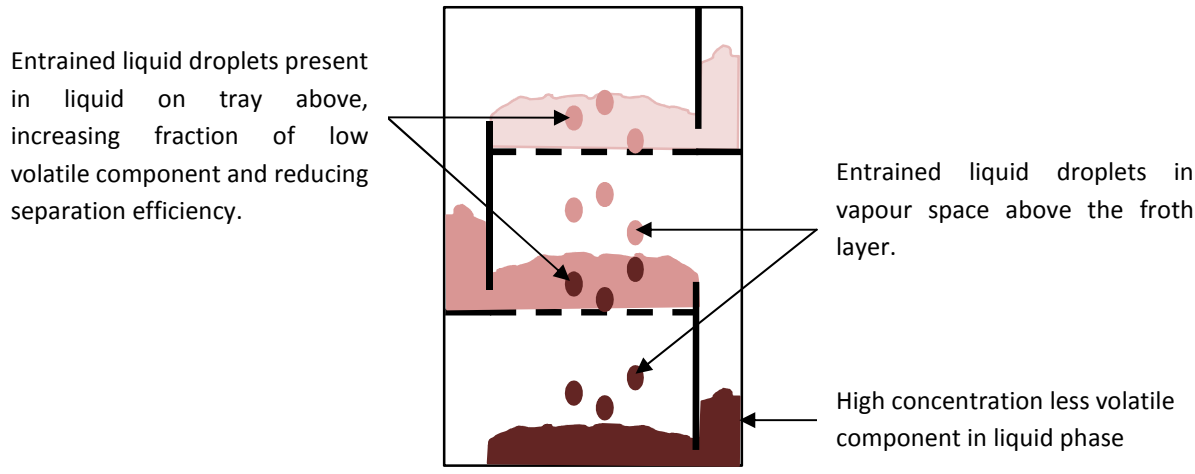

Figure 1.5 Schematic representation of the influence of entrainment on the separation efficiency.

The study of entrainment is categorised as part of the hydrodynamic behaviour inside the distillation column and is generally influenced by the following parameters:

1. Gas and liquid flow rates

2. Gas and liquid physical properties
3. Column and tray geometry

Weeping:

Another hydrodynamic phenomenon is found when the vapour rate is low enough for liquid dumping (weeping) to occur. Under these conditions the vapour rate is so low that the liquid weeps through the holes in the tray to the tray below. Weeping is therefore the inverse of entrainment and also negatively influences the separation efficiency.

Flooding:

Excessive entrainment can cause the liquid flow rate to exceed the downcomer capacity (Seader and Henley, 1998). As the downcomer exceeds capacity, liquid will build-up on the trays and go back up the column causing the column to flood. Column flooding can also occur when the liquid feed flow rate exceeds the downcomer capacity while the gas flow rate is sufficiently high enough to prevent weeping, resulting in a liquid build-up on the tray. Another mechanism for column flooding occurs during low liquid rates when the vapour velocity is high enough so that the amount of liquid entrained exceeds the liquid rate flowing through the downcomer (and column).

1.3 Project scope

In this study the focus is on entrainment and the hydrodynamic behaviour that constitutes entrainment. In order to investigate the hydrodynamic behaviour inside the tray column it was decided to use a thermally stable gas and liquid system (air/water) to ensure that no mass transfer occurred between the phases. To further simplify the investigation it was decided not to test the effects of foaming on entrainment.

Currently the entrainment rate is expressed and measured as the mass of liquid entrained over the mass of rising vapour (Hunt *et al.* (1955), Kister and Haas (1988) and Bennett *et al.* (1995)). This expression does not consider the amount of liquid on the tray and can therefore not be linked to the rate of liquid entrained compared to the liquid flow rate entering the tray. A correlation is therefore required to predict entrainment as a function of the liquid entering the tray so that the effect of entrainment on the separation efficiency can be determined directly.

Work has been done on the effect that gas and liquid flow rates, tray geometry, tray spacing and weir height have on entrainment. Since most of the work done in the literature focused on entrainment in the spray regime for low liquid loads. Very little is mentioned about the hydrodynamic behaviour at excessive entrainment for high liquid (> $45m^3/(h.m)$) and vapour

loads (> 3m/s). No extensive research has been done on the effects that gas and liquid physical properties have on entrainment because most of the work has been done with the air/water system, resulting in a lack of non-air/water system data. The limited existing non-air/water data is obtained from various sources with different column geometries and sampling methods.

Based on the shortcomings in the literature there is a need to generate entrainment data over a wide range of experimental conditions including conditions of excessive entrainment. The data should be generated by using a range of gas/liquid systems so that the influence of system (gas and liquid) physical properties on entrainment can be determined. To eliminate the effect of different column geometries and sampling methods, one experimental setup of known geometry should be used to generate entrainment data. Foaming is another hydrodynamic phenomenon that negatively affects mass transfer in distillation and especially stripping applications. However, due to the limited time available for this project it was decided that the influence of foaming systems on entrainment should not be part of the project scope.

The majority of correlations in literature assume that the influence of droplet drag on the froth height and entrainment rate is of little significance, as will be shown in Chapter 2. There is however a need to determine the validity of this assumption at high vapour rates and for low surface tension liquids. The influence of high vapour and liquid flow rates on excessive entrainment should therefore be investigated.

Entrainment will be redefined so that the entrainment rate relates to the amount of liquid on the tray. It is anticipated that the redefined entrainment rate should give an indication of the influence of entrainment on the separation efficiency of the distillation process.

1.4 Objectives

This study is aimed at investigating some of the shortcomings that have been identified in literature. The objectives of this study are described as follows:

1. Conduct a literature survey to gain insight into the hydrodynamic behaviour in sieve tray columns and how this relates to entrainment.
2. Design and construct an experimental setup capable of testing a range of different gasses and liquids as well as gas and liquid flow rates so that the influence of gas and liquid physical properties and their flow rates on entrainment can be determined in a continuation of this project.
3. The experimental setup must be able to measure weeping rates.
4. Commission the experimental setup with an air/water system.

5. Redefine and measure entrainment as the amount of liquid entrained over the amount of liquid entering the tray for a wide range of gas and liquid flow rates for the air/water system.
6. Compare excessive entrainment data for the air/water system at high vapour (superficial velocities > 3 m/s) and liquid flow rates (Q_L > 17.2 m^3/(h.m)) with predictive trends from literature.
7. Finally, recommendations will be made as to how the investigation can be continued in a doctoral dissertation.

1.5 Thesis layout

Based on the objectives mentioned above, the layout of the thesis is shown in Table 1.2.

Table 1.2 The structural layout of the thesis.

Goal	Method	Chapter
Conduct a Historical Overview of the Hydrodynamic Characterization in Sieve Tray Distillation Columns	Literature Review	2
Design Experimental Setup	1. Concept Design 2. Detail Design 3. Construction	3
Commissioning of Experimental Setup	1. Test system for leaks 2. Validate sensor readings 3. Calibrate control system analog signals 4. Test system repeatability	3
Compare air/water system data with predictive trends from the literature	Generate entrainment data for air/water system and range of gas-and-liquid flow rates	4
Discussion of experimental results	Refer to literature and comparison with predictive trends	4
Make Conclusions	Based on the findings from the results	5
Suggest Recommendations	Based on conclusions and shortcomings in literature	6

2 A historical overview of the hydrodynamic characterization in sieve tray distillation columns

In order to understand the parameters that influence entrainment it was necessary to investigate the hydrodynamic behaviour inside the column. In this section a literature survey will review some of the work done on hydrodynamics in sieve tray distillation columns following a time line, see Figure 2.1, starting in 1955 with work done by Hunt *et al.* (1955) and ending in 2003 with the contribution made by Van Sinderen *et al.* (2003). Since entrainment is influenced by other hydrodynamic phenomena like liquid hold-up and flow regimes, some attention will be given to these factors in the literature review. At the end of the literature survey a critical evaluation will be conducted on the work done on entrainment. The different entrainment correlations will then be compared and their limitations revealed. Based on the short-comings found in the literature the aim of this project will be developed.

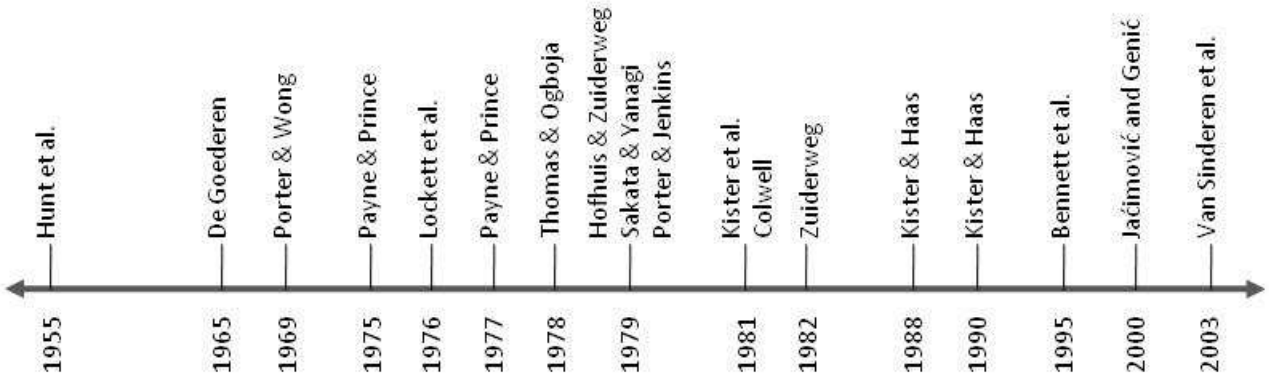

Figure 2.1 The timeline followed in the literature review.

2.1 Work done on Hydrodynamic behaviour in Sieve Tray Columns

2.1.1 Hunt *et al.* (1955) – Capacity factors in the performance of perforated plate columns.

Before 1955 sieve trays were mainly used for liquid systems that contained a large amount of solid matter. In systems that did not contain solid matter bubble-cap trays were used due to the fact that they could operate with much lower gas flow rates than sieve trays. After

Arnold *et al.* (1952) and Mayfield *et al.* (1952) showed that sieve trays have an economic advantage over bubble-cap trays Hunt et al. (1955) investigated the factors affecting the vapour capacity of sieve tray columns.

Hunt *et al.* (1955) found that the liquid flow over the weirs in a 0.152m diameter column is unstable. They therefore chose to use a 0.152m diameter column with no liquid cross flow and the liquid hold-up was controlled with a constant head tank placed at different heights above the tray. The gas was circulated through the column with a centrifugal blower and the flow rate measured and controlled with an orifice and slide valve. A heat exchanger cooled with running tap water was used to remove heat added by the centrifugal blower from the air. Water-filled manometers were used to determine column gauge pressure, orifice gauge pressure and the resultant column pressure drop. The orifice pressure drop was measured with an inclined manometer.

The entrained liquid was collected on a similar tray as the test tray and placed at different spacings above the test tray. The entrainment catchment section of the column tapered to increase the gas flow path area and reduce the superficial gas velocity. Entrainment was measured using a vented and calibrated Buret to measure volume as a function of time.

The following systems were used to generate total pressure drop and entrainment data:

- Methane – Water
- Freon 12 – Water
- Air – Kerosene (ρ_l = 704 kg/m^3, σ = 25 mN/m)
- Air – Hexane
- Air – Carbon Tetrachloride
- Air – water & glycerine (μ = 10 – 80 mPa.s)

Hunt *et al.* (1955) developed a dry tray pressure drop correlation, Eq. 2.1, based on the entrance and exit losses of a small tube with an empirical constant of 1.14 obtained from their data.

$$h^*_{DP} = 1.14 \frac{u_h^{*2}}{2.g_c} \left[0.4 \left(1.25 - \frac{A_h}{A_n} \right) + \left(1 - \frac{A_h}{A_n} \right)^2 \right] \qquad 2.1$$

In this case the dry tray pressure drop is measured in meters vapour. From Eq. 2.1 it can be seen that the dry tray pressure drop depends on the hole velocity (u_h^*) and the ratio of hole area (A_h) to net column area (A_n) which, in this case, is similar to the column area.

Hunt *et al.* (1955) found that entrainment is independent of hole velocity and depended on the superficial gas velocity. Entrainment increased exponentially with decreasing tray spacing and increasing superficial gas velocity. Entrainment was found to be a function of the distance between the froth height and the tray above, called the effective tray spacing. Since they could not measure the froth height they assumed a foam density, based on their scope of work, of 0.4 times the clear liquid density in order to develop their correlation. They found that the gas density has no effect on entrainment and the only physical property that contributes to entrainment is the surface tension of the liquid. Eq. 2.2 was developed to predict the entrained liquid mass per mass of gas flowing, based on surface tension, tray spacing, column gas velocity and the clear liquid height.

$$E = 0.22\left(\frac{73}{\sigma}\right)\left(\frac{u_s^*}{S^* - 2.5h_L^*}\right)^{3.2} \qquad 2.2$$

Using high speed photography, 0.5m above the bottom tray, they found the droplet size to be too large for droplet drag to have an influence on entrainment and that entrainment is caused by droplets ejecting from the liquid froth. This finding was supported by the dependency of entrainment on the tray spacing as shown in Figure 2.2. A summary of test ranges used by Hunt *et al.* (1955) is shown in Table 2.1.

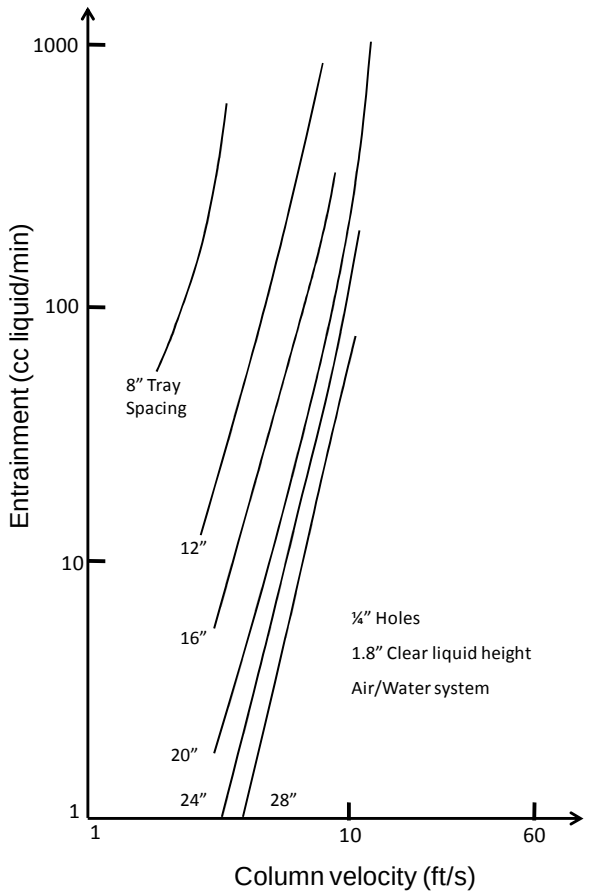

Figure 2.2 Effect of plate spacing on entrainment, redrawn from Hunt *et al.* (1955) Fig. 9.

Table 2.1 Summary of the column geometry, test ranges and systems used by Hunt *et al.* (1955).

Column Shape and Dimensions	Tray Spacing [m]	Gas Superficial Velocity [m/s]	Fractional Hole Area	Liquid Flow Rate [$m^3/(h.m)$]	Correlations	Systems Used
0.152m Round	0.2 – 0.711	1.0 – 4.3 m/s	0.05 – 0.215	No liquid cross flow	1. Dry Tray Pressure Drop (H_{DP}^*) 2. Entrainment (L'/G)	Methane – Water Freon 12 – Water Air – Kerosene Air – Hexane Air – Carbon Tetrachloride Air – water & glycerine

Hunt *et al.* (1955) developed a correlation for predicting entrainment without liquid cross flow. Since commercial tray columns operate with liquid cross flow the applicability of their correlation, Eq. 2.2, which neglects the effect of liquid cross flow, is therefore questioned. They found that entrainment depends on the liquid surface tension, tray spacing, clear liquid height and superficial vapour velocity. They assumed a froth density of 0.4 times the clear liquid density based on their range of operation and acknowledge that this assumption is not necessarily valid for all systems and operating conditions. They found that droplet drag has no effect on entrainment and that the droplet ejection velocity, from the liquid froth, contributes to entrainment.

2.1.2 Porter and Wong (1969) – The transition from spray to bubbling on sieve plates.

While investigating the effect of liquid properties on mass transfer in the gas phase De Goederen (1965) found that two forms of dispersion exist on the tray. He described the dispersions as liquid dispersion in the form of droplets at gas velocity and low liquid hold-up, and gas/vapour dispersion as bubbles at low gas velocity and higher liquid hold-up. Based on the findings made by, De Goederen (1969), Porter and Wong (1969) decided to investigate the transition from the spray to bubbling (froth) regime. They defined the regimes at a fixed gas velocity where a small amount of liquid hold-up would produce a spray and by increasing the liquid hold-up would produce froth.

The experiments were conducted in a square 0.457m x 0.457m column with no liquid cross flow with more detail shown in Table 2.2. Table 2.3 is a summary of the experimental conditions used to determine the froth to spray transition. Superficial gas velocity is defined as open column velocity.

Table 2.2 Summary of the column geometry, test ranges and systems used by Porter and Wong (1969).

Column Shape and Dimensions	Tray Spacing [m]	Gas Superficial Velocity [m/s]	Fractional Hole Area	Hole Diameter [mm]	Liquid Flow Rate [m^3/(h.m)]	Correlations/ Work Done	Systems Used
0.457x0.457m Square	single tray	0.24 – 2.01	0.032 – 0.094	3.18 – 12.7	No liquid cross flow	1. $h_{L,t}$* Clear liquid height at froth to spray transition	Freon/Air, He/Air, CO_2/Air gas mixtures with NaCl solutions to vary liquid density, Glycerol dilutions to vary viscosity, and Kerosene to represent organic liquids

The transition between the spray and bubbling regimes was determined using a light transmission technique. The experimental procedure was started with a clear liquid height of around 5mm and a fixed superficial gas velocity. The light source was placed just above where they expected the froth interface to be and more liquid was slowly added. In the spray regime the amount of light transmitted was small due to the thick spray of droplets. With the addition of more liquid, fewer droplets were formed and the amount of light transmitted increased suddenly. This sudden increase in the amount of light transmitted was defined as the regime transition point. The light transmission height was varied at three different distances (75mm, 90mm and 100mm) above the tray and found to be independent of the regime transition for the same amount of liquid hold-up on the tray.

Table 2.3 Experimental conditions used by Porter and Wong (1969).

Variable	Description	Range
u_S [m/s]	Superficial Velocity	0.24 – 2.01
u_h [m/s]	Hole vapour velocity	4.9 – 47.2
ρ_L [kg/m^3]	Liquid density	769 - 1177
ρ_g [kg/m^3]	Gas/vapour density	0.33 – 4.24

Table 2.3 Experimental conditions used by Porter and Wong (1969).

Variable	Description	Range
F [$u_S\rho_g^{0.5}$]	F-factor based on gas superficial velocity and density	0.07 – 1.95
μ [mPa.s]	Liquid viscosity	0.94 - 15
σ [mN.m]	Surface Tension	32 - 74

It was found that the liquid hold-up at the transition:

- Increases with increasing gas velocity
- Increases with increasing gas density
- Increases with decreasing liquid density
- Is not affected by the liquid viscosity
- Increases with increasing hole diameter

They found that surface tension only influenced droplet diameter in the spray regime and that the important drop size for transition results from droplet coalescence at liquid hold-up values close to the regime transition. The effect of hole diameter on the transition was determined with trays having the same pitch to hole diameter ratio, 4:1, but with different hole diameters and hole areas.

Porter and Wong (1969) developed a model that relates droplet terminal velocity to the rate of change of the gas velocity above the tray. The droplet terminal velocity was determined by measuring the time a water droplet of know diameter fell over a measured vertical distance through air. They assumed that at the regime transition the drop size distribution is determined by droplet coalescence and droplet breakdown in the spray. The spray consists of liquid droplets that are rising, falling or suspended in the rising gas stream. By increasing the liquid hold-up more droplets are formed increasing the probability for coalescence to create larger drops until the droplets all have the same terminal velocity. They showed that droplets exceeding 5mm diameter all have the same terminal velocity. This test was done by measuring the terminal velocity of water droplets with ranging diameters through stagnant air at atmospheric conditions.

The transition from spray to froth (bubbling) is assumed to be at the point where sufficient liquid has been added so that multiple droplet coalescence can take place. This liquid hold-up is then used to predict the transition.

For trays with a pitch to hole diameter ratio of 4:1 and for conditions where $0 < \frac{u_h - u_t}{u_h - u_s} < 0.8$ (difference between hole velocity and droplet terminal velocity over the difference between hole velocity and gas superficial velocity) the liquid hold-up at the transition can be determined with Eq. 2.3

$$\frac{h_{L,t}^{*}}{d_H^{*}\varepsilon} = 4 + 9\left[\frac{\left[1 - 1.04 A_f (\rho_l / \rho_g)^{0.5} / u_s^{*}\right]}{(1 - A_f)}\right] \qquad 2.3$$

Alternatively:

$$\frac{h_{L,t}^{*}}{d_H^{*}\varepsilon} = 4 + 9\left[\frac{u_h - u_t}{u_h - u_s}\right] \qquad 2.4$$

If the hole velocity, and superficial velocity is measured in ft/s then the droplet terminal velocity can be calculated with Eq. 2.5 (Porter and Wong (1969)):

$$u_t^{*} = 1.04\left(\frac{\rho_l}{\rho_g}\right)^{0.5} \qquad 2.5$$

They do acknowledge that this model may be an oversimplification of the transition from the spray to froth regime.

The work done by Porter and Wong (1969) applies to columns with no liquid cross flow and can therefore not be applied in industrial applications with liquid cross flow. Their work does, however, give more insight regarding the transition from the spray to froth regime and the methods used to measure the transition. Porter and Wong (1969) found that the liquid hold-up is larger for larger hole diameter trays. By changing the fractional hole area

(total hole area divided by the perforation area) and hole diameter the hole velocity is changed which might have an effect on the liquid hold-up at the transition. The effect of hole diameter on the liquid hold-up can therefore not be determined with different hole diameter trays, each having a different fractional hole area, as was done by Porter and Wong (1969).

2.1.3 Lockett *et al.* (1976) – The effect of the operating regime on entrainment from sieve trays.

Locket *et al.* (1976) were one of the first to investigate the effect of the flow regime on entrainment for sieve trays with liquid cross flow. All the work done prior to their investigation ignored the effect of the flow regime on entrainment. They wanted to show that a change in the flow regime from spray to froth would cause a sudden decrease in entrainment and that this change can be caused by increasing the liquid flow rate. They measured entrainment as the mass of liquid entrained per mass of vapour flowing through the tray.

Locket *et al.* (1976) used a 0.46m diameter round Perspex column with three trays evenly spaced at 0.36m intervals. Air and water were circulated through the column using a centrifugal blower and pump. The entrainment from the middle tray to the top tray was determined by a tracer mass balance around the top tray. A $NaNO_2$ tracer was continuously introduced at the bottom of the downcomer feeding the middle tray. Liquid samples were taken at the bottom of the downcomers feeding the top and middle trays and at the exit of the middle tray. Tracer concentrations were determined using a conductivity bridge.

The clear liquid height on the tray was determined by taking the average between five liquid manometers mounted flush to the tray floor. Four different tray geometries were used in the tests to determine the influence of hole diameter on entrainment and the transition between the flow regimes. The liquid flow rate (per weir length) and hole velocity ranged between 3.6 – 21.6 m^3/(h.m) and 8.4 – 31.1 m/s respectively.

Table 2.4 Summary of the column geometry, test ranges and systems used by Lockett *et al.* (1976).

Column Shape and Dimensions	Tray Spacing [m]	Hole Gas Velocity [m/s]	Fractional Hole Area	Hole Diameter [mm]	Liquid Flow Rate [m^3/(h.m)]	Correlations/ Work Done	Systems Used
0.46m Round	0.36m	8.4 – 31.1	0.033 – 0.173	3.2 – 12.7	3.6 – 21.6	No correlations	Air and Water

A sudden decrease in entrainment was found as the liquid flow rate increased (see Figure 2.3) for a fixed hole gas velocity. During each run the hole velocity remained constant. The liquid rate at which the sudden decrease in entrainment occurred was called the critical liquid flow rate. They found that the critical liquid flow rate, and liquid hold-up at the transition, increases with increasing hole diameter and hole velocity.

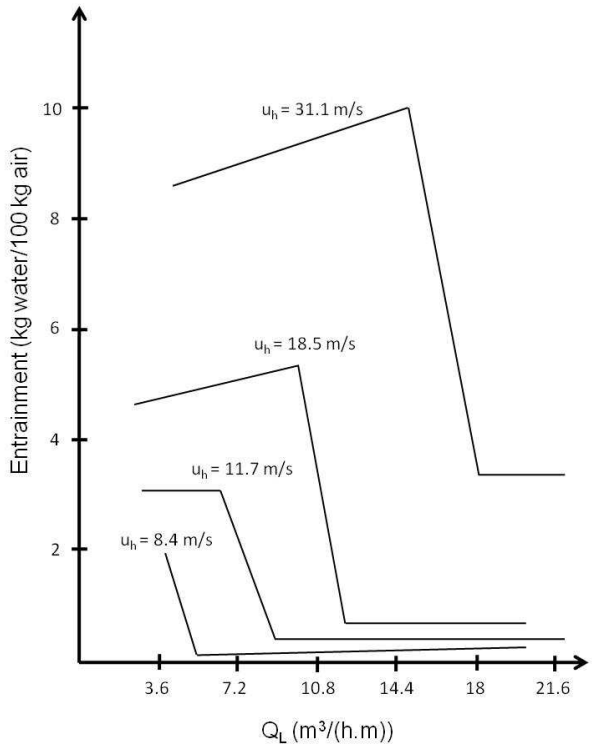

Figure 2.3 Effect of liquid flow rate on entrainment, redrawn from Fig 2 in Lockett *et al.* (1976).

Locket *et al.* (1976) showed that by increasing the liquid flow rate, while maintaining the gas velocity, the flow regime can change from spray to froth and simultaneously reduce the amount of liquid entrained in the rising gas. The critical liquid flow rate, causing the transition change, increased with increasing hole velocity. The sudden reduction in entrainment at constant hole velocity and increasing liquid flow rate was show graphically and no correlation predicting this transition was published.

2.1.4 Payne and Prince (1977) – Froth and spray regimes on distillation plates.

In their publication, Payne and Prince (1977) showed that the transition between the spray and froth regimes in a sieve tray column corresponds to transition from bubbling to jetting

at the orifices of the tray. They conducted tests in a 0.431m x 0.452m square Perspex column with three sieve trays (see Table 2.5 for more information regarding test ranges). The liquid cross flow was kept very low from 2.9 – 3.5 m^3/(h.m) compared to the range (3.6 – 21.6 m^3/(h.m)) covered by Lockett *et al.* (1976). They found that the clear liquid height at the transition for a gas hole velocity of 29.8 m/s and liquid flow rate of 3.5 m^3/(h.m) to be 19.3 mm. This corresponds very well with the entrainment transition data from Lockett *et al.* (1976) at similar hole velocities and tray geometry, although Lockett *et al*. (1976) did not specify the liquid flow rate at this transition. Payne and Prince (1977) do suggest that liquid flow rate contributes to the liquid hold-up which will have an effect on the transition conditions. However for the limited liquid flow range used in their test they found that the liquid flow rate does not have an influence on the regime transition. They therefore recommended that more research is required to relate the transitional liquid hold-up to the liquid loading.

Air and water was used in their tests and they can therefore not predict the influence of gas and liquid physical properties on the spray to froth transition. They recommend that more work should be done to fully understand the effects of gas and liquid physical properties on the regime transition.

Table 2.5 Summary of the column geometry, test ranges and systems used by Payne and Prince (1977).

Column Shape and Dimensions	Tray Spacing [m]	Hole Gas Velocity [m/s]	Fractional Hole Area	Hole Diameter [mm]	Liquid Flow Rate [m^3/(h.m)]	Correlations/ Work Done	Systems Used
0.43 x 0.45 Square	610	12.6 – 40	0.04 – 0.09	3.2 – 12.7	2.9 – 3.5	No correlations	Air and Water

2.1.5 Thomas and Ogboja (1978) – Hydraulic studies in sieve tray columns.

Most of the hydrodynamic data generated before 1978 was for sieve trays with hole diameters ranging between 3.2mm – 9.5mm. Small hole diameter trays can not be used in columns with liquids containing solid material due to problems created by fouling and hole blockage. Thomas and Ogboja (1978) therefore decided to test the influence of two 25.4mm hole diameter sieve trays on entrainment, dynamic pressure drop, residual pressure drop, total tray pressure drop and froth height. The operating regime observed on the trays is defined as a “frothy mass”. No more information is given regarding this regime and no

comparison is made with the definitions for the spray and froth regimes provided in literature.

The experimental setup used consisted of a 0.3m x 0.91m rectangular column and 0.81m diameter round column. The rectangular column consisted of three compartments, evenly spaced at 0.61m in height, with the test tray placed between the top and middle compartments. External downcomers are used with Perspex side windows for visual observation. More information regarding the setup is given by Thomas and Haq (1976). The round column is made from glass sections with 1.02m tray spacing and internal downcomers. For all the tests an air-water system was used.

For the entrainment studies a special entrainment collection (catch-pot) device was made. The cylindrical catch-pot had a 25.4mm packed bed of 3.2mm diameter silica gel spheres. The catch-pot was placed inside the columns at three different heights (0.305m, 0.381m and 0.457m) above the tray floor. Once the conditions inside the column had stabilised the bed of silica spheres will be exposed to the environment above the tray by opening a sliding mechanism, at the catch-pot underside, for 10 seconds. The amount of liquid entrained was determined by the increase in weight of the silica gel. Fresh silica gel was used every time and allowance was made for the effect of the saturated air. The liquid flow rate and gas hole velocities covered during the experiments ranged between 4.5 – 40.3 m^3/(h.m) and 13 – 25.5 m/s respectively. A summary of their experimental setup and test conditions are given in Table 2.6 below:

Table 2.6 Summary of the column geometry, test ranges and systems used by Thomas and Ogboja (1978).

Column Shape and Dimensions	Tray Spacing [m]	Hole Gas Velocity [m/s]	Fractional Hole Area	Hole Diameter [mm]	Liquid Flow Rate [m^3/(h.m)]	Correlations/ Work Done	Systems Used
0.3 x 0.91m Rectangular	0.61m	13 – 25.5	0.124	25.4	4.5 – 40.3	1. h_t Total tray pressure drop 2. h_d Dynamic pressure drop 3. h_f Froth height 4. (L'/G) Entrainment	Air and Water
0.81m Round	1.02m		0.118				

Dynamic pressure drop measurements were made by a series of liquid manometers. Each manometer had one leg flush with the tray floor and the other leg protruding into the

vapour space above the tray. Froth height measurements were obtained visually with the aid of Cine film.

Thomas and Ogboja (1978) found that the total tray pressure drop increased with an increase in gas and liquid flow rates. The equation predicting total tray pressure drop for the rectangular column with 25.4mm holes is given in Eq. 2.6 which is a function of the liquid flow rate (Q_L) and the gas velocity times the square root of the gas density (F_P):

$$h_t^* = 0.024Q_L^+ + 0.2F_P^{*2} + 3.66 \qquad 2.6$$

The total pressure drop for the round column with 25.4mm hole diameter tray is shown in Eq. 2.7:

$$h_t^* = 0.038Q_L^+ + 0.533F_P^{*2} + 2.0 \qquad 2.7$$

The tray dynamic pressure drop was found to decrease with increasing hole velocity at a constant liquid rate. Increasing the liquid flow rate increased the dynamic pressure drop for similar hole gas velocities. According to Thomas and Ogboja (1978) hole size has a small effect on the dynamic pressure drop while column geometry showed a significant influence.

The dynamic pressure drop for the rectangular and round column with a 25.5mm hole diameter tray can be determined with Eq. 2.8 and Eq. 2.9 respectively.

$$h_d^* = 0.02Q_L^+ - 0.4F_P^{*2} + 2.4 \qquad 2.8$$

$$h_d^* = 0.02Q_L^+ - 0.16F_P^{*2} + 3.15 \qquad 2.9$$

No correlation was developed to predict the residual pressure drop for the different trays while the influence of the gas hole velocity and liquid flow rate on the residual pressure drop is given graphically. The froth height was measured at the centre of the trays. They showed that the froth height increased with increasing gas superficial velocity and increasing liquid flow rate. The froth height for the rectangular and round tray column with 25.5mm hole diameter tray can be predicted using Eq. 2.10 and Eq. 2.11:

$$h_f^* = 0.08Q_L^+ + 1.56F_P^* + 3.52 \quad 2.10$$

$$h_f^* = 0.055Q_L^+ + 2.16F_P^* + 4.83 \quad 2.11$$

The entrainment data were collected at 0.305m, 0.381m and 0.457m above the tray floor. By injecting a dye into the liquid entering the lower tray, it was found that no liquid was transported to the tray above the test tray. The possible influence which the upper and lower trays might have on entrainment is therefore not accounted for in the sampling process. It was found that an increase in gas velocity (based on the bubbling area) will result in an increase in entrainment. Entrainment was measured in mass of liquid captured in the catch-pot over time. The entrainment data was used to create an entrainment prediction correlation based on the correlation, Eq. 2.2, developed by Hunt *et al.* (1955):

$$E = 0.88\left(\frac{u_p^*}{S^* - h_f^*}\right)^{0.77} \quad 2.12$$

The difference between the entrainment predicting correlation provided by Hunt *et al.* (1955) and equation 2.12 is that Hunt *et al.* (1955) considered the effect of liquid surface tension on entrainment. Hunt *et al.* also assumed a constant froth density while Thomas and Ogboja (1978) developed a froth height correlation based on their results. Hunt *et al.* (1955) acknowledged that their assumption of a constant froth density is not regarded to be representative.

By using an entrainment catch-pot device that only partially covers the vapour flow path area (column net area), Thomas and Ogboja (1978) assumes that the amount of entrainment is uniform across the column net area. However this assumption was not justified and may not be true. The entrainment catch-pot was placed in the vapour space between two trays and it was proven by dye studies that no liquid was transported from the tray below to the tray above during the tests. The effect of entrainment from the tray below the test tray was thus not accounted for and not representative of entrainment situations in industrial applications.

Previous work done by Lockett *et al.* (1976) showed that the flow regime above the tray influences the mass of liquid entrained in the vapour. Thomas and Ogboja (1978) did not mention any change in flow regime even though tests were conducted over a similar gas and liquid flow rate range as that of Lockett *et al.* (1976).

2.1.6 Hofhuis and Zuiderweg (1979) – Sieve plates: Dispersion density and flow regimes.

Until 1979 very little work has been done regarding flow regimes on sieve tray columns with liquid cross flow, Hofhuis and Zuiderweg (1979) decided to investigate the significance of the flow regime on liquid hold-up and flooding (they did not define flooding). By using the gamma ray absorption technique they studied the flow regimes on sieve trays for an air/water and toluene/toluene vapour system. Helium – air and Freon – air mixtures with densities of 0.5 – 3.5 kg/m^3 were also used with water as test systems in a 0.15m diameter column.

The rectangular column used for the air/water system tests was 1.4m x 0.8m with a 0.8m x 0.8m bubbling (perforated) area. The toluene/toluene vapour column had a 0.45m diameter. Air was circulated through the rectangular column using 2 centrifugal blowers. The air flow rate was measured using a vane anemometer, which is not highly accurate, and the liquid flow rate was measured using a rotameter and an orifice plate. Table 2.7 is a summary of the tray and column geometry used by Hofhuis and Zuiderweg (1979) during their tests.

Table 2.7 Summary of the column geometry, test ranges and systems used by Hofhuis and Zuiderweg (1979).

Column Shape and Dimensions	Tray Spacing [m]	Superficial Gas Velocity [m/s]	Fractional Hole Area	Hole Diameter [mm]	Liquid Flow Rate [$m^3/(h.m)$]	Correlations/ Work Done	Systems Used
1.4x0.8m Rectangular	unknown	0.5 - 2.2	0.04 – 0.071	3.0 – 10.0	unknown	1. ε, froth density 2. H_L, liquid hold-up	Air/water
0.45m Round	unknown		0.064	7.0			Toluene/Toluene
0.15m Round	unknown	unknown	unknown	unknown			Freon-air mixture/water Helium-air mixture/water

The gas/liquid dispersion density on and above the trays were measured using a gamma ray absorption technique. A narrow, 1cm, radiation beam was moved both horizontally and vertically across the gas and liquid flow paths to determine the density profiles. The vertical profiles were used to identify the bed height, defined as the height above the tray were the dispersion density equalled 0.01. The accuracy of this technique is approximately 3%. The clear liquid hold-up was determined by integrating the vertical density profiles between the tray floor and the bed height. The average bed density is calculated by the ratio of the clear liquid hold-up divided by the bed height as shown in Eq. 2.13:

$$\varepsilon = \frac{h_L}{h_b} \qquad 2.13$$

Hofhuis and Zuiderweg (1979) found that the bed height increases with increasing gas velocity and the dispersion density increased with increasing liquid hold-up. It was found that gas and liquid densities influences the dispersion density profiles. However surface tension had no significant influence on the dispersion density which contradicts the predictions made by Payne and Prince (1977) that decreasing surface tension will cause decreasing dispersion density at the regime transition. From visual observation of the

dispersion behaviour a change was observed at the weir location. A flow ratio group, Eq. 2.14 was introduced to define the transition at the weir.

$$\psi = \frac{Q_L}{3600 u_b}\sqrt{\frac{\rho_l}{\rho_g}} \qquad 2.14$$

At ψ < 0.2m the clear liquid level (it is unclear of the level refers to clear liquid height) is below the weir edge and the liquid is moved over the weir as "drops and slugs". At ψ > 0.2m the clear liquid level is equal to the weir edge and the liquid/gas dispersion flows over the weir as a homogeneous mixture. The majority of the gas was also found to be emulsified to small bubbles.

After observing this transition a new regime was defined at ψ > 0.2m called the emulsified flow regime. The transition is also described as the condition where the horizontal momentum flux of the liquid becomes equal to the vertical momentum flux of the rising gas. The liquid hold-up at this transition was found to be 0.025m with the hole gas velocity "about" 10 times the gas bubbling velocity. They did not, however, investigate the influence of weir height on the liquid hold-up and it is unclear what weir height was used in this particular experiment. Gas bubbling velocity is defined as the velocity based on column area minus two times the downcomer area. For a hole diameter range of 7mm – 10mm they proposed a clear liquid height correlation as shown in Eq. 2.15:

$$H_L = 0.6\psi^{0.25} H_w^{\ 0.5} P^{0.25} \qquad 2.15$$

The dispersion density (h_L/h_F) ranged between 0.05 – 0.4 and depends on the gas velocity (it is not clear if this velocity refers to the bubbling or hole velocity), the liquid hold-up and the gas/liquid density ratio. Plate geometry and surface tension had no significant effect.

Hofhuis and Zuiderweg (1979) found that liquid surface tension and viscosity have no significant effect on the spray regime transition and only hole diameter showed some influence. The lowest gas flow rate where spray is still dominant was determined with a Froude number ($Fr = \frac{u_b}{\sqrt{gH_L}}$) correlation as shown in Eq. 2.16:

$$\frac{H_L}{D_H} = \frac{1.1u_b}{A_f\sqrt{gH_L}}\sqrt{\frac{\rho_g}{\rho_l}} \qquad 2.16$$

Eq. 2.16 applies to trays with hole diameters of approximately 6.3mm. For hole diameters around 12.6mm the constant of 1.1 in Eq. 2.16 should be changed to 1.2.

The free bubbling regime was found to range between a Froude number ($u_b/(gH_L)^{0.5}$) of 1 – 1.4 and is independent of tray geometry and gas density. The free bubbling regime was found to be close to the weeping limit. The mixed froth regime was defined as the regime between the spray regime and the emulsion regime. The flow regime ranges and limits are presented in Figure 1.4 as a function of the capacity factor, C_b, and flow parameter, ϕ.

By using the gamma ray absorption technique Hofhuis en Zuiderweg (1979) defined the four flow regimes namely the spray regime, mixed froth regime, free bubbling regime and the emulsion regime. The average two phase density is controlled by the tray Froude number, which accounts for the gas superficial velocity and liquid hold-up on the tray, and the gas to liquid density ratio. The free bubbling regime occurs if the Froude number is smaller than 1.2. The regime was found to be close to the weeping limit making this regime, according to Hofhuis and Zuiderweg (1979), less important. They did not specify the applicability of the free bubbling regime to commercial operation.

The work done by Hofhuis and Zuiderweg (1979) gave more insight into the effects of gas and liquid properties as well as tray geometry, on the different flow regimes. Only two main gas/liquid systems were used to develop their correlation for predicting the clear liquid height. Based on only two liquids, they found that surface tension did not have an influence on bed height. This finding is limited to low (< 0.3m) bed heights where droplet drag is expected to have no influence. They did show that for bed heights larger than 0.3m and low dispersion densities, droplet drag has a significant influence on the bed height.

2.1.7 Sakata and Yanagi (1979, 1982) – Performance of a commercial scale sieve tray.

Up to 1979 very little commercial sieve tray performance data existed in the literature and most of the available data for sieve tray columns with liquid cross flow was for air/water systems only. Sakata and Yanagi (1979) therefore decided to record performance data for a 1.2m diameter sieve tray distillation column. In order to cover a range of systems they used the following systems:

1. Cyclohexane/n – heptane at 34 and 165 kPa

2. Isobutane/n-butane at 1138, 2068 and 2758 kPa

The data generated by Sakata and Yanagi (1979) was used by others to develop non air/water correlations to predict froth height, froth density, clear liquid height and entrainment.

The trays had a fractional hole area of 8% (1979) and 14% (1982), tray spacing of 0.61m and 12.7mm diameter holes as shown in Table 2.8. The entrainment collection tray was similar to the other trays without a downcomer and no liquid cross flow. No more information is given regarding the entrainment collection section. It is unclear if all the entrained liquid was removed from the vapour and if any liquid carried over to the column outlet and condenser. The liquid feed rate and reflux stream flow rate was measured using orifices. They did not state how the vapour flow rate was recorded. The one possibility is that the condensate flow rate, measured by monitoring the condensate level in the condenser, was converted to a vapour flow rate.

Table 2.8 Summary of the column geometry, test ranges and systems used by Sakata and Yanagi (1979).

Column Shape and Dimensions	Tray Spacing [m]	Superficial Gas Velocity [m/s]	Fractional Hole Area	Hole Diameter [mm]	Liquid Flow Rate [m^3/(h.m)]	Correlations/ Work Done	Systems Used
1.2m Round	0.61m	0.015 – 2 approximately	0.08 & 0.14	12.7	9.3 – 88.9	No correlations only data	Cyclohexane/n-Heptane Iso-butane/n-Butane

The experimental data was generated from a cyclohexane/n-heptane system, at 34kPa and 165kPa, and an isobutane/n-butane system at 1138, 2068, 2758kPa. The entrainment measurements, measured as entrained liquid mass flow over the bubbling area (kg/s/m^2), were conducted under total reflux conditions and constant liquid loads. The data showed the strong dependence of entrainment on the vapour rate. The 14% fractional hole area tray proved to have a 5 – 10% higher vapour capacity than the 8% fractional hole area tray. Sakata and Yanagi (1979) found that at some conditions it was difficult if not impossible to predict entrainment rates. Testing was conducted over a liquid range from 9.3 – 88.9 m^3/(h.m). It was found that at low liquid rates the vapour velocity had to increase as the liquid flow rate increased to maintain a constant entrainment rate until a certain liquid flow rate (see maxima in trend shown in Figure 2.4) was reached where after the vapour velocity was decreased with increasing liquid flow rates to maintain the constant entrainment rate, as shown in Figure 2.4:

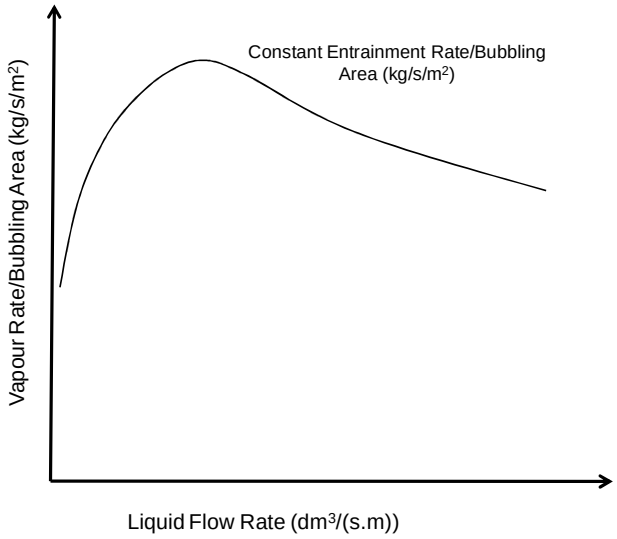

Figure 2.4 The influence of vapour and liquid flow rates on entrainment.

Most of the data generated is published in graphs and the recorded tabled data could be obtained by special request to the authors (at the time of printing the data was not received yet).

Sakata and Yanagi (1979) were the first to publish entrainment and performance data for non air/water systems from an industrial column. It is however unclear how the vapour rate was determined and the accuracy thereof. Nothing is mentioned to confirm that the de-entrainment section collected 100% of the entrained liquid and they acknowledged that for some conditions it is almost impossible to predict the amount of entrainment. The reliability and accuracy of the data is therefore questionable. Porter and Jenkins (1979), Zuiderweg (1982), Kister and Haas (1990), and Bennett *et al.* (1995) used the data from Sakata and Yanagi (1979, 1982) to develop their entrainment prediction correlations. Van Sinderen *et al.* (2003) compared their minimum entrainment data with that of Sakata and Yanagi (1982).

2.1.8 Porter and Jenkins (1979) – The Interrelationship between industrial practice and academic research in distillation and absorption.

The purpose of the paper written by Porter and Jenkins (1979) was to “relate research to practise”. This was done so that areas that required attention could be identified for future research. They therefore used published data, mostly by Sakata and Yanagi (1979), Lockett

et al. (1976) and Porter and Wong (1969), to interpret certain conditions in a distillation column.

Based on the difficulties Sakata and Yanagi (1979) experienced with accurately measuring entrainment they recommended more work should be done to generate accurate data. They found that the differences between the correlations predicting the transition from the froth regime to the spray regime are partly due to the different techniques used to measure and define the regime change and partly due to the modelling of a multi-orifice sieve tray with a single hole plate experiment. The transition between the spray and mixed (bubbly) regimes is therefore redefined as the condition where minimum entrainment is achieved. This will occur at the liquid cross flow rate (for a constant gas velocity) where the rate of liquid entrainment is a minimum as shown in Figure 2.5, relating the transition to the capacity of the tray.

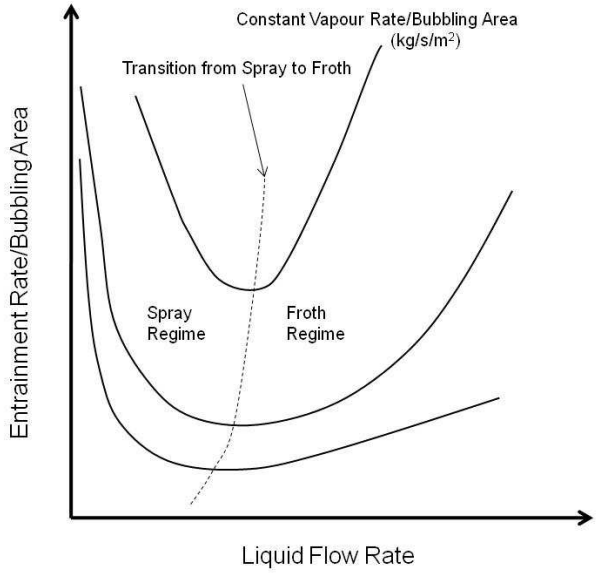

Figure 2.5 Minimum Entrainment trend based on data from Sakata and Yanagi (1979).

They then determined a correlating line using the capacity factor based on superficial gas velocity, $C_s = u_s\sqrt{\frac{\rho_g}{\rho_l - \rho_g}}$, liquid flow rate, $\frac{Q_L}{3600}$, and minimum entrainment data from Sakata and Yanagi (1979) and Lockett *et al.* (1976) to determine the spray to bubbly regime transition. The line, Eq. 2.17, is based on the correlation developed by Hofhuis and Zuiderweg (1979), Eq. 2.14:

$$\psi = \frac{Q_L}{3600 u_s}\sqrt{\frac{\rho_l - \rho_g}{\rho_g}} = 0.07 \qquad 2.17$$

The transition between spray and mixed bubbly regime and mixed bubbly and emulsified regime can therefore be predicted as shown in Figure 2.6:

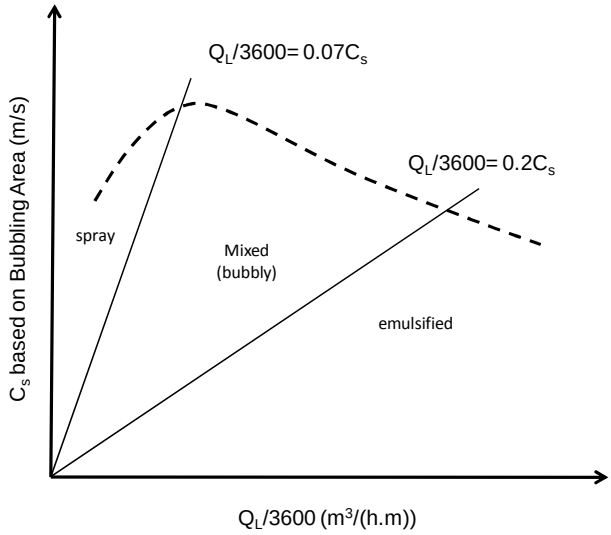

Figure 2.6 Transition between spray to mixed and mixed to emulsified regimes, redrawn from Porter and Jenkins (1979) Fig. 13.

Porter and Jenkins (1979) acknowledge that their definition of spray to bubbly regime is based on very little data and that more work is required to validate the concept. Porter and Jenkins (1979) developed a correlation predicting the transition between spray and bubbly (mixed) regime based on the idea of minimum entrainment. This also agrees with the findings of Payne and Prince (1977). Since entrainment is one of the tray capacity limits, this is found to be a practical interpretation.

2.1.9 Kister *et al.* (1981) – Entrainment from sieve trays operating in the spray regime.

Kister *et al.* (1981) found that until 1981 most of the correlations predicting entrainment were developed using data from small scale laboratory units (Hunt *et al.* (1955), Fair (1961) and Smith and Fair (1963)) which operated in the froth regime and gave poor predictions for entrainment in larger scale columns operating in the spray regime. Kister *et al.* (1981)

therefore found a need to develop a correlation for entrainment in the spray regime. They applied froth to spray transition criteria (based on work done by Porter and Jenkins (1979)) on data taken from their laboratory together with published data from the literature to develop a data set which represents the spray regime; see Table 2.9 for more detail. The data are only for the air-water system since limited non air-water system data existed. Using the data set they investigated the effect of tray design parameters on entrainment in the spray regime and developed a correlation for predicting entrainment in the spray regime.

Kister *et al.* (1981) proposed that the mechanism for entrainment between the froth regime (liquid continuous) and the spray regime (vapour continuous) is significantly different and it is therefore unlikely that entrainment can be predicted with one correlation for both regimes. In the froth regime the majority of the sieve tray holes will be bubbling. The mechanism for entrainment in the froth regime is therefore the break-up of bubbles emerging from the liquid sheets but on the other hand the spray regime is characterised by the droplet formation of the liquid at the tray floor caused by the vapour jetting through the sieve tray holes.

Table 2.9 Range of data used for correlating by Kister *et al.* (1981).

Column Shape and Dimensions	Tray Spacing [m]	Superficial Gas Velocity [m/s]	Fractional Hole Area	Hole Diameter [mm]	Liquid Flow Rate [$m^3/(h.m)$]	Correlations/ Work Done	Systems Used
From various authors, no information provided on their experimental setup	0.305 – 0.914	1.27 – 3.2 (estimated from graphs)	0.05 – 0.161	3.175 – 25.4	4.2 – 19.0	1. (L'/G) Entrainment in spray regime	Air/Water

They found that the main factors affecting entrainment are the tray free area, hole diameter, weir height, tray spacing and liquid flow rate. At constant liquid load with changing superficial gas loading they found that entrainment increases with decreasing tray free area (fractional hole area), increases with increasing hole diameter, is not affected by weir height, increases with decreasing tray spacing and decreases with increasing liquid load.

The air-water data showed that entrainment in the spray regime depends on gas velocity, liquid loading, tray spacing and tray geometry. They also found that liquid hold-up plays a significant role predicting entrainment and though constant in the spray regime with

increasing gas flow rate, liquid hold-up strongly depends on tray hole diameter and tray free area. They found it convenient to express the parameters influencing entrainment in the following dimensionless groups representing the primary fluid mechanic phenomena on the tray:

1. A hole Weber to hole Reynolds number ratio, $\left(\frac{u_s \rho_L \mu_G}{\rho_G \sigma_L}\right)$
2. Dimensionless hole diameter to clear liquid height ratio, $\left(\frac{d_H}{h_L}\right)$
3. Dimensionless tray spacing to clear liquid height ratio, $\left(\frac{s}{h_L}\right)$
4. A dimensionless group they introduced which accounts for the effect of liquid cross flow, $\left(\frac{u_s{}^3 \rho_G}{\rho_L Q_L g}\right)$

Using these groups the correlation predicting the rate of entrainment is written as follows:

$$E \ \alpha \left(\frac{u_s{}^3 \rho_G}{\rho_L Q_L g}\right)^a \left(\frac{u_s \rho_L \mu_G}{\rho_G \sigma_L}\right)^b \left(\frac{d_H}{h_L}\right)^c \left(\frac{s}{h_L}\right)^e \qquad 2.18$$

Where *E* is the dimensionless rate of entrainment expressed as mass liquid entrained per mass of vapour. The values for the exponents *a, b, c* and *e* were evaluated from experimental entrainment data for the air-water system. None of the experimental data they used included tray liquid hold-up measurements and the liquid hold-up was therefore estimated from measurements at the froth to spray transition. They assumed that the liquid hold-up for a given tray in the spray regime will remain fairly constant with increasing gas flow rate. The data generated at the froth to spray regime transition was then used as an approximation to the liquid hold-up of trays operating in the spray regime.

They used the correlation of Jeronimo and Sawistowski (1973) for liquid hold-up at the froth to spray transition for the air-water system, as shown in Eq. 2.19, which correlates the data with an average error of 8%:

$$h_{L,t} = \frac{1.059 A_f{}^{-0.791} d_H{}^{0.833}}{1 + 0.013 Q_L{}^{-0.59} A_f{}^{-1.79}} \qquad 2.19$$

Using Eq. 2.19, with the measured entrainment rates from the experimental data, the values for the exponents in Eq. 2.18 are:

$$a = b = 1.17$$

$$c = e = -2.34$$

Eq. 2.18 can then be written as:

$$E \ \alpha \left(\frac{u_s{}^3 \rho_G}{\rho_L Q_L g} \right)^{1.17} \left(\frac{u_s \rho_L \mu_G}{\rho_G \sigma_L} \right)^{1.17} \left(\frac{h_L}{(d_H s)^{1/2}} \right)^{4.68} \qquad 2.20$$

Eq. 2.20 suggests that surface tension, gas viscosity and gas and liquid density are the fluid properties influencing entrainment in the spray regime. Liquid viscosity was not included based on results from single hole studies which showed no effect on entrainment for liquid viscosities in the range of 0.89 – 2.42 mPa.s. Unfortunately the proportional constant required to calculate the entrainment rate was not supplied, thus the equation can not be applied directly.

The assumption made by Kister *et al.* (1981) that the liquid hold-up in the spray regime is similar to that at the transition is not validated. The influence on viscosity was only tested over a very small range (0.89 – 2.42 mPa.s) and the true effect of viscosity on entrainment in the spray regime can therefore not be determined with confidence.

2.1.10 Colwell (1981) – Clear liquid height and froth density on sieve trays.

Colwell (1981) developed a correlation that predicts clear liquid height and froth density in the froth regime based on the Francis weir equation, Eq. 2.21, given by Bolles (1963):

$$h_L = h_{wo} + 6.65 \left(\frac{Q_L}{3.6} \right)^{2/3} \qquad 2.21$$

The Francis weir equation formed the basis for determining the clear liquid height in bubble cap trays under conditions where the liquid flows over the weir as a non-aerated liquid. In sieve trays however the liquid flows over the weir as froth and the Francis weir equation can not be used directly.

In order to use the Francis weir equation the flow over the weir has to be uniform per weir length, free flowing with no obstructions and a uniform froth existing as a continuous layer adjacent to the tray floor. In order to develop a clear liquid height correlation Colwell avoided data from the spray regime because of the non-uniform froth densities that exist. Only directly measured clear liquid height data from various sources and various systems (although mostly air/water) as shown in Table 2.10 were used.

Table 2.10 Range of data used for correlating by Colwell (1981).

Column Shape and Dimensions	Tray Spacing [m]	Gas velocity based on bubbling area [m/s]	Fractional Hole Area	Hole Diameter [mm]	Liquid Flow Rate [m^3/(h.m)]	Correlations/ Work Done	Systems Used
From various authors	unknown	0.24 – 3.54	0.0416 – 0.12	1.6 – 22	0.468 – 86.4	1. $h_{L,f}$, Clear liquid height in the froth regime 2. ε, froth density in froth regime	Mostly Air/Water Isopentane/n-pentane Air/Isopar-M Air/55 wt % Glycerol Steam/Water MEK/toluene

The methods for determining the clear liquid heights ranged from using manometers, bubblers and blocking and draining. The effect of momentum heads, calculated with Eq. 2.22, was added to the manometer readings if not done by the authors of the data.

$$h_M = \frac{1000\rho_g u_b^{\,2}}{\rho_l g}\left(\frac{1}{A_h / A_b} - 1\right) \qquad 2.22$$

After fitting of the data a new semi-empirical adaptation of the Francis weir equation for predicting clear liquid height, Eq. 2.23, was proposed.

$$h_{L,f} = \varepsilon h_w + 7.3\left(\frac{\varepsilon^{0.5} Q_L}{3.6 C_d}\right)^{2/3} \qquad 2.23$$

With C_d calculated as:

$$C_d = 0.61 + 0.08\frac{h_{ow}}{h_w} \text{ for } \frac{h_{ow}}{h_w} \le 8.135$$
$$C_d = 1.06\left(1 + \frac{h_w}{h_{ow}}\right)^{1.5} \text{ for } \frac{h_{ow}}{h_w} > 8.135 \qquad 2.24$$

where

$$h_{ow} = h_F - h_w \qquad 2.25$$

and

$$\varepsilon = \frac{h_{L,f}}{h_F} = \frac{1}{\eta + 1} \qquad 2.26$$

with

$$\eta = 12.6 Fr^{0.4}\left(\frac{A_h}{A_b}\right)^{-0.25} \qquad 2.27$$

The Froude number is an indication of the kinetic energy of the vapour compared to the potential energy of the liquid hold-up:

$$Fr = \frac{\rho_g u_b^{\ 2}}{g\left(\frac{h_{L,f}}{1000}\right)\left(\rho_L - \rho_g\right)} \qquad 2.28$$

Colwell (1981) suggests the following trial and error procedure to determine the clear liquid height in the froth regime in Eq. 2.23:

1. Assume an initial $h_{L,f}$ of 50mm;
2. Calculate the Froude number with Eq. 2.28 followed by η using Eq. 2.26. Use the calculated η value to calculate ε using Eq. 2.26;
3. Calculate C_d (Eq. 2.24) by calculating h_F using Eq. 2.26 and h_{ow} using Eq. 2.25;
4. Calculate the h_{Lf} using Eq. 2.23;
5. Repeat steps 2 – 4 until the clear liquid height (h_{Lf}) value converges.

According to Colwell (1981) froth densities can be calculated with ±8% accuracy and clear liquid heights with ±7% accuracy. Colwell did not mention the definition used to categorise the data used to develop his correlation between froth and spray regime. No definition is given for the froth regime so it is unclear to what extent the correlation is applicable. Kister and Haas (1988) used the correlations developed by Colwell (1981) to calculate clear liquid height and froth height for entrainment databases lacking clear liquid height and froth height data. Bennett *et al.* (1995) also developed froth height and froth density correlations for both the froth and spray regimes. They did however not compare their results with those of Colwell (1981).

2.1.11 Zuiderweg (1982) – Sieve Trays: A view on the state of the art

Zuiderweg (1982) compared the results from the theoretical and experimental model studies of Hofhuis and Zuiderweg (1979) with commercial data from Sakata and Yanagi (1979, 1982). The data for liquid hold-up and entrainment fitted the respective correlations well within the comparison range. Performance correlations were also developed with the aim of implementation in practise.

Zuiderweg (1982) used a correlation developed by Hofhuis (1980) that defines the transition into the emulsion regime as a ratio of the horizontal liquid momentum flow and the vertical vapour momentum flow:

$$\frac{u_l}{u_b}\left(\frac{\rho_l}{\rho_g}\right)^{0.5} = \frac{FP}{bh_L} > 3 \qquad 2.29$$

According to Zuiderweg (1982) the transition range between the spray and emulsion regimes is called the “mixed regime” or “froth regime”. The free bubbling regime, characterized by bubble formation at the sieve plate orifices, occurs close to the weeping limit at relatively low liquid flow rates and is of little significance for commercial trays.

The froth density was determined with the gamma ray absorption technique using the data from Hofhuis and Zuiderweg (1979). From the two phase (froth) density profiles the bed height, liquid hold-up and therefore the average two phase density was determined. The two phase density was found to be a function of the tray Froude number:

$$\frac{1}{\varepsilon} = c_1\left[\frac{u_b}{\left(gH_L\right)^{0.5}}\left(\frac{\rho_g}{\rho_l}\right)^{0.5}\right]^n$$

$$\text{for spray regime: } c_1 = 265, n = 1.7$$

$$\text{mixed/emulsion: } c_1 = 40, n = 0.8 \qquad 2.30$$

with the liquid hold-up calculated using an equation developed by Hofhuis (1980):

$$H_L = 0.6 H_w{}^{0.5} P^{0.25}\left(\frac{FP}{B}\right)^{0.25} \qquad 2.31$$

According to Zuiderweg (1982) heavy entrainment occurs only in the spray regime where the ratio between the froth bed height and tray spacing are the main variables responsible for entrainment. The probability that the liquid reaches the tray above depends on the settling characteristics of the droplets. This can be predicted by the ratio of the superficial liquid velocity to the hole vapour velocity. Eq. 2.32 was proposed to predict the fraction of liquid entrained on the net liquid down flow in the spray regime.

$$\frac{L'}{L} = 1.0 \times 10^{-8} \left(\frac{H_b}{S} \right)^3 \left(\frac{u_h}{u_l} \right)^2 \qquad 2.32$$

Sieve tray flooding is one of the capacity limits of the column and occurs in the spray regime when the bed height is equal to the tray spacing.

$$S = H_b = \frac{H_L}{\varepsilon} \qquad 2.33$$

Or when

$$C_{b,\max} = u_b \sqrt{\frac{\rho_g}{\rho_l - \rho_g}} = 0.037 g^{0.5} \frac{\left(S - H_L\right)^{0.59}}{H_L^{0.09}} \qquad 2.34$$

Zuiderweg (1982) also presented a tray pressure drop correlation, Eq. 2.35. The total pressure drop is calculated as the sum of the dry tray pressure drop (Eq. 2.36) and the hydrostatic pressure caused by the clear liquid height.

$$\Delta P = \Delta P_{dr} + \rho_l g H_L \qquad 2.35$$

with

$$\Delta P_{dr} = \frac{\rho_g}{2} \left(\frac{u_h}{C_D} \right)^2 \qquad 2.36$$

and

$$C_D = 0.7 \left[1 - 0.14 \left(\frac{g h_L \rho_l}{u_h^{\,2} \rho_g} \right)^{2/3} \right] \qquad 2.37$$

Zuiderweg (1982) proposed correlations predicting the operating flow regime (Eq. 2.29), entrainment in the spray regime (Eq. 2.32), clear liquid height (Eq. 2.31), froth density (Eq. 2.30), froth height (Eq. 2.33), spray regime flooding capacity (Eq. 2.34) and tray pressure

drop (Eq. 2.35). According to the specific correlations only gas and liquid density is used to represent system physical properties. According to Sakata and Yanagi (1979) and Porter and Jenkins (1979) entrainment flooding occurs in the froth (bubbly) regime as well. The correlation predicting entrainment developed by Zuiderweg (1982) is limited to the spray regime only and a different correlation should be used for entrainment in the froth (emulsion) regime.

2.1.12 Kister and Haas (1988) – Entrainment from sieve trays in the froth regime.

According to Kister and Haas (1988) entrainment in the froth regime was poorly understood. They therefore used published entrainment data for the air/water system and columns with tray spacing exceeding 300mm to investigate the effects of tray geometry as well as air and water flow rates on entrainment in the froth regime. In the froth regime bubbling occurs at most of the sieve tray holes and entrainment is caused by sheets of liquid that break due to the emerging bubbles. This causes small drops to form with low projection velocities resulting in low entrainment. The froth regime is encountered in columns operating above atmospheric pressure and high liquid flow rates. Since they only used air/water data to develop their entrainment prediction correlations, Kister and Haas (1988) did not mention the effect of gas and liquid physical properties on the froth regime. Kister and Haas (1988) measured entrainment as the amount of liquid entrained per mass of rising gas.

Kister and Haas (1988) also developed a correlation for predicting entrainment when weeping and entrainment occurs simultaneously. The correlation previously developed by Kister *et al.* (1981) to predict entrainment in the spray regime is presented in Eq. 2.43, with the proportional constant which was previously omitted in the publication of Kister *et al.* (1981)

In the froth regime Kister and Haas (1988) found that:

1. At low and moderate liquid rates an increase in hole diameter will result in an increase in entrainment.

2. The effect of tray spacing on entrainment was found to be inversely proportional to a power of between 2 and 3.

3. Fractional hole area (hole area divided by bubbling area) has no significant effect on entrainment in the froth regime.

4. Increasing the weir height reduces entrainment at low liquid rates, < 25 m^3/(h.m). At high liquid flow rates, > 25 m^3/(h.m), and high gas rates, > 1.15 m/s, weir height has

no effect on entrainment. At low, < 1.15 m/s, gas rates and high liquid rates, > 25 m^3/(h.m) entrainment will be increased with increasing weir height.

5. Entrainment generally increases with increasing liquid rate except with low fractional hole area (<0.06) and or large hole diameter (>19mm) where liquid flow rate has a small effect on entrainment.

6. Increasing the gas velocity will always increase the amount of entrainment, however, the rate at which entrainment increases with gas velocity varies.

Most of the correlations predicting entrainment in the froth regime, developed prior to the work of Kister and Haas (1988), were developed from small diameter columns (150mm), columns with no liquid cross flow and a relatively small data bank. Large differences were observed between the data and correlation predictive trends at low liquid rates (<10m^3/(hm)), large hole diameters (>12.7mm), small fractional hole areas (<0.07) and trays without weirs. They therefore went about developing a new correlation.

Kister and Haas (1988) based their correlation on that of Hunt *et al.* (1955), Eq. 2.2, simulating the hydraulic conditions above the tray with no liquid cross flow. After refitting the correlation of Hunt *et al.* (1955), Eq. 2.2, and empirically adding a hole diameter dependence and correction term for non-uniformity at low clear liquid heights, Eq. 2.38 was developed.

$$E_f = 111\left(\frac{u_b}{s - h_F}\right)^2 d_H{}^{0.5}\left(1+\zeta\right) \qquad 2.38$$

The froth height is calculated using the correlation provided by Colwell (1981), Eq. 2.26. The correction terms is calculated with Eq. 2.39:

$$\zeta = \frac{0.00225}{A_f{}^3}\left(\frac{h_{L,t}}{h_L} - 1\right) \quad \text{for } h_{L,t} > h_L$$
$$\zeta = 0 \quad \text{for } h_{L,t} \le h_L \qquad 2.39$$

The clear liquid height at the froth to spray transition for the air/water system is calculated from a correlation, Eq. 2.40, developed by Jeronimo and Sawistowski (1973):

$$h_{L,t} = \frac{0.4974 A_f^{-0.791} d_H^{0.833}}{1 + 0.013 L^{-0.59} A_f^{-1.79}} \qquad 2.40$$

Very low gas velocities, high weirs, large hole diameters and large fractional hole areas generally causes weeping to take place. For entrainment in this region Eq. 2.41 was empirically developed from the data:

$$E_w = \frac{0.3 d_H p^2}{h_L \left(s - h_F\right)^2} \qquad 2.41$$

With the hole pitch calculated as:

$$p = 0.951 \frac{d_H}{A_f^{0.5}} \qquad 2.42$$

The spray regime entrainment correlation previously proposed by Kister *et al.* (1981) is given in Eq. 2.43:

$$E_s = 4.742^{(10/\sqrt{\sigma})^{1.64}} \left[872 \left(\frac{u_b h_{L,ct}}{\sqrt{d_H S}} \right)^4 \left(\frac{\rho_g}{Q_L \rho_l} \right) \left(\frac{\rho_l - \rho_g}{\sigma} \right)^{0.25} \right]^{\left(10/\sqrt{\sigma}\right)} \qquad 2.43$$

With

$$h_{L,ct} = \frac{h_{L,t}}{1 + 0.00262 h_w} \left(\frac{996}{\rho_l} \right)^{0.5\left(1 - 0.00091 d_H / A_f\right)} \qquad 2.44$$

Kister and Haas (1988) did not propose a regime defining correlation. The correlation (Eq. 2.38, 2.41 and 2.43) which gives the largest amount of entrainment represents the flow regime on the tray and should be used to predict entrainment. The application range of the correlations for the air/water system at atmospheric pressures on sieve trays is shown in Table 2.11:

Table 2.11 Recommended range of application for Eq. 2.38, 2.41 and 2.43.

Variable	Description	Minimum Value	Maximum Value
u_b [m/s]	Bubbling velocity	0.3	3.5
Q_L [m^3/(hm)]	Liquid flow per weir length	2	130
s [mm]	Tray spacing	300	1000
d_H [mm]	Hole diameter	1.5	25
A_f [-]	Fractional hole area	0.04	0.2
h_w [mm]	Weir height	0	80

Kister and Haas (1988) proposed that entrainment in the froth regime is caused by ascending bubbles, breaking up liquid sheets at the surface of the froth and not at the tray floor. Therefore tray geometry (hole diameter, fractional hole area and weir height) only has a small effect on entrainment. As the gas velocity is increased jetting starts to occur at the holes until jetting replaces bubbling as the mechanism for entrainment and the spray regime is entered resulting in entrainment to be described by Eq. 2.43. Tray geometry (hole diameter, fractional hole area and weir height) and low liquid rates play a significant role the spray regime.

Kister *et al.* (1981) suggests that weir height does not have a significant influence on entrainment in the fully developed spray regime. Kister and Haas (1988) did, however, show that weir height could have an influence on entrainment in the froth regime. The correlation developed by Kister and Haas (1988) to predict entrainment in the froth regime for air/water systems gave a much better fit to the data than the correlation proposed by Hunt *et al.* (1955). It is unclear how Kister and Haas (1988) classified the data used in developing their correlation as spray regime or froth regime data. The proposed correlations are limited to the air/water system.

2.1.13 Kister and Haas (1990) – Predict entrainment flooding on sieve and valve trays

Since the capacity of sieve trays are limited by the onset of entrainment flooding, Kister and Haas (1990) developed a correlation that predicts the flood point caused by entrainment.

They also wanted to predict the influence of gas and liquid physical properties, operating conditions and tray geometry on the flood point.

According to Kister and Haas (1990) most commercial tray spacings are between 380 and 457mm where the froth surface is seldom within reach of the tray above when operating in the froth regime. Kister and Haas (1990) therefore stated that the mechanism for entrainment flooding is related to spray regime entrainment. Flooding is expressed in terms of the Souders and Brown constant or more commonly known as the flooding C-factor. At incipient flooding the force of the rising gas equals the gravity force on a liquid droplet causing the droplet to stay suspended between the trays. The flooding C-factor is defined in Eq. 2.45:

$$C_f = u_{s,\,flood}\sqrt{\frac{\rho_g}{\rho_l - \rho_g}} \qquad 2.45$$

Using the Froude number, Bond number and the gas-to-liquid velocity ratio as dimensionless groups, Kister and Haas (1990) developed a correlation for the flooding C-factor that includes the effects of gas and liquid physical properties:

$$C_f = 0.0277\left(\frac{{d_H}^2\sigma}{\rho_l}\right)^{0.125}\left(\frac{\rho_g}{\rho_l}\right)^{0.1}\left(\frac{S}{h_{L,t}}\right)^{0.5} \qquad 2.46$$

With the clear liquid height at the froth to spray transition calculated as:

$$h_{L,t} = \left(\frac{0.4974 {A_f}^{-0.791} {d_H}^{0.833}}{1 + 0.013 L^{-0.59} {A_f}^{-1.79}}\right)\left(\frac{996}{\rho_l}\right)^{0.5\left(1-0.00091 d_H / A_f\right)} \qquad 2.47$$

For surface tensions exceeding 25 mN.m Kister and Haas (1990) recommends using a surface tension of 25 mN.m. They found in previous studies (Kister and Haas (1987) that entrainment becomes insensitive to surface tension for values greater than 25 mN.m. The data used to fit correlation, Eq. 2.46, was obtained from different authors representing different column geometries and gas-liquid systems. According to Kister and Haas (1990), Eq. 2.46 fits most of the sieve tray data with ±15% accuracy.

The application range of Eq. 2.46 for sieve trays is shown in Table 2.12:

Table 2.12 Recommended range of application for Eq. 2.46.

Variable	Description	Minimum Value	Maximum Value
u_s [m/s]	Superficial velocity	0.5	4
Q_L [m^3/(hm)]	Liquid flow per weir length	5	110
s [mm]	Tray spacing	350	900
d_H [mm]	Hole diameter	3	25
A_f [-]	Fractional hole area	0.06	0.2
h_w [mm]	Weir height	0	80
σ [mN/m]	Surface Tension	5	80
ρ_L [kg/m3]	Liquid density	300	1200
ρ_g [kg/m3]	Gas/vapour density	0.5	180
μ [mPa.s]	Liquid viscosity	0.05	2

The data used by Kister and Haas (1990) was obtained from various sources, systems and column geometries. The advantage of this is that a broad range of systems and column geometries were covered. The disadvantage is that the errors caused using data obtained from different system parameters, column geometries and sampling methods can not be accounted for. The criteria on which the data was selected to develop there correlation is not clear. According to Kister and Haas (1990) the mechanism of entrainment flooding relates to entrainment in the spray regime yet no correlation was given to identify this regime. Kister and Haas (1990) also did not relate the flooding factor to entrainment. It is therefore unclear how flooding relates to the entrainment rate.

2.1.14 Bennett *et al.* (1995) – A mechanistic analysis of sieve tray froth height and entrainment

Bennett *et al.* (1995) developed a model to predict the sieve tray froth height and entrainment. They compiled a data base which included data from Lockett *et al.* (1976), Thomas and Ogboja (1978), Sakata and Yanagi (1979), and Nutter (1979). Table 2.13 summarises the flow, column and tray geometry, and system property ranges for the air/water and non-air/water data.

Table 2.13 Data used by Bennett *et al.* (1995).

Variable	Description	Minimum Value	Maximum Value
u_s [m/s]	Superficial velocity	0.45	2.41
Q_L [m^3/(hm)]	Liquid flow per weir length	4.18	134.28
s [mm]	Tray spacing	152	914
d_H [mm]	Hole diameter	1.59	25.4
A_f [-]	Fractional hole area	0.059	0.124
h_w [mm]	Weir height	0	76.2
σ [mN.s]	Surface Tension	5	73.5
ρ_L [kg/m3]	Liquid density	493	1000
ρ_g [kg/m3]	Gas/vapour density	1.13	28

Bennett *et al.* (1995) used the correlation, Eq. 2.48, proposed by Pinczewski and Fell (1982) to classify the data as either spray regime or froth regime related. Pinczewski and Fell (1982) used data from Porter and Wong (1969), Hofhuis and Zuiderweg (1979), and Sakata and Yanagi (1979) to predict the froth to spray transition on sieve trays using gas and liquid flow rates, tray geometry and system physical properties. The advantage of their correlation, Eq. 2.48, is that the liquid hold-up is not required to determine the transition. Bennett *et al.* classified the data in their data bank for $\psi > 1$ as froth like regime data:

$$\psi = \frac{2.75\left(q_L\sqrt{\rho_L}\right)^{0.91D_H/A_f}}{u_s\sqrt{\rho_g}} \qquad 2.48$$

Bennett *et al.* (1995) defined the froth as consisting of a liquid-continuous and vapour-continuous region. In the liquid-continuous region vapour is distributed as bubbles in the liquid layer and as the bubbles break at the liquid layer surface, droplets are formed which is then ejected into the vapour-continuous region. The froth height is defined as the maximum height a droplet ejected from the liquid-continuous region will reach. The height the liquid droplets ejected from the liquid-continuous region will reach is influenced by a force balance between the droplet momentum, gravity and droplet drag. Bennett *et al.* (1995) showed that droplet drag is significant at high superficial vapour velocities and Froude and Weber numbers are used to determine the extent of the drag contribution.

Bennett *et al.* however decided to use a no-drag solution to determine the froth height and entrainment correlations. For systems other than air and water where surface tension may have an influence, Figure 2.7, is needed to correct the predicted froth height.

When the superficial gas velocity exceeds the droplet ejection velocity (see Figure 2.7 (a) and (b)) vapour drag will transport liquid droplets higher than when there was no drag contribution, resulting in more entrainment than predicted. It is therefore evident that contribution of vapour drag is most significant at high gas velocities. The effect of vapour drag on the projected droplet is less when the vapour superficial velocity is close to the droplet ejection velocity as shown in Figure 2.7 (c) and (d). In the case where the gas superficial velocity is lower than the droplet ecjection velocity, as shown in Figure 2.7 (e) and (f) the vapour space above the froth will slow the projected droplet down and the maximum height the droplet will reach is lower than predicted, resulting in less entrainment than predicted. The magnitude of the drag contribution is determined by the Froude and Weber numbers.

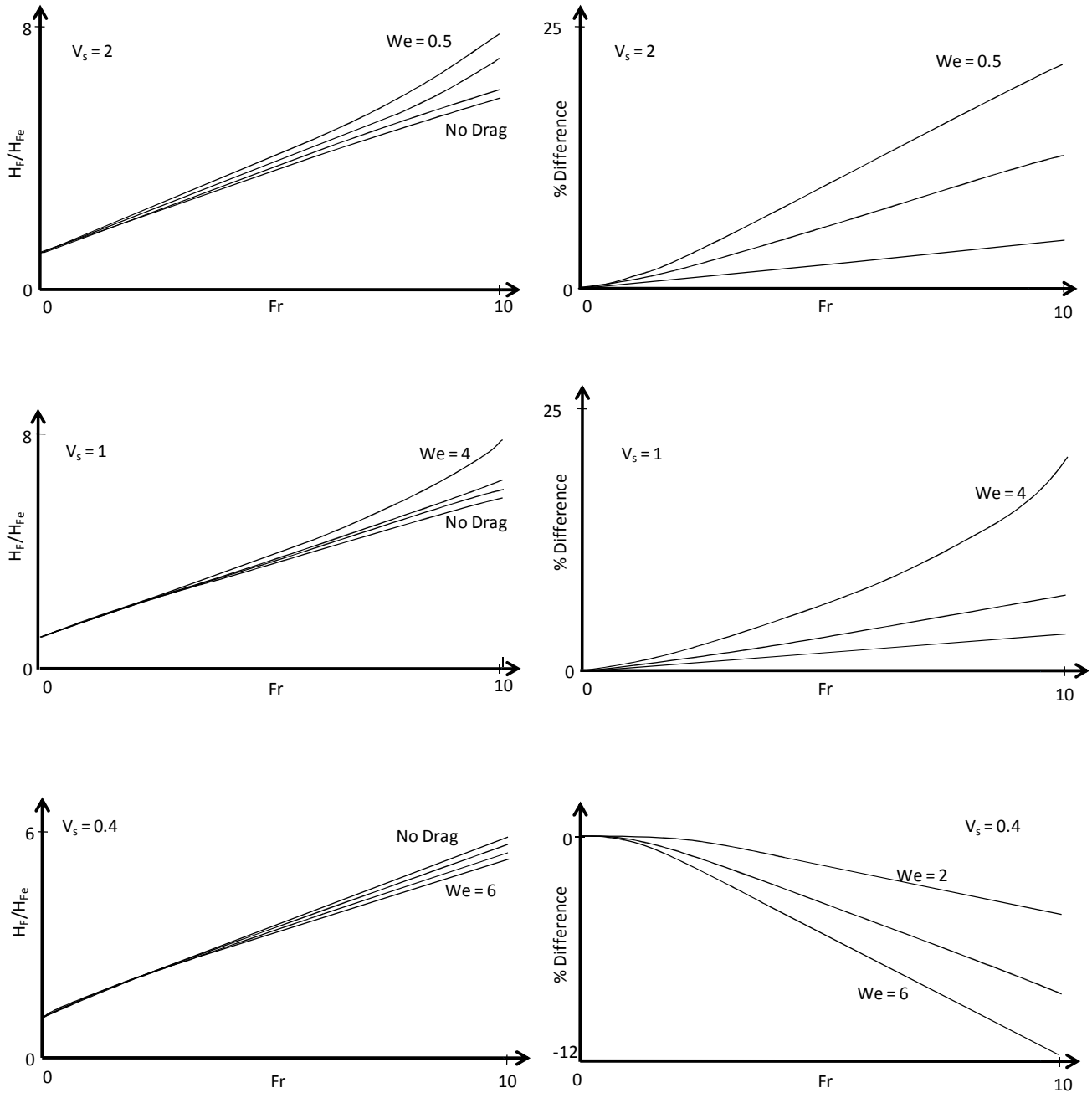

Figure 2.7 Difference in froth height between the solution which accounts for droplet drag and no drag assumption by Bennett *et al.*, based on the Froude and Weber numbers, and the $V_s = u_D/u_{D0}$ ratio redrawn from Fig. 1 in Bennett *et al.* (1995).

Using the gamma ray data from Hofhuis and Zuiderweg (1979), Bennett *et al.* (1995) developed a new correlation, Eq. 2.49, to predict the froth height in the froth regime:

$$\frac{H_f}{H_{Fe}} = 1 + \left(1 + 6.9\left(\frac{H_L}{D_H}\right)^{-1.85}\right)\frac{Fr}{2} \qquad 2.49$$

On average Eq. 2.49 under estimates the froth height by less than 1cm. With the effective froth height calculated as:

$$H_{Fe} = H_w + C\left(\frac{q_L}{\phi_e}\right)^{2/3} \quad 2.50$$

$$C = 0.501 + 0.439\exp[-137.8H_w] \quad 2.51$$

$$\phi_e = \exp[-12.55K_s^{0.91}] \quad 2.52$$

$$K_s = u_s\sqrt{\frac{\rho_g}{\rho_l}} \quad 2.53$$

The Froude number is a function of the droplet ejection velocity, the gravitational constant and the effective froth height:

$$Fr = \frac{u_{D0}^2}{gH_{Fe}} \quad 2.54$$

$$u_{D0} = 3K_s\sqrt{\frac{\sqrt{3}}{A_f\phi_e}} \quad 2.55$$

The clear liquid height is the product of the effective froth density times the effective froth height:

$$H_L = \phi_e H_{Fe} \quad 2.56$$

Entrainment is defined as the mass flux of entrained liquid over the mass flux of vapour approaching the tray deck. Using the Pinczewski and Fell (1982) correlation for the froth to spray transition, Bennett *et al.* (1995) proposed the following correlation for predicting entrainment in the froth regime for the air/water system:

$$E_f = 0.00164\left(\frac{K_s^2}{g\phi_e S}\right)^{1.86}\left[\frac{gH_L}{K_s^2}+\frac{9\sqrt{3}}{2A_f}\left(1+6.9\left\{\frac{D_H}{H_L}\right\}^{1.85}\right)\right]^{1.86}\left(\frac{\rho_L}{\rho_g}\right)^{0.5} \quad 2.57$$

At low liquid rates and high vapour velocities entrainment will increase with increasing hole diameter or decreasing fractional hole area. Entrainment is found to be inversely proportional to the tray spacing to the power of 1.86 compared to the suggested power of 2-3 by Kister and Haas (1988). The effect of vapour velocity on entrainment depends on the $\frac{gH_L}{K_s^2}$ ratio. For low liquid rates and high vapour rates this functionality is less important and entrainment depends on K_s to a power of 5. As $\frac{gH_L}{K_s^2}$ increases to around 100, entrainment depends on K_s to a power of 3.

Again using the criteria of Pinczewski and Fell (1982), air/water data in the spray regime was selected to develop the following entrainment prediction correlation for the air/water system in the spray regime:

$$E_s = 0.0050\left(\frac{K_s^2}{g\phi_e S}\right)^{1.26}\left[\frac{gH_L}{K_s^2}+\frac{9\sqrt{3}}{2A_f}\left(1+4.77\left\{\frac{D_H}{H_L}\right\}^{3.29}\right)\right]^{1.26}\varepsilon^{\beta}\left(\frac{\rho_L}{\rho_g}\right)^{0.5} \quad 2.58$$

With

$$\varepsilon = \frac{H_L}{H_F} \quad 2.59$$

and

$$\beta = 0.5\left(1-\tanh\left[1.3\ln\left(\frac{H_L}{D_H}\right)-0.15\right]\right) \quad 2.60$$

The froth height in the spray regime is correlated by Eq. 2.61:

$$\frac{H_F}{H_{Fe}} = 1 + \left(1 + 4.77\left\{\frac{D_H}{H_L}\right\}^{-3.29}\right)\frac{Fr}{2} \qquad 2.61$$

Bennett *et al.* (1995) found that the main difference between entrainment in the froth and spray regimes is the dependence of entrainment on the average froth density. In the spray regime entrainment is approximately proportional to the average froth density whereas entrainment in the froth regime has little dependency on the average froth density. Entrainment is dependent on hole diameter in the spray regime and independent of hole diameter in the froth regime when $H_L/D_H > 10$.

Bennett *et al.* (1995) stated that the specific flow regime (froth or spray) is characterised by the dependency of the average froth density on entrainment. The clear liquid height to hole diameter ratio is used to determine the flow regime.

$$\begin{aligned} \frac{H_L}{D_H} &< 1 \text{ Spraylike} \\ 1 < \frac{H_L}{D_H} &< 2 \text{ Transition} \\ \frac{H_L}{D_H} &> 2 \text{ frothlike} \end{aligned} \qquad 2.62$$

Using data from cyclohexane/n-heptane, isobutane/n-butane and air/Isopar-M oil systems Bennett *et al.* (1995) developed entrainment prediction correlations for the froth and spray regimes for non-air/water (naw) systems:

$$E_{f,NAW} = 0.742\left(\frac{K_s^2}{g\phi_e S}\right)^{2.77}\left(\frac{gH_L}{K_s^2}\right)^{1.81}\left(\frac{\rho_L}{\rho_g}\right)^{1.19} \qquad 2.63$$

$$E_{s,NAW} = 8\times10^{-18}\left(\frac{K_s^2}{g\phi_e S}\right)^{1.56}\left[\frac{gH_L}{K_s^2} + \frac{2.48}{A_f}\left(1 + 8.27\left\{\frac{D_H}{H_L}\right\}^{-0.614}\right)\right]^{7.4}\varepsilon^{\beta}\left(\frac{\rho_L}{\rho_g}\right)^{1.08} \qquad 2.64$$

Table 2.14 summarises the system parameter range used by Bennett *et al.* (1995):

Table 2.14 System parameter range used by Bennett *et al.* (1995).

Parameter	Minimum (Air/water)	Maximum (Air/water)	Minimum (Non-Air/water)	Maximum (Non-Air/water)
K_s [m/s]	0.0158	0.081	0.017	0.122
ϕ_e	0.28	0.75	0.158	0.737
H_{Fe} [m]	0.0169	0.145	0.052	0.162
H_L [m]	0.0073	0.0481	0.017	0.064
Fr	0.134	9.29	0.084	12.3
We	0.015	1.81	0.196	1.535
u_D/u_{D0}	1.029	1.941	0.122	1.714

Bennett *et al.* (1995) developed different entrainment prediction correlations for air/water and non-air/water systems based on data obtained from various sources. The disadvantage of this is that the errors caused by using data obtained from different system parameters, column geometries and sampling methods can not be accounted for. They found that the flow regime is dependant on the average froth density and is characterised by the clear liquid height to hole diameter ratio. From their work it is evident that droplet drag has a significant influence on the average froth height and entrainment for high superficial vapour velocities and low surface tension liquids. In their work they focussed mainly on the air/water system and low (2.31 m/s) superficial vapour velocities. Industrial sieve tray columns can operate at higher superficial velocities (3 – 4.5 m/s) during allowable flooding conditions (when through put is more important than mass transfer efficiency). It is of significant importance to understand the hydrodynamic behaviour under flooding conditions so that the effect of entrainment on the mass transfer efficiency can be determined and the appropriate action taken to reduce entrainment if necessary.

2.1.15 Jaćimović and Genić (2000) – Froth porosity and clear liquid height in trayed columns

Jaćimović and Genić (2000) questioned the accuracy of the correlations in literature and decided to develop new correlations for froth porosity and clear liquid height for bubble cap, sieve and valve trays based on air/water data from their experimental runs.

A 314mm diameter glass column was used for their air/water runs with more detail in Table 2.15 below:

Table 2.15 Range of data used for correlating by Jaćimović and Genić (2000).

Column Shape and Dimensions	Tray Spacing [m]	Superficial Gas Velocity [m/s]	Fractional Hole Area	Hole Diameter [mm]	Liquid Flow Rate [$m^3/(h.m)$]	Correlations/ Work Done	Systems Used
314mm Round	0.4	0.2 – 1.9	unknown	6	2 – 19.8	1. ε, froth porosity 2. H_L, clear liquid height	Air/Water

They found that the froth porosity for all three tray types and the air/water system can be correlated with a standard deviation of 16.0% by:

$$\varepsilon = \frac{\sqrt{Fr}}{1+\sqrt{Fr}} \qquad 2.65$$

with the Froude number as a function of the superficial gas velocity based on column area:

$$Fr = \frac{u_c^2}{gH_L} \qquad 2.66$$

From the clear liquid height data obtained in their column for the three tray types, they suggested the following correlation which fitted their data with a standard deviation of 22.5%:

$$H_L = (0.04 + 0.9H_w)\frac{V_l}{V_g}\sqrt{\frac{\rho_l}{\rho_g}} \qquad 2.67$$

Since they only tested with an air water system and for limited column geometry Jaćimović and Genić (2000) suggested that the constants (0.04 and 0.9) in Eq. 2.67 should be investigated for systems other than air/water and different column geometries. Colwell (1981) showed that froth porosity (density) and clear liquid height is a function of both the weir height and the fractional hole area. Since the correlations (Eq. 2.65 and 2.67) proposed only consider weir height as the column geometrical dependant variable, the applicability of their correlations for a range of tray and column geometries needs to be investigated.

2.1.16 Van Sinderen *et al.* (2003) – Entrainment and maximum vapour flow rate of trays.

Van Sinderen *et al.* (2003) found that the behaviour of the gas-liquid mixture on trays, despite all the research done before 2003, is not fully understood. They conducted entrainment tests in a 0.2 x 0.2m square column with a changeable weir height (0 – 0.3m) and splash baffle placed above the weir. In their tests they used sieve, fixed valve and valve trays. The liquid flow rate stayed fixed at 5.04 m^3/(h.m) and three gas velocities (ranging from 1 – 2 m/s, based on column area). They only used one tray and the effect of entrainment from a "bottom" tray is therefore not accounted for. Their entrainment measurements were limited to a maximum of 4.8% (entrained liquid per liquid exiting the downcomer) for the given flow rate. A summary of the test ranges used by Van Sinderen *et al.* is shown in Table 2.16 below:

Table 2.16 Range of data used for correlating by Van Sinderen *et al.* (2003).

Column Shape and Dimensions	Tray Spacing [m]	Superficial Gas Velocity [m/s]	Fractional Hole Area	Hole Diameter [mm]	Liquid Flow Rate [$m^3/(h.m)$]	Correlations/ Work Done	Systems Used
0.2 x 0.2m Square	`0.25 – 0.45 this refers to collection tray	1 – 2	0.06 & 0.076	6 & 12	fixed at 5.04	1. H_L, clear liquid height	Air/Water Compared Data with that of Sakata and Yanagi (1979)

Van Sinderen *et al.* (2003) used an inclined mesh pad (see Figure 2.8) with a rectangular discharge cutter to capture and measure the entrained liquid. They found that the position of the mesh pad above the tray greatly contributes to the amount of entrainment collected. Since their inclined mesh pad is not parallel with the test tray and the froth layer above the tray, the representativeness of their entrainment measurements are therefore questioned. This also differs from commercial tray columns where the trays are placed parallel above each other. When they compared their data with those of Sakata and Yanagi (1979, 1982) they found some discrepancies which they suggest is due to the difference in column scale. The more logic suggestion would be to investigate the influence of their entrainment collection system.

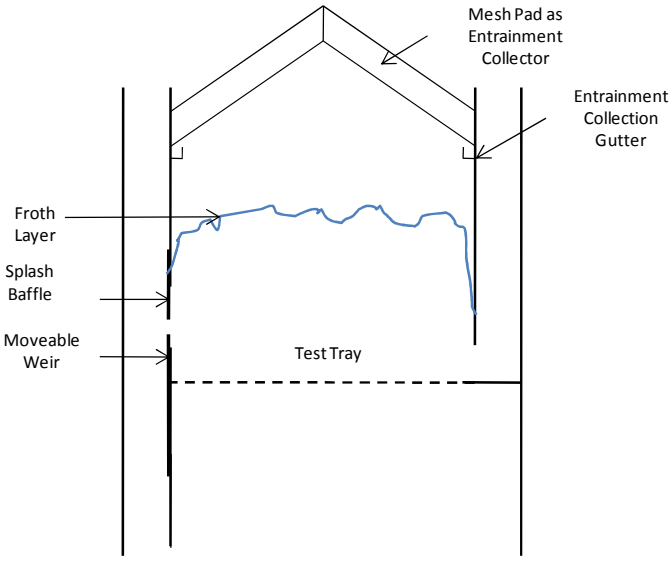

Figure 2.8 Section view of the experimental setup used by Sinderen *et al.* (2003).

The structure of the froth was redefined in terms of three layers, a bottom layer, middle layer and a top layer. In the *bottom layer* bubbles or jets are formed at the holes in the tray which in turn determines the size of the bubbles or jets. The velocity used to characterise the bottom layer is the hole gas velocity. The *middle layer* is formed by erupting bubbles which create droplets that are projected into the top layer. The velocity of rising bubbles characterise this layer and was found to be between 0.3 – 1m/s. In the *top layer* drops are found. These drops reached vertical heights of 0.05 – 0.5m with horizontal distances, caused by liquid horizontal momentum, ranging between 0.1 – 0.3m. They found the velocity of the ejecting droplets to be between 1 and 2m/s.

Not all three layers were always found to be present. They defined two regimes, namely, the low-liquid-height and the high-liquid-height regimes. In the low-liquid-height regime the middle layer is absent and was found at low weir heights. By increasing the weir height and therefore increasing the clear liquid height (liquid hold-up) they found the amount of liquid entrained into the vapour space above the tray to decrease. In this regime entrainment depended on tray geometry and tray type. As the liquid height is increased further a transition was found as the middle layer began to form. At the transition the amount of liquid entrained into the vapour space was found to be a minimum. By further increasing the liquid height the amount of liquid entrained will increase and entrainment is independent of tray geometry and tray type. This is not in agreement with the findings of Hunt *et al.* (1955), Kister and Haas (1988) and Bennett *et al.* (1995) who found entrainment to be dependent on column and tray geometry in both the froth and spray regimes. Even though Van Sinderen *et al.* (2003) do not relate their low – and – high-liquid-height regimes to the "commonly" known froth and spray regimes, the test ranges used correspond to those of the previously mentioned authors except at weir heights exceeding 76mm (which is supposedly high enough for the high-liquid-height regime to exist).

Van Sinderen *et al.* proposed the following entrainment prediction correlation for the high-liquid-height regime and all three tray types:

$$\frac{L'}{\rho_l A_p} = 0.029\left(\pm 0.01\right)\exp\left[-4.38\left(\sqrt{2g\left(S - 0.7H_W + \frac{130C_p^2}{g}\right)} - 17C_p\right)\right] \qquad 2.68$$

Their definition for both the low – and – high-liquid-layer regimes are the same ($H_L<H_{L,tr}$), defined as the condition where the clear liquid height is smaller than the clear liquid height at the regime transition. This is confusing and it is assumed, based on their description of the regimes, that this is a type error and that the high-liquid-height layer is found where $H_L>H_{L,tr}$. In order to calculate both the clear liquid height and the clear liquid height at the regime transition the gas fraction of bubbles in the liquid layer and liquid volume fraction in

the plane of droplet origin is required. They did not specify how these parameters are calculated from known system parameters like tray geometry and gas and liquid flow rates.

Based on the work done by Van Sinderen *et al.* (2003) the influence of the liquid flow rate on entrainment and the froth behaviour is questioned. They mention that both the weir height and the liquid flow rate will increase the liquid hold-up which is responsible for the different regimes and the rate of entrainment. However, the while the liquid flow rate increases both the liquid hold-up and the liquid horizontal momentum increases. It is the effect of liquid momentum on froth behaviour and entrainment that needs to be investigated so that both effects can be determined and accounted for in correlating the data. Since they only used an air/water system during their tests the influence of gas and liquid physical properties was not investigated.

2.2 Critical evaluation

In the literature review it was found that the mechanisms and the extent to which they affect entrainment differ between the froth and spray regimes. All the latest regime (layers in the case of Van Sinderen *et al.* (2003)) prediction correlations (Bennett *et al.* (1995) and Van Sinderen *et al.* (2003)) relate the clear liquid height (also referred to as liquid hold-up) to the transition between the froth and spray regimes. It was found that the liquid hold-up directly affects the entrainment rate (Hunt *et al.* (1955), Kister and Haas (1988), Bennett *et al.* (1995), and Van Sinderen *et al.* (2003)).

Colwell (1981) found that the liquid hold-up in the froth regime depends strongly on gas velocity, liquid flow rate, gas and liquid density, fractional hole area and weir height. This agrees with the findings of Bennett *et al.* (1995) even though the latter correlated the influence of these parameters differently. Due to the complexity of their correlations it is difficult to compare the differences in the correlations proposed by Colwell (1981) and Bennett *et al.* (1995) directly. The advantage of the correlation developed by Bennett *et al.* (1995) over that of Colwell (1981) is that no iteration of the liquid hold-up is required.

Each author (Hunt *et al.* (1955), Thomas and Ogboja (1978), Kister and Haas (1988) and Bennett *et al.* (1995)) found different complex relationships between the system parameters (gas velocity, liquid flow rate and gas and liquid physical properties), tray and column geometry and entrainment. It is therefore difficult and in most cases impossible to directly compare the influences of these parameters on entrainment between the various authors. To show how the different correlations compare (see Table 2.17 and Table 2.18), they are plotted against each other for a range of gas velocities, liquid flow rates and tray spacings (see Figure 2.10, Figure 2.11 and Figure 2.12) based on the ranges used by most of the authors. Hunt *et al.* (1955) did not test with liquid cross flow, but used clear liquid

height in their correlation. Kister and Haas (1988) used the clear liquid height correlation (Eq. 2.23) from Colwell (1981), (see Eq. 2.26) to calculate entrainment with the correlation of Hunt *et al.* (1955). Both entrainment correlations from Hunt *et al.* (1955) and Kister and Haas (1988) are based on clear liquid height. It was therefore decided to use the clear liquid height correlation developed by Colwell (1981) for both the Hunt *et al.* (1955) and Kister and Haas (1988) entrainment correlations in the comparisons shown in Figure 2.10, Figure 2.11 and Figure 2.12.

Table 2.17 Application range summary of entrainment predictive correlations from literature.

Author	Column Shape and Dimensions	Tray Spacing [m]	Gas Superficial Velocity [m/s]	Fractional Hole Area	Hole Diameter [mm]	Liquid Flow Rate [$m^3/(h.m)$]	Entrainment Correlation/s	Systems Used
Hunt *et al.* (1955)	0.152m Round	0.2 – 0.711	1.0 – 4.3 m/s	0.05 – 0.215	3.18 – 12.7	No liquid cross flow	$E = 0.22\left(\frac{73}{\sigma}\right)\left(\frac{u_s^*}{S^* - 2.5h_L^*}\right)^{3.2}$ Eq. 2.2 Short-comings: 1. No liquid cross flow. 2. Single tray measurements.	Methane/Water, Freon 12/Water, Air/Kerosene, Air/Hexane, Air/CCl_4, Air/water & glycerine

Table 2.17 Application range summary of entrainment predictive correlations from literature.

Author	Column Shape and Dimensions	Tray Spacing [m]	Gas Superficial Velocity [m/s]	Fractional Hole Area	Hole Diameter [mm]	Liquid Flow Rate [$m^3/(h.m)$]	Entrainment Correlation/s	Systems Used
Thomas & Ogboja (1978)	0.3 x 0.91m Rectangular	0.3 – 0.457	1.9 – 3.2	0.124	25.4	4.5 – 40.3	$E = 0.88\left(\frac{u_p^*}{S^* - h_f^*}\right)^{0.77}$ Eq. 2.69 Short-comings: 1. Questionable catch pot entrainment measuring device. 2. Single tray measurements. 3. Influence of fractional hole area on entrainment not incorporated in correlation. 4. Only air/water system used in tests.	Air/Water
	0.81m Round			0.118				

Table 2.17 Application range summary of entrainment predictive correlations from literature.

Author	Column Shape and Dimensions	Tray Spacing [m]	Gas Superficial Velocity [m/s]	Fractional Hole Area	Hole Diameter [mm]	Liquid Flow Rate [$m^3/(h.m)$]	Entrainment Correlation/s	Systems Used
Kister & Haas (1988)	Used data from various sources	0.3 – 1	0.3 – 3.5	0.04 – 0.2	1.5 – 25	2 - 130	$$E_f = 111\left(\frac{u_b}{s-h_F}\right)^2 d_H{}^{0.5}(1+\zeta)$$ Eq. 2.38 $$E_w = \frac{0.3 d_H p^2}{h_L (s-h_F)^2}$$ Eq. 2.41 $$E_s = 4.742^{(10/\sqrt{\sigma})^{1.64}}\left[872\left(\frac{u_b h_{L,ct}}{\sqrt{d_H S}}\right)^4\left(\frac{\rho_g}{Q_L \rho_l}\right)\left(\frac{\rho_l-\rho_g}{\sigma}\right)^{0.25}\right]^{(10/\sqrt{\sigma})}$$ Eq. 2.43 Short-comings: 1. Used data from various sources to develop their correlations and can therefore not account for measurement and/or experimental errors. 2. Empirical correlations are limited to experimental parameter ranges they were developed from. 3. Applicable to only air/water system. Advantages: 1. Consider different flow regimes, and tray and column geometry	Air/Water

Table 2.17 Application range summary of entrainment predictive correlations from literature.

Author	Column Shape and Dimensions	Tray Spacing [m]	Gas Superficial Velocity [m/s]	Fractional Hole Area	Hole Diameter [mm]	Liquid Flow Rate [$m^3/(h.m)$]	Entrainment Correlation/s	Systems Used
Bennet *et al.* (1995) (air/water)	Used data from various sources	0.15 - 0.91	0.45 – 2.31	0.06 - 0.124	1.6 – 25.4	4.2 – 134	$E_f = 0.00164\left(\frac{K_s^2}{g\phi_e S}\right)^{1.86}\left[\frac{gH_L}{K_s^2}+\frac{9\sqrt{3}}{2A_f}\left(1+6.9\left\{\frac{D_H}{H_L}\right\}^{1.85}\right)\right]^{1.86}\left(\frac{\rho_L}{\rho_g}\right)^{0.5}$ Eq. 2.57 $E_s = 0.0050\left(\frac{K_s^2}{g\phi_e S}\right)^{1.26}\left[\frac{gH_L}{K_s^2}+\frac{9\sqrt{3}}{2A_f}\left(1+4.77\left\{\frac{D_H}{H_L}\right\}^{3.29}\right)\right]^{1.26}\varepsilon^{\beta}\left(\frac{\rho_L}{\rho_g}\right)^{0.5}$ Eq. 2.58 Short-comings: 1. Used data from various sources to develop their correlations and can therefore not account for measurement and/or experimental errors. 2. Applicable only to air/water system. 3. Low gas velocities, therefore not considering effect of droplet drag. Advantages: 1. Semi-empirical correlations, therefore more likely to be accurate when extrapolated beyond developed parameter range.	Air/Water

Table 2.17 Application range summary of entrainment predictive correlations from literature.

Author	Column Shape and Dimensions	Tray Spacing [m]	Gas Superficial Velocity [m/s]	Fractional Hole Area	Hole Diameter [mm]	Liquid Flow Rate [$m^3/(h.m)$]	Entrainment Correlation/s	Systems Used
Bennet *et al.* (1995) (non-air/water)	Used data from various sources	0.61	0.07 - 2.41	0.08 - 0.12	12.7 – 25.4	0.25 - 100	$$E_{f,NAW} = 0.742\left(\frac{K_s^2}{g\phi_e S}\right)^{2.77}\left(\frac{gH_L}{K_s^2}\right)^{1.81}\left(\frac{\rho_L}{\rho_g}\right)^{1.19}$$ Eq. 2.70 $$E_{s,NAW} = 8\times10^{-18}\left(\frac{K_s^2}{g\phi_e S}\right)^{1.56}\left[\frac{gH_L}{K_s^2}+\frac{2.48}{A_f}\left(1+8.27\left\{\frac{D_H}{H_L}\right\}^{-0.614}\right)\right]^{7.4}\times \varepsilon^{\beta}\left(\frac{\rho_L}{\rho_g}\right)^{1.08}$$ Eq. 2.71 Short-comings: 1. Based on data from limited number of systems, mostly under mass transfer conditions. 2. Used data from various sources to develop their correlations and can therefore not account for measurement and/or experimental errors. 3. Low gas velocities, therefore not considering effect of droplet drag. 4. Data from a fixed tray spacing of 0.61m.	Non-air/Water systems nl.: Cyclohexane/n-Heptane, Isobutane/n-Butane, Air/Isopar-M oil

Table 2.18 Parameter ranges used to compare different entrainment prediction correlations.

System	Tray Spacing [m]	Superficial Gas Velocity [m/s]	Weir Height [mm]	Fractional Hole Area	Hole Diameter [mm]	Liquid Flow Rate [$m^3/(h.m)$]	Fs $[(kg/m)^{1/2}/s]$
Air/Water @ 25°C and 1atm	0.3 – 0.6	1.5 – 3.0	57	0.098	12.7	10 - 60	1.6 – 3.2

The first comparison between the entrainment prediction correlations was made by keeping the tray spacing and liquid flow rate constant while changing the gas velocity (see Figure 2.9). Entrainment (L'/G) was plotted against the gas superficial velocity.

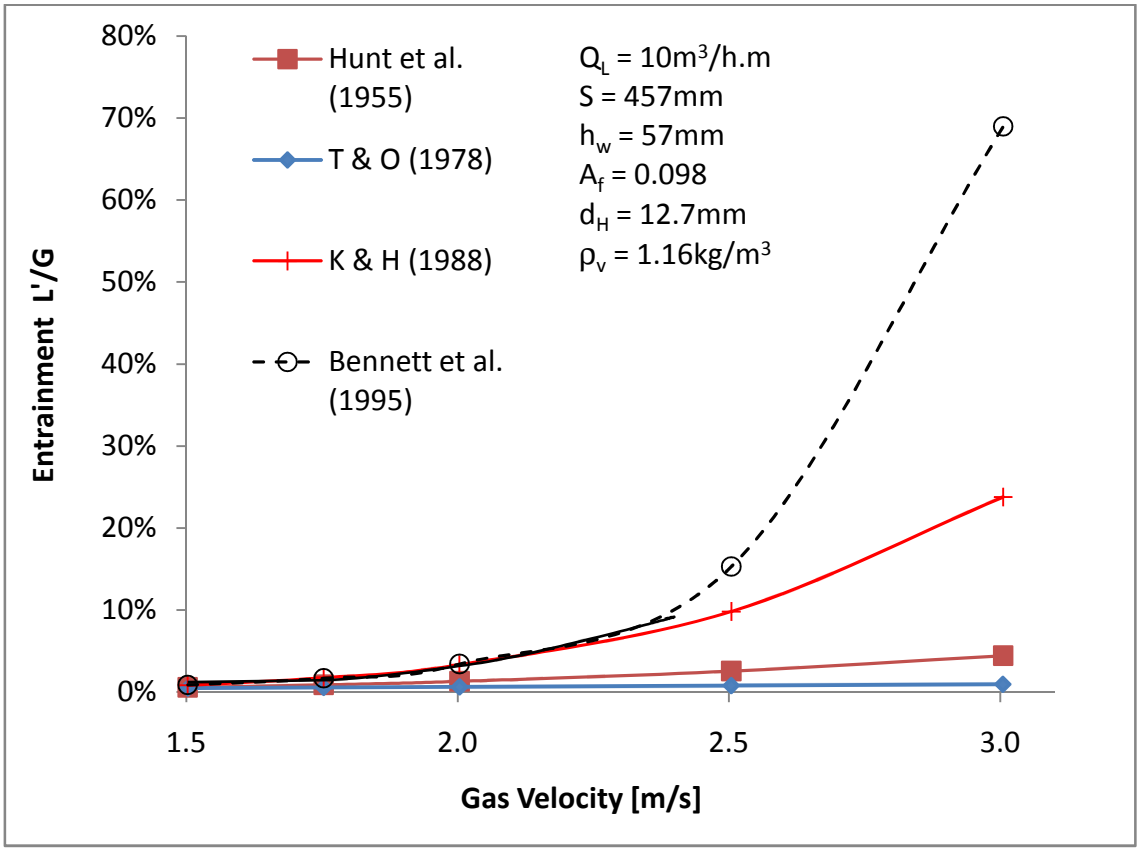

Figure 2.9. Comparing the effect of gas velocity on entrainment between the different entrainment prediction correlations. Dotted lines indicate extrapolation beyond recommended range of application.

Figure 2.9 shows that at low gas velocities (1.5 – 2m/s) there is no significant difference between the correlations. However, when the gas velocity exceeds 2m/s the correlations deviate significantly. Hunt *et al.* (1955) assumed that the froth density stays constant. Both Colwell (1981) and Bennett *et al.* (1995) later showed that froth density is a function of gas velocity, liquid flow rate, gas and liquid density, and column and tray geometry. The assumption of constant froth density by Hunt *et al.* (1955) is therefore an oversimplification. Kister and Haas (1978) only used the low gas velocity data (0.8 – 1.5m/s) from Thomas and Ogboja (1978) to develop their prediction correlation even though Thomas and Ogboja generated entrainment data for gas velocities up to 3.2m/s. One of the reasons for the deviation in entrainment prediction by Thomas and Ogboja (1978) could be the use of a catch pot device filled with silica gel to measure entrainment. The effectiveness and representativeness of such a device that does not cover the total column area is questionable, particularly at high entrainment rates. Kister and Haas (1988) used a larger data bank than Hunt *et al.* (1955) and Thomas and Ogboja (1978) to develop their correlation and it is therefore expected that their correlation should perform better than the latter over a large range of operating conditions. However, since they used data from various sources to develop their empirical entrainment prediction correlation, possible deviations are expected when operating outside the range of the data used. Systematic errors caused by poor experimental setup design and measurement errors from the different experimental setups used to generate data are not accounted for and could also lead to deviations between predictions and real column operation. Bennett *et al.* (1995) developed a semi-empirical correlation to predict entrainment over a large range of operating and system parameters. It is therefore expected that their correlation should perform better when extrapolated beyond their recommended application range. Bennett *et al.* (1995) did however mention that deviations are to be expected at high gas velocities due to their assumption that droplet drag will have negligible effect on entrainment at their proposed low operating gas velocity (<2.31m/s) range.

The next comparison, Figure 2.10, between the correlations was made by changing the liquid flow rate while keeping the tray spacing and gas velocity constant. The gas velocity was kept low, 2m/s, since the entrainment prediction between the correlations agreed well at low gas velocities as shown in Figure 2.9.In this example entrainment will be given as mass entrained liquid per mass of rising gas (Figure 2.10 (a)) and as mass entrained liquid per mass of liquid entering the tray (Figure 2.10 (b)).

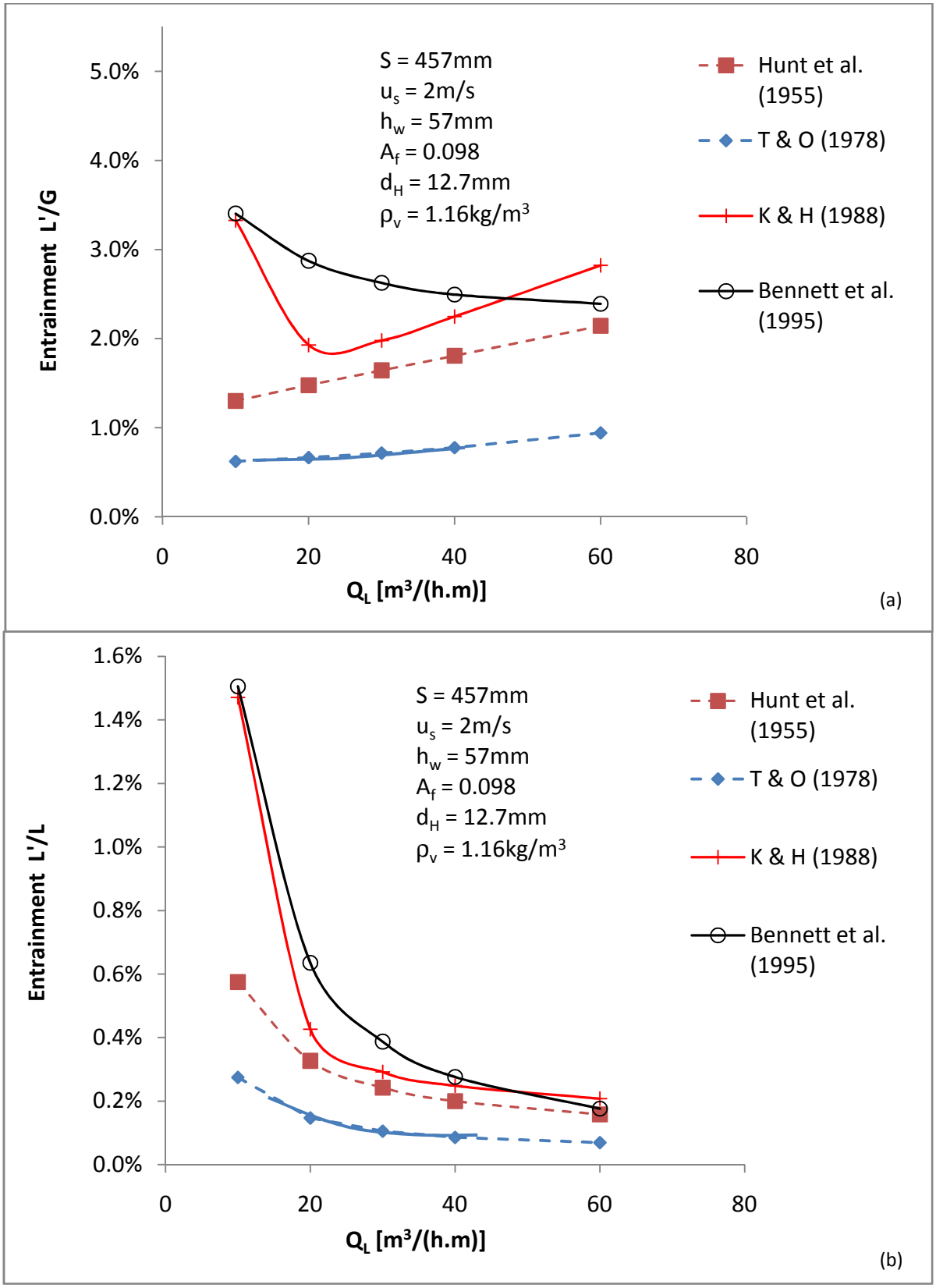

Figure 2.10 Investigating the influence of liquid flow rate on entrainment for the different entrainment prediction correlations, plotted as (a) mass entrained liquid per mass rising vapour (b) mass entrained liquid per mass liquid entering the tray under exactly the same conditions. Dotted lines indicate extrapolation beyond recommended range of application or testing.

Figure 2.10 (a) shows that an increase in liquid flow rate will result in an increase in entrainment (L'/G) in the froth regime as mentioned by Kister and Haas (1988). However, when entrainment is measured as the mass of liquid entrained over the mass of liquid entering the tray (L'/L), a different trend is observed (see Figure 2.10 (b)) where entrainment decreases with increasing liquid flow rate. Figure 2.10 (b) gives a much better understanding of the influence of the liquid flow rate on the percentage entrainment from an operating point of view. By relating the entrained liquid with the liquid entering the tray it is easier to determine the fraction of liquid and their components (in distillation operation) that is transported with entrainment to the tray above.

The sudden inflexion in the trend by Kister and Haas (1988) in Figure 2.10 (a) is caused by their anticipation of a regime change from spray to froth. However, according to Bennett *et al.* (1995) the flow regime is the froth regime and does not change for the liquid flow rate range presented. After reinspection of their correlation it was found that the correlation for regime transition by Kister and Haas (1988) is not accurate. This was found when their regime correlation was compared to conditions they specified as froth regime (Figure 5 in Kister and Haas (1988)) and their spray regime entrainment correlation matched the data while the froth regime correlation deviated significantly. It should be noted that the correlation for entrainment in the froth regime by Kister and Haas (1988) is only an adaptation from the Hunt *et al.* (1955) correlation. At a liquid flow rate of 60 m^3/(h.m) the correlation by Hunt *et al.* (1955) agrees with that of Bennett *et al.* (1995). It is interesting to note that at this specific point the froth density and clear liquid height of Hunt *et al.* (1955) is the same as that predicted by Bennett *et al.* (1995). When entrainment is plotted as the entrained liquid per liquid entering the tray (Figure 2.10 (b)) the trends follows a very similar curvature. It should also be noted that the percentage entrainment in both Figure 2.10 (a) and (b) is very low and the correlations are not extrapolated beyond the recommended range of application.

The last comparison (Figure 2.11) between the entrainment prediction correlations was made by changing the tray spacing while maintaining a constant gas and liquid velocity.

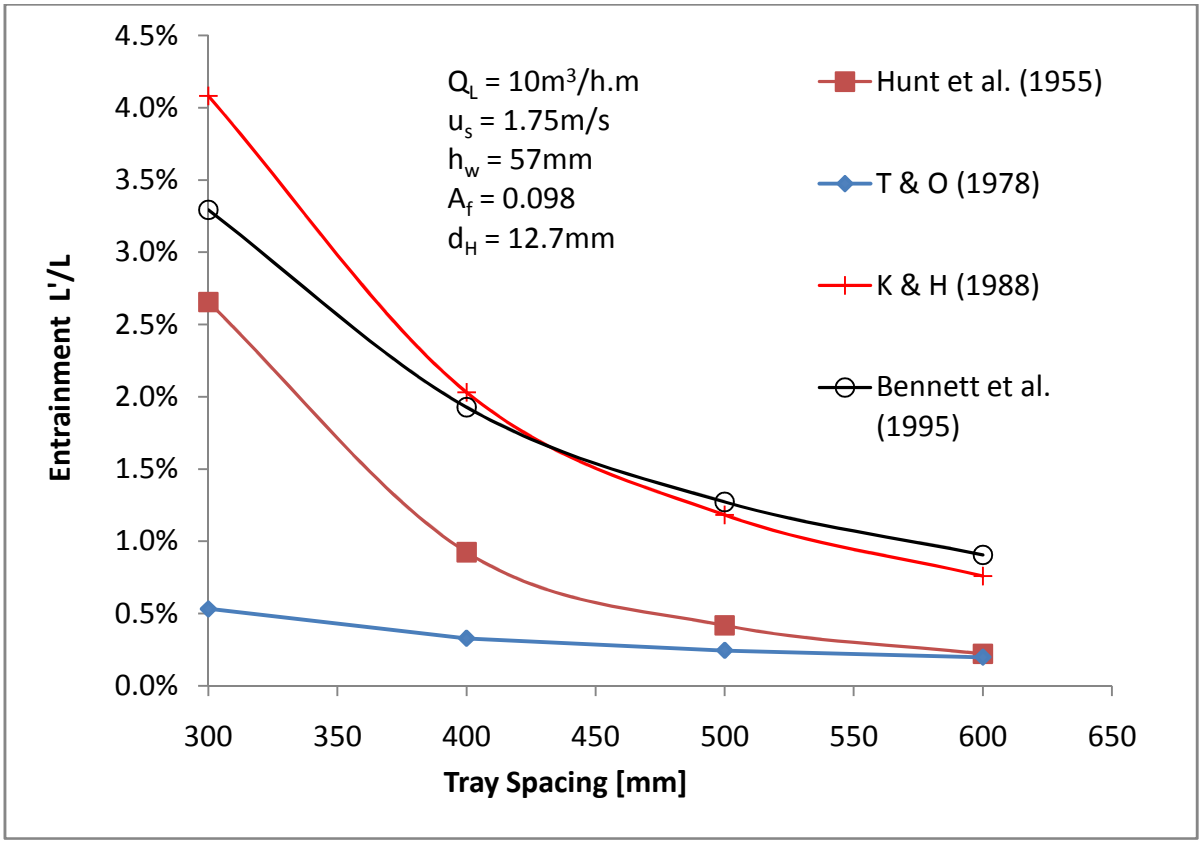

Figure 2.11 Investigating the influence of tray spacing on entrainment for the different entrainment prediction correlations. Dotted lines indicate extrapolation beyond recommended range of application or testing.

Figure 2.11 shows that a decrease in tray spacing will result in an increase in entrainment under constant froth height conditions. This decrease is not linear which shows that the froth density is not constant with height above the tray floor. This agrees with the findings of Hofhuis and Zuiderweg (1979) that the froth density decreases with elevation from the tray floor. At 300mm tray spacing the correlation from Hunt *et al.* (1955) agrees with that of Bennett *et al.* (1995) at this point however the froth densities predicted by Hunt *et al.* and Bennett *et al.* differed. The prediction by Kister and Haas (1988) shows a much higher dependency on tray spacing than that of Bennett *et al.* (1995). The deviation could be due to the fact that Kister and Haas (1988) develop an empirical correlation while Bennett *et al.* (1995) developed a more fundamental (semi-empirical) model. The curvature of the Hunt *et al.* (1955) and Kister and Haas (1988) correlations corresponds which shows the influence of the empirically derived non-uniformity adaptation made by Kister and Haas (1988) to the Hunt *et al.* (1955) correlation at low clear liquid heights. Once again the prediction by Thomas and Ogboja (1978) shows significant deviation from the others.

The graphs in Figure 2.12 (a) and (b) are plotted to show how the froth height correlations of various authors compare over a range of gas and liquid flow rates.

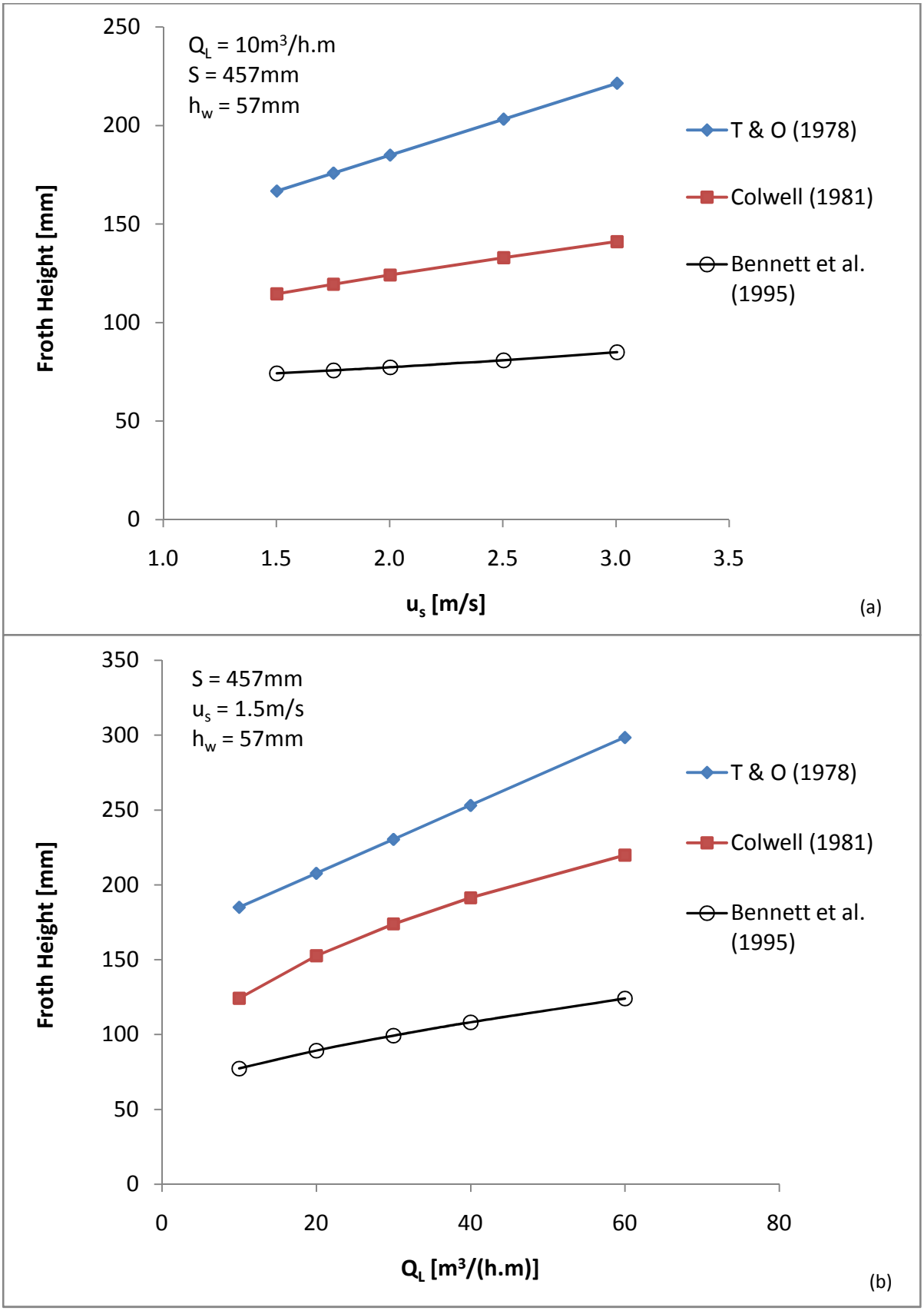

Figure 2.12 Investigating the influence of (a) gas and (b) liquid flow rate on entrainment for the different entrainment prediction correlations.

Figure 2.12 (a) and (b) shows that an increase in gas velocity and liquid flow rate will result in an increase in froth height. All the trends follow a similar curvature with Thomas and Ogboja (1978) predicting the highest froth height. One would therefore expect Thomas and Ogboja (1978) to over predict entrainment in Figure 2.9 and Figure 2.10. Since this is not the case it has to be assumed that the accuracy of their entrainment measuring device is questionable given that they developed an empirical entrainment prediction correlation from their entrainment data.

2.3 Summary of literature survey

Based on the content covered in the literature review and the critical evaluation the following summary was made:

Correlations have been developed to:

1. Predict the flow regime of the dispersion above the tray based on system conditions and tray geometry.
2. Predict the froth height and froth density for mainly air/water systems.
3. Predict entrainment in both the froth and spray regime for mainly air/water systems. Entrainment prediction correlations developed for non-air/water systems were developed based on limited data with questionable reliability.
4. Determine the tray pressure drop as a function of the residual and dynamic pressure drop, and momentum heads at the sieve tray holes.

Figure 2.9 - Figure 2.12 compared the different entrainment and froth height prediction correlations with each other. The largest deviations between the entrainment prediction correlations of the various authors were found at higher (>2 m/s) superficial gas velocity. At low liquid rates and low tray spacing the correlations also tend to differ significantly with the entrainment prediction correlation from Thomas and Ogboja (1978) which showed the largest deviation when compared to trends of the other correlations. Most of the variations between the trends are caused by the limited range (gas and liquid flow rates, gas and liquid physical properties) of testing and in some cases poor experimental setup design. The variation between the trends in Figure 2.9 - Figure 2.11 is proof that more work is required to improve understanding of the mechanisms that affect entrainment. In order to investigate these mechanisms a large range of gas and liquid flow rates, gas and liquid physical properties, and, tray and column geometry should be investigated in a single experimental setup. This will eliminate systematic errors caused by experimental setup design and different sampling methods.

Very little reliable non-air/water data exists compared to the work done with air/water systems. The correlations developed by Kister (1990) and Bennett *et al.* (1995) are based on data generated from different column geometries and from different experimental setups. It is unclear how accurate and representative the data is since limited information is given regarding the collection of the data. Sakata and Yanagi (1979) acknowledged that they experienced difficulties measuring entrainment. Most of the non-air/water correlations are based on the data from Sakata and Yanagi (1979).

In the publications reviewed the definition for the different flow regimes varied between the different authors. Porter and Jenkins (1979) related the froth to spray transition to the minimum entrainment that is achieved when the liquid flow rate is increased while the vapour velocity is kept constant. This related the tray capacity to the respective regime. The only problem is that their definition for the entrainment rate (ratio of the mass entrained liquid to the mass of vapour) does not relate to the amount of liquid on the tray. The effect of entrainment on the concentration of the high and low volatile components in the liquid phase on the tray is therefore not considered.

All the authors defined entrainment as the mass of liquid entrained over the mass of rising vapour or as the amount of entrained liquid that reached the entrainment collection section. Therefore ten percent entrainment for a fixed gas flow rate is the same amount of liquid entrained irrespective of the liquid flow rate. This is better explained in the following example (see Figure 2.10 (a) and (b)):

If for a constant vapour flow rate of 1 kg/s and a liquid flow rate of 1 kg/s an entrainment rate of 100% is reached all the liquid on the tray (1kg/s liquid) will be moved from the tray below to the tray above. In the case where the liquid flow rate is 10 kg/s with a 1 kg/s vapour flow rate, 100% entrainment rate is still 1 kg/s liquid that are moved to the tray above. The significant difference is that 1 kg/s in this case is only 10% of the total liquid flow rate entering the tray and would therefore not influence the mass transfer efficiency to the extent as when all the liquid is moved from the tray below to the tray above. The definition of entrainment is therefore not related to the amount of liquid on the tray and can therefore not be directly linked with the mass transfer separation efficiency.

Most of the correlations developed to predict froth height and entrainment assumes that the effect of droplet drag can be neglected. Bennett *et al.* (1995) showed that at high superficial vapour velocities and for high Froude and Weber numbers droplet drag does have a significant influence on entrainment. The effect of liquid viscosity on the hydrodynamic behaviour has not been focused on. Most of the work done on the influence of viscosity on entrainment used a small range (0.8 – 2 mPa.s) of viscosities. No entrainment predicting correlation has been developed that can accurately predict entrainment for air/water and non-air/water systems over a broad operating range.

2.4 Scope for potential research

Based on the summary made of the literature review, the following areas in sieve tray hydrodynamics require investigation:

1. The influence of a large range of gas and liquid physical properties, with fixed tray geometry, on:
    i. the clear liquid height (liquid hold-up);
    ii. froth density;
    iii. entrainment at different tray spacings to investigate the influence of droplet drag for low surface tension liquids;
    iv. weeping
2. The influence of the liquid flow rate on entrainment and froth behaviour at fixed clear liquid heights (liquid hold-up).
3. The minimum entrainment, for a range of system physical properties, as a function of liquid entering the tray through the downcomer.

Most of the deviations found between the entrainment prediction trends of the various authors (in Figure 2.9 - Figure 2.11) and others (Van Sinderen *et al.* (2003)) can be related to poor experimental setup design and sampling methods. Therefore, in order to achieve the above it is of utmost importance to spend time on the design of an experimental setup to ensure representative and accurate results.

2.4.1 Scope for this work

The aim for this project was therefore to develop an experimental setup to investigate hydrodynamic behaviour in sieve tray columns while isolating the effects of mass transfer which occurs in commercial distillation. An overview of the different column geometries used in the past by different research groups with their findings acted as a guide to approach the optimum column design. Some advice and suggestions regarding column and tray geometry were proposed by Koch – Glitsch (international tray and packing supplier and developer).

To verify system accuracy and representativeness air/water tests were conducted and the results compared with entrainment prediction correlations from Hunt *et al.* (1955), Thomas and Ogboja (1978), Kister and Haas (1988) and Bennett *et al.* (1995).

3 Design of a distillation sieve tray column for hydrodynamic characterisation

3.1 Introduction

In order to generate entrainment data with non-mass transfer systems an experimental setup had to be designed. Different column geometries have been used in the past to generate data representing the hydrodynamic behaviour in sieve tray columns. Table 2.17 is a summary of the column geometries previously used by different research groups.

Hunt *et al.* (1955) found that the liquid flowing over the weirs in a small diameter round column is unstable and therefore conducted their studies with no liquid cross flow. Porter and Jenkins (1979) showed that round columns will have a constriction effect on the cross flowing liquid at the outlet weir. The sudden expansion in the liquid flow path, after exiting the downcomer, could also contribute to non-uniform froth development. It was therefore decided to use a column with rectangular shape to eliminate entrance and wall effects. To eliminate a possible effect of mass transfer on entrainment, and to focus on hydrodynamic behaviour, it was decided to design the pilot plant for thermally stable non-reacting, and non-foaming, gas and liquid systems. By using a zero mass transfer system, the gas and liquid flow rate measurements will be simplified compared to industrial distillation where the composition of the components and flow rate of the phases and fractions change throughout the column.

3.1.1 Objective

The objective of this section is to describe the development of an experimental setup that would allow generation of reliable entrainment data for:

1. a range of gasses with different densities;
2. a range of liquids with different;
    a. Densities
    b. Viscosities
    c. Surface tensions
3. different tray spacings;
4. a range of gas and liquid flow rates.

It was decided that the experimental setup should also be able to measure weeping rates even though it does not fall within the scope of this project.

3.1.2 Scope and Limitations

The following is a summary of the limitations that determined the scope for constructing the experimental setup:

1. Time
2. Laboratory Space
3. Gas and liquid systems
4. Gas and liquid flow rates
5. Materials for Construction
6. Safety

Time:

Construction and commissioning of the experimental setup is limited to two years since a year is needed for testing with an air/water system, generating entrainment data and reporting the findings.

Laboratory space:

Space for the development of an experimental setup was limited. The experimental setup could not exceed a height of 8m and only 20m^2 of floor space was available. The available space had to be shared with another column (that will be used to investigate the hydrodynamic behaviour for structured and random packing) that will make use of the same utilities as this experimental setup.

Gas and liquid systems:

The aim was to generate data that represents a large fraction of the systems used in distillation, absorption and stripping applications. Since one of the objectives is to eliminate the possible influence of mass transfer on the hydrodynamic behaviour, care was taken with the selection of the liquid systems. If the flash point is low and or the vapour pressure high, evaporation will take place which would include the effect of mass transfer on the measurements. Flammable liquid in the vapour phase will also increase the risk of fire and explosion.

Since it is expensive and nearly impossible to create gas mixtures of known concentration in such a large system it was decided to use pure (technical grade) gasses. To reduce the possibility of air leakage into the system, especially at the blower shaft seal, the operating pressure should be slightly above atmospheric pressure. Air that leaks into the system when using a flammable liquid will increase the probability of fire and an explosion.

The range of liquid and gas systems therefore depended on the availability, cost, corrosive properties and safety.

Gas and liquid flow rates:

According to the entrainment rate (ratio of liquid entrained over liquid entering the tray) prediction correlation of Bennett *et al.* (1995) for the froth regime a superficial gas velocity of 5.4 m/s is required to achieve 20% entrainment for a liquid rate of 120 m^3/(h.m). Since the exact superficial velocity required for excessive entrainment is uncertain (the superficial velocity exceeds the range, 0.5 - 2.3m/s, used by Bennett *et al.* (1995)) a maximum velocity of 7 m/s was chosen (this velocity had to be excessive since the required velocity for entrainment for Helium gas is uncertain).

The correlation developed by Bennett *et al.* (1995) covered a liquid range of 4.18 – 134.28 m^3/(h.m). It was therefore decided to test for a liquid range of 11 – 114 m^3/(h.m) since more than one flow meter would be required for a larger flow range. This flow range should be sufficient to test the influence of excessive entrainment for high liquid rates. The liquid flow rate is based on the volumetric flow rate per weir length.

Materials for construction:

Organic solvents are known for their corrosive properties on seals and polymeric compounds. PTFE (polytetrafluoroethylene) or Viton (a fluoropolymer elastomer) seals were therefore used. Due to the corrosiveness of the organic solvents glass should be used for viewing ports. Polycarbonate (LEXAN) was used as viewing ports since glass would tend to crack and create sealing problems.

Water will be used therefore the construction material should be stainless steel, grade 304 or 316.

Safety:

With the use of flammable liquids and gasses special rules and legislation apply. Based on the MSDS (material safety data sheet) properties and the operating conditions, precautions regarding sensor and electronic device selection and placement have to be made. Since the safety legislation was not the aim of the study an in depth investigation of the rules and legislation will not be covered in this work.

To ensure safe operation a proper HAZOP (Hazard and Operability Study) was conducted. In order to reduce the probability of fire and explosions, contact with air should be eliminated by maintaining a system pressure greater than the atmospheric pressure, the area should be well ventilated and the system should be free of gas and liquid leaks.

3.2 Concept design

3.2.1 Pilot Plant Unit Selection

The pilot plant will need the following main units:

1. The distillation hydrodynamic characterisation sieve tray column.
2. A blower to circulate the gas (since no re-boiler will be used).
3. A pump to circulate the liquid (since no condenser will be used).
4. Vessels than can measure the entrainment and weeping rates.
5. A surge tank that will act as a dampener to possible system pressure fluctuations. This vessel should also act as a droplet settling tank to remove and measure droplets which can be carried over with the gas from the de-entrainment section of the column.
6. Heat exchanger to control the operating temperature.
7. Sensors that will measure flow rate, absolute pressure, pressure drop, and temperature.
8. Control system to control temperature, flow rate and pressure.
9. A catwalk structure to make visual observation, manual settings, sampling and maintenance possible.

3.2.2 Pilot plant layout

The process flow diagram in Figure 3.1 represents the schematic layout of the plant. The function of each unit will be discussed in section 3.3 with the detailed specifications in Appendix A (section 8).

Liquid circulation loop:

Liquid is circulated from the sump with a centrifugal pump through a flow meter and control valve to the heat exchanger where excess process heat is removed. From the heat exchanger the liquid is fed into the downcomer above test tray 1 of the column. As the liquid enters test tray 1, it is brought in contact with the rising gas. In the event where no entrainment occurs, all the liquid will exit test tray 1 and enter test tray 2. The main purpose of test tray 2 is to cool and distribute the gas coming from the blower as well as to represent flow conditions found in multi tray columns. The liquid will then exit test tray 2 through a downcomer, which is isolated from the chimney tray section, to the sump. Alternatively the

liquid can be circulated from the heat exchanger through the sump, bypassing the trays and any gas contact.

During entrainment conditions the gas velocity is sufficiently high to transport the liquid on test tray 1 to the de-entrainment section. The entrained liquid is then removed from the rising gas stream and fed through MV-204 to the sump. To determine the rate of entrainment the valve below MV-204 will be closed (low entrainment rates) or the entrained liquid will be fed to MV-202 (high entrainment rates). The mass inside either MV-202 or MV-204 is then logged over time to determine the rate of entrainment.

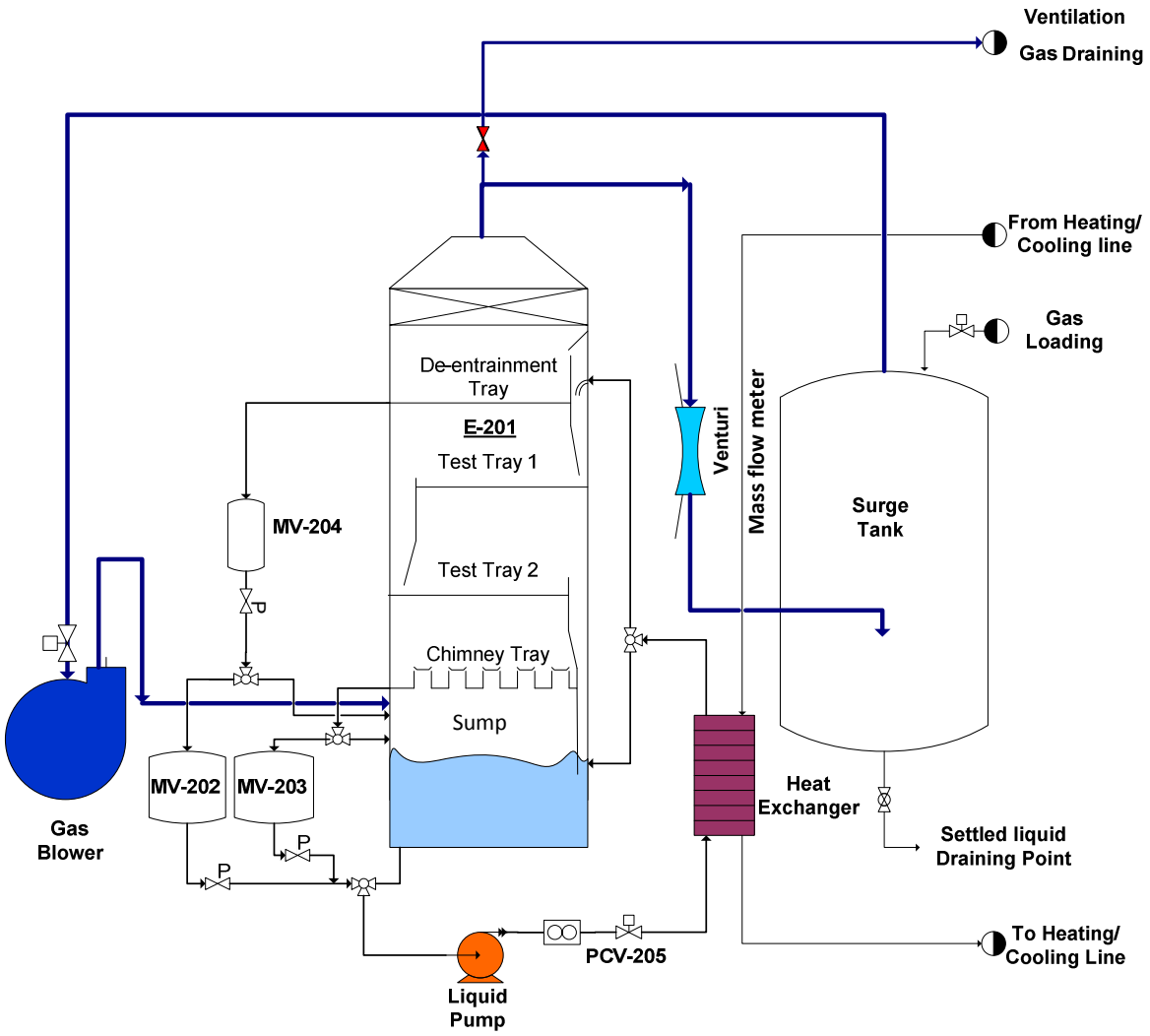

Figure 3.1 Schematic representation of the pilot plant setup.

Weeping occurs when the gas velocity is sufficiently low for the liquid to 'leak or dump' through the perforations in the tray to the chimney tray. The chimney tray is sealed so that no liquid on the tray can leak through to the sump. The 'chimneys' or gas distributors are elevated above the tray deck to prevent gas-liquid contact. The liquid exits the chimney tray section through a 3-way valve to either the sump or MV-203 which will measure the weeping rate over time.

To evacuate MV-202 or MV-203 valves are switched so that the pump is no longer fed from the sump. As soon as MV-202 or MV-203 is emptied the valves will switch back so that the pump is fed from the sump.

Gas circulation loop:

Gas is fed to the column by a centrifugal blower through a gas distributor, shown as the chimney tray in Figure 3.1. The gas will then rise through the column exiting through a venturi meter to a surge tank. The surge tank absorbs pressure fluctuations as well as separates any remaining liquid droplets from the gas. From the surge tank the gas is fed to the blower completing a closed loop.

3.3 Detail design

3.3.1 Choosing gas and liquid systems

In order to conduct sensor, unit, and pipe sizing, the range of gas and liquid physical properties that will be used to generate the required data were needed. To generate data that represents a large fraction of the systems found in commercial distillation applications it was decided to look at the physical properties of a range of hydrocarbons around their boiling points (at saturation). The physical properties of the gas and liquid systems should compare to a hydrocarbon range of C1 – C12 (methane to dodecane) to represent the physical properties of most systems used in commercial distillation, as shown in Table 3.1. This range was also selected based on the molecular mass range (16 – 170 kg/kmol) which covers most systems used in commercial distillation. The objective for the design includes that it should be able to test the influence of a range of gas and liquid physical properties on entrainment. In stripping applications where volatile components are removed from waste water or in the case where some polymers might be present in the liquid, the viscosity and surface tension range had to be increased beyond distillation applications. The effect of foaming on the hydrodynamic behaviour does not form part of this investigation and will therefore not be investigated.

Table 3.1 Vapour/liquid physical properties found in commercial stripping and distillation applications obtained from www.nist.gov.

Description	Chemical Formula	Mr [kg/kmol]	Temp [°C]	Absolute Pressure [kPa]	Liquid density [kg/m³]	Vapour Density [kg/m³]	Liquid Viscosity [mPa.s]	Surface tension [mN/m]
Methane	CH_4	16	-162	100	422	1.8	0.12	13
Butane	C_4H_{10}	58	-0.8	100	602	2.7	0.20	15
Pentane	C_5H_{12}	72	36	100	610	2.9	0.20	14
Octane	C_8H_{18}	114	125	100	612	3.7	0.20	12
Decane	$C_{10}H_{22}$	142	174	100	604	4.1	0.20	11
Dodecane	$C_{12}H_{26}$	170	216	100	595	4.5	0.20	9
Oxygen	O_2	32	-183	100	1142	4.4	0.20	13
Oxygen	O_2	32	-153	1000	976	38.5	0.10	6
Cyclohexane	C_6H_{12}	84	80.	100	720	2.97	N/A	18
Water	H_2O	18	100	100	958	0.59	0.28	59
Water	H_2O	18	20	2.3	998	0.017	1.00	73
Water	H_2O	18	25	3.2	997	0.023	0.89	72
Ethylene Glycol	$C_2H_6O_2$	62	25	100	1113	N/A	15.00	48

Since the aim of this investigation is to study entrainment (hydrodynamics) and not thermodynamics, the liquids which will be used for testing should have a low saturated vapour pressure to prevent evaporation at 25°C (the chosen operating temperature). At 25°C no excessive cooling or heating is required for temperature control. The gas/liquid range is also limited to availability, cost and safety. Most of the work done in the literature focused on the gas and liquid densities, future work will focus on a large range of liquid surface tensions and especially a large range of liquid viscosities to represent commercial distillation and stripping applications. Table 3.2 and Table 3.3 is a summary of the chosen gasses and liquids with their properties. The values are only approximations and will be analytically verified and measured during and after testing.

Table 3.2 Approximated Gas Properties (obtained from www.nist.gov).

Gas	Mr [kg/kmol]	Density [kg/m³]	Dynamic Viscosity [mPa.s]	Kinematic Viscosity [m²/s]
He	4	0.16	1.98E-02	1.24E-04
Air	29	1.18	1.82E-02	1.54E-05
CO_2	44	1.78	1.49E-02	8.37E-06
SF_6	146	5.96	1.53E-02	2.56E-06

Table 3.3 Approximated Liquid Properties (obtained from www.nist.gov).

Liquids	Mr [kg/kmol]	Density [kg/m³]	Dynamic Viscosity [mPa.s]	Surface Tension [mN/m]	Boiling Point @ 1 atm [°C]
Water	18	997	0.89	73	100
Ethylene Glycol	62	1113	15.4	48	198
Silicone Oil	74	963	50	19	130
n-Butanol	74	810	2.6	24.9	118
Isopar G	not specified	748	0.84	23.1	160

The gas density range cover the vapour density range found in most commercial applications. The liquid density range does, however, not cover the low liquid densities found in commercial applications. However, the liquid density range is large enough so that the effect of liquid density on entrainment can be determined and extrapolated to lower density liquid applications. The liquids also cover a large surface tension and viscosity range which was not previously tested for by other research groups.

3.3.2 Column design

The main column design was proposed by Koch-Glitsch and modified to meet the requirements of this project. The gas enters at the bottom of the column through a gas distributor that also acts as the weeping collection tray. Above the weeping collection tray, two test trays are followed by a de-entrainment tray and a mist eliminator pad, see Figure 3.1. The liquid enters the column through a sealed downcomer placed in the de-entrainment section. This ensures that the liquid rate entering the tray can be measured and are representative of real column operation. Some changes and adjustments, regarding tray spacing and the viewing ports, were then made to meet the objectives.

The following was considered in the design of the column:

1. The column shape
2. Tray spacing
3. Tray geometry
4. Visibility
5. Downcomer clearance area (downcomer escape area)
6. De-entrainment section
7. Weeping collection section
8. Liquid sump

Column shape:

The column shape was chosen to be rectangular to eliminate possible entrance (expansion), exit (constriction) and wall effects of the liquid flow path on the hydrodynamics in the column associated with small to medium size round columns. The column size was chosen to be 175 x 635mm. Koch-Glitsch provided the de-entrainment and mist eliminator devices, the test trays and the gas distributor. Figure 3.2 and Figure 3.3 are detailed drawings of the column with some dimensions.

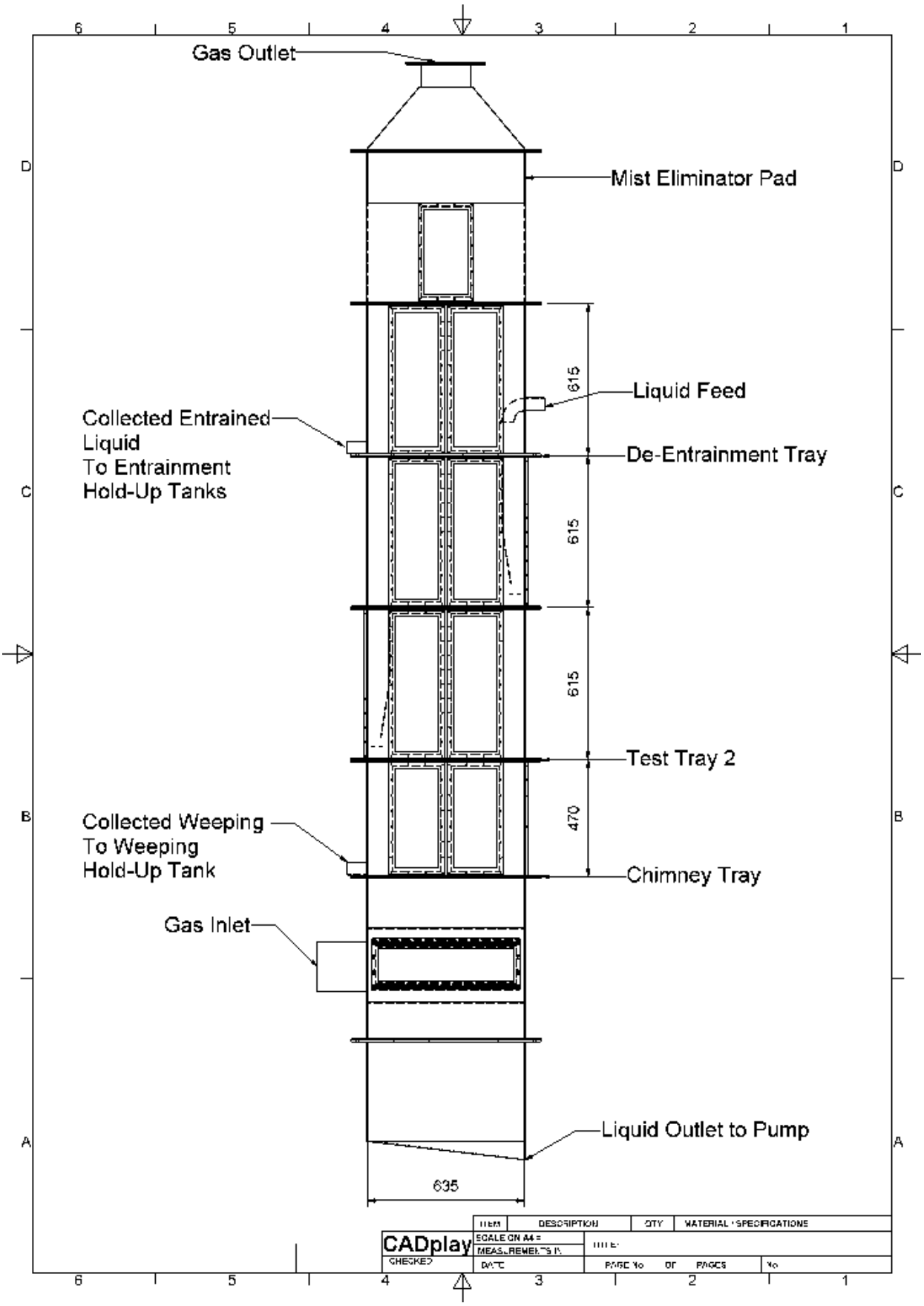

Figure 3.2 Column front view with dimensions in millimetres.

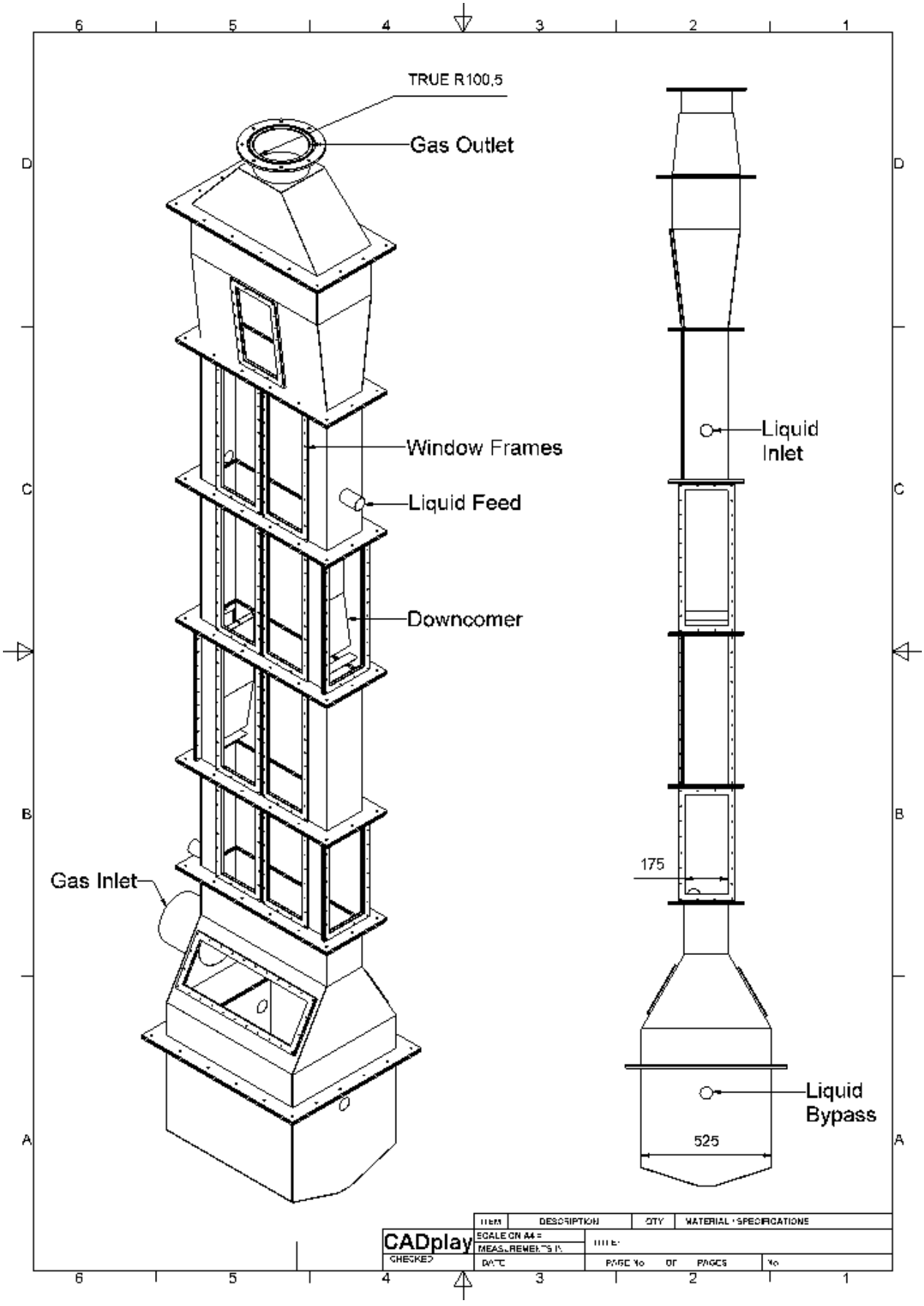

Figure 3.3 Column side-and-isometric views with dimensions in millimetres.

Tray spacing:

It was decided to use two trays in order to represent the hydrodynamic behaviour of a multi-tray distillation column. The hydrodynamic effect that the bottom tray has on the top tray during entrainment will therefore be included in the test results.

Most of the work done in the literature was for a tray spacing range between 300 and 600mm. It was therefore decided to design the column to accommodate 4 tray spacings; 315, 415, 515 and 615mm. In order to change the tray spacing separate sections had to be constructed. This influenced the piping that connects the gas and liquid lines to the column.

Tray geometry information:

Table 3.4 is a summary of the test tray geometry:

Table 3.4 Sieve Tray and Column Geometry.

Variable	Description	Value
A_b [m^2]	Bubbling Area	0.0796
A_d [m^2]	Downcomer Area	0.0158
A_f [m^2]	Fractional hole area	0.155
A_h [m^2]	Hole area	0.0143
A_p [m^2]	Perforated Area	0.0919
	Number of Holes (including bubble promoters)	458
d_H [mm]	Hole diameter	6.3
h_w [mm]	Weir height	57
l [mm]	weir length	175
p [mm]	Hole triangular pitch	14
s [mm]	Tray spacing	615

Figure 3.4 is a picture of the sieve trays used in this work:

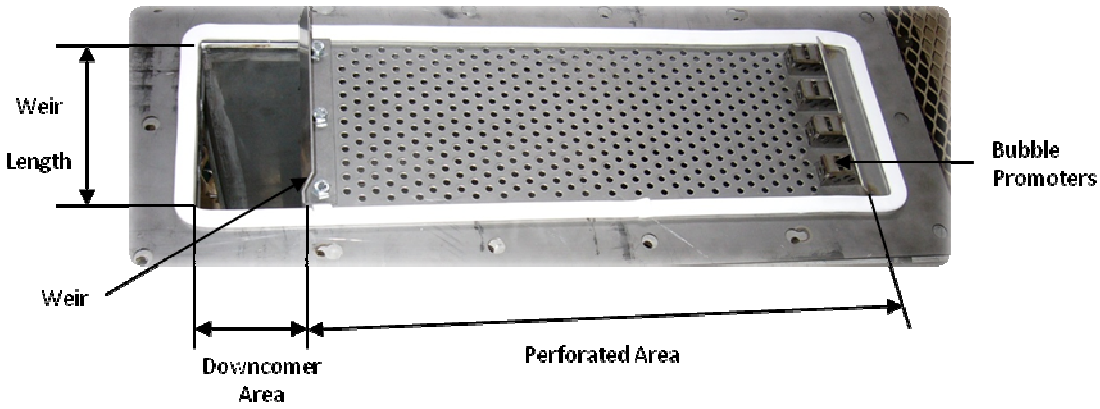

Figure 3.4 Picture of a sieve tray used in this work.

Visibility:

Since the aim of this investigation is to characterise the hydrodynamic behaviour inside the column, visual observation is needed to monitor:

1. When entrainment and weeping occur.
2. The froth development.
3. If the downcomer is flooding.
4. If there is sufficient liquid in the downcomer (downcomer seal) to prevent gas bypass through the downcomer.
5. If the de-entrainment section is flooding or at maximum capacity
6. If the weeping section is at maximum capacity.

Glass or transparent sections are therefore needed in the column walls to create visibility. The challenge is therefore to design and construct window frames that seal and allow the glass to be removed to allow access to the column internals from the outside. The glass should be flush with the inside of the column wall to retain a smooth gas and liquid flow path.

Downcomer clearance area:

The downcomer clearance (escape) area should be adjustable to:

1. Prevent the downcomer from flooding (downcomer flooding occurs when the downcomer is overfilled with liquid preventing the liquid from the tray above to exit).

2. Provide a sufficient liquid level in the downcomer (downcomer seal) to prevent gas from bypassing through the downcomer instead of flowing through the column.

Koch-Glitsch suggested that the velocity of the liquid exiting the downcomer should be between 0.3 and 0.6 m/s.

De-entrainment section:

The de-entrainment section consists of a de-entrainment tray responsible for separating most of the entrained liquid from the gas, and a mist eliminator pad (see Figure 3.5) which should capture the remaining droplets. Both the de-entrainment tray and mist eliminator pad was supplied and tested by Koch-Glitsch.

To separate the liquid from the rising gas, the gas/liquid mixture passes through angled louvers in the de-entrainment tray deck. The liquid is then separated from the rotating gas with centrifugal force, and settles to the tray deck on the outside of the cylindrical risers. The separated liquid is sent to the entrainment measuring units, MV-202/204, through a pipeline exiting through the wall of the de-entrainment section, mounted level with the tray deck to minimise the liquid hold-up in the de-entrainment section.

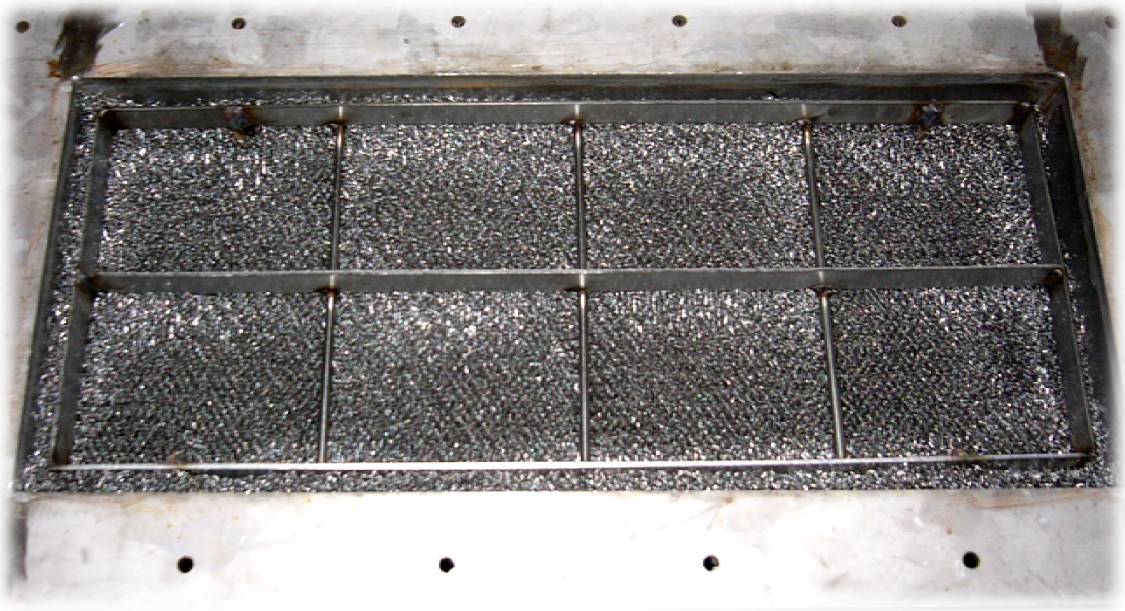

Figure 3.5 Top view of the mist eliminator pad.

Weeping collection section:

The weeping collection tray, designed and supplied by Koch-Glitsch, acts as a gas distributor and a weeping collection tray. The tray consists of "chimneys" protruding the tray deck (approximately 250mm) which act as gas distributors. The liquid that weeps through the bottom test tray is therefore collected on the tray deck and fed to the weeping measuring vessel, MV-203. A sealed downcomer is used to transport the liquid exiting test tray 2 to the liquid sump to ensure isolation of the weeping collection section.

Liquid sump:

The liquid sump was elevated to supply a net positive suction head (NPSH) of 6.5m (64kPa) to the pump. Since the liquid entering the sump form test tray 2 contains entrained gas bubbles a splash deck was placed at the bottom of the downcomer to redirect the liquid flow path so that the bubbles have sufficient time to disengage from the liquid. A vortex breaker was placed inside the exit pipe feeding the pump to prevent the formation of a vortex that will cause the pump to suck gas into the pipeline and cause cavitation.

3.3.3 Gas blower (E-102)

It was chosen to use a centrifugal blower to circulate the gas through the pilot plant. After the pressure drop calculations for the gas line (piping, fittings and column) were completed the design specifications as shown in Table 8.1 in Appendix A were sent to the supplier.

The blower was placed in an acoustic enclosure outside the laboratory to reduce noise levels. A plinth was specially designed and constructed to support the blower with the acoustic enclosure. To further ensure flexible operation of the blower, especially at low volumetric flow rates, an inverter was connected to the blower that controls the rotational speed and therefore the gas flow rate.

3.3.4 Liquid pump (E-204)

Since the pressure required to circulate the liquid through the liquid pipeline, heat exchanger and column, is below 10 bar a centrifugal pump with specifications shown in Table 8.2 was chosen.

3.3.5 Entrainment and weeping measuring vessels (MV-202, 203, 204)

Since the pressure head available from the entrainment and weeping collection sections are too low to use conventional flow meters it was decided to use hold-up tanks to measure the entrainment and weeping rates. This required vessels of known volume to measure the entrainment and weeping rates over time. To do this a three way ball valve was placed above the hold-up tank (MV-202 and MV-203 in Figure 3.1) which would change the liquid flow direction from the sump to the liquid hold-up tank. For small entrained liquid rates a smaller hold-up vessel (MV-204) was required. This vessel was placed in the pipeline feeding the larger entrainment hold-up vessel (MV-202) with a valve at the bottom to enable measuring.

The simplest method to measure the entrainment and weeping mass flow rates would be to use electronic balances. In order to execute this with high accuracy the mass from the electronic balances has to be logged and monitored by the programmable logic controller (PLC) that controls the system. There was no simple solution to achieve communication between the balances and the local (PLC) control system and a different method had to be devised.

It was then decided to use digital differential pressure transmitters, see placement configuration in Figure 3.6 and Figure 3.7, and the correlation provided in Eq. 3.2 to measure the mass of the liquid inside the hold-up vessels.

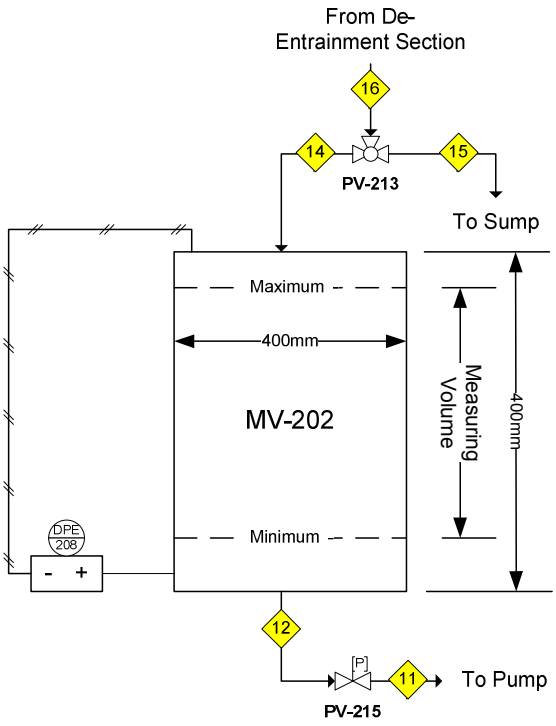

Figure 3.6. Entrainment measuring hold-up tank configuration for larger entrained liquid rates (L'>0.07kg/s).

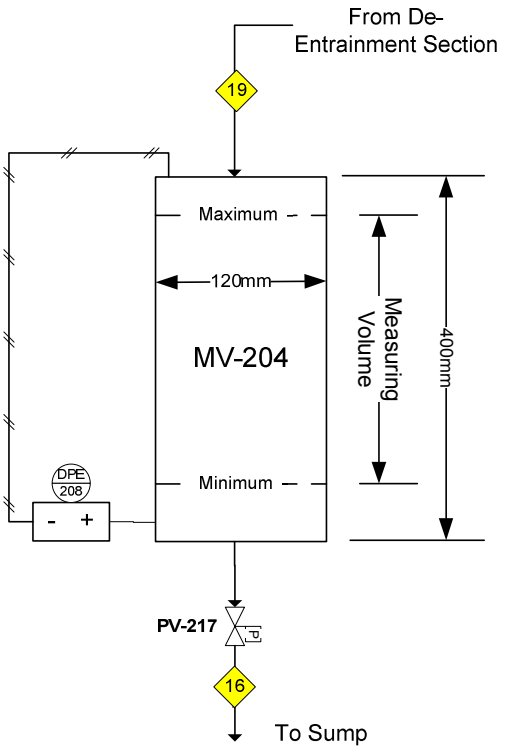

Figure 3.7 Entrainment measuring hold-up tank configuration for small entrained liquid rates (L'<0.07kg/s).

The correlation used to measure the mass inside the vessels was derived from the static head correlation:

$$p = \rho g h \tag{3.1}$$

Since the area of the hold-up vessel is known and constant the correlation can be rearranged:

$$m = \frac{pA}{g} \tag{3.2}$$

By using differential pressure transmitters, instead of absolute pressure transmitters, the influence of system pressure fluctuations was filtered out. The mass of the liquid inside the hold-up vessel was then sampled over time and linear regression was used to determine the average mass flow rate. The convenience of this sampling method is that the density of the liquid and temperature does not have to be known to determine the inventory mass. System vibration would also not affect the measurements as much as it would influence the electronic balance measurements. Since the liquid momentum entering the hold-up vessel is approximately constant (if the entrainment rate is constant) over the sampling period, the effect was assumed to be negligible.

The size of the hold-up tanks (MV-202/3) was determined for 20% entrainment (liquid entrained over liquid entering the tray) at the maximum liquid flow rate, 114m^3/(h.m). At this rate a minimum of 20 samples (2 seconds for each sample), of the mass inside the hold-up tank over time, should be recorded. To do this the volume required is 45 litres.

The size of the small entrainment hold-up tank (MV-204) was determined for 1% entrainment (liquid entrained over liquid entering the tray) at the maximum liquid flow rate, 114m^3/(h.m). At the maximum flow rate, 80 seconds will be required to measure 1% entrainment and 180 seconds will be required for the 17.2m^3/(h.m) flow rate.

3.3.6 Surge tank (E-101) design

Since pulsation of the froth, which will cause pressure fluctuations, is expected a surge tank was designed to act as dampener to prevent the system from oscillating. The surge tank was also used to separate any small liquid droplets that passed or escaped the mist eliminator pad. The effectiveness of the de-entrainment section can therefore be determined. The size of the surge tank was determined using the method proposed by Coulson and Richardson (1999) (Chemical Engineering, Volume 6).

The surge tank design was based on the vertical separator design as shown in Figure 8.1.

3.3.7 Heat exchanger (E-205) design

In order to maintain a constant temperature inside the column a heat exchanger is needed. The operating temperature was decided to be 25°C since most of the gas and liquid properties are available at this temperature. In the case where liquid properties are to be changed by increasing the temperature, the heat exchanger should be able to heat the liquid to a maximum of 80 degrees Celsius. This maximum temperature, 80°C, was chosen so that normal pump and heat exchanger seals could be used since the scope of this project does not involve testing at high temperatures.

To maintain an operating temperature of 25°C an energy balance was performed. Table 3.5 is a summary of the energy balance conducted for the pilot plant.

Table 3.5 Summary of Energy balance for the pilot plant.

Energy Source	Energy Flow	Values	Units
Blower [37kW motor]	Into system, maximum	14.8	kW
Pump [5.5kW motor]	Into system, maximum	2.75	kW
Environment	Unidirectional	-	-
Cooling Water	From system, variable	17.55+	kW

Since the temperature difference between the environment and the system is never expected to exceed 15°C it was assumed to have negligible effect on the energy balance. Table 8.4 in Appendix A is a summary of the heat exchanger design specifications.

3.3.8 Venturi design (E-103)

It was impossible to find one gas flow meter that would accurately measure the gas flow for all the different gasses mentioned in Table 3.2. The other options were therefore to use a Pitot tube, Orifice plate or venturi. The latter was found to be more accurate with a friction coefficient that is a more linear function of the Reynolds number over the operating range. The challenge was then to design the venturi meter, construct it and to add the necessary sensors that will be used to measure and record the gas mass flow. The detail venturi design with correlations and measurements can be found in section 8.2.1 of Appendix A.

3.3.9 System pressure control

In the case where flammable liquids and gasses other than air will be used the system pressure should be maintained slightly above atmospheric pressure. To achieve this a pressure control valve (PCV-107, see Figure 3.8) is place between the regulator valve of the gas cylinder and the surge tank (E-101). To prevent the system from overpressure a liquid seal was constructed and attached to the surge tank. The liquid height in the seal (see pipeline 39 in Figure 3.8) will prevent the system from exceeding a pressure of 10kPa above the atmospheric pressure.

3.3.10 Sensor placing

Digital pressure transmitters:

By measuring the pressure drop across the different trays and sections in the column, the system stability can be monitored. The pressure drop across the de-entrainment section indicates if the mist-eliminator pad is flooded, accumulating liquid, and whether the liquid hold-up on the de-entrainment tray stays constant during sampling. Digital differential pressure transmitters were therefore placed:

1. Over the Chimney (gas distributing section) tray (DPE-201)
2. Over Test trays 1 and 2 (DPE-203/2)
3. Over the de-entrainment tray (DPE-204)
4. Over the mist eliminator pad (DPE-205)
5. Between the Venturi Pressure Tapings (DPE-101)
6. The bottom of the entrainment and weeping hold-up tanks (DPE-208/7)

Absolute pressure transmitters:

The absolute pressure transmitters are used to determine the gas physical properties (density) at the venturi (PE-102) and test tray 1 (PE-206).

Temperature sensors:

In order to control and monitor the system thermal stability and temperature, sensors were placed:

1. At the exit of the heat exchanger, to control temperature (TE-201)
2. At the inlet to the column (TE-202)
3. In the liquid flow path on test tray 1 (TE-203)
4. In the gas flow path between test tray 1 and 2 (TE-204)
5. In the liquid flow path on test tray 2 (TE-205)
6. In the gas flow path between test tray 2 and the chimney tray (TE-206)
7. In the liquid sump close to the exit (TE-207)
8. At the liquid flow meter to convert volumetric flow to mass flow when needed (TE- 210)
9. In the weeping and entrainment hold-up vessels (TE-208/9)
10. At the gas inlet to the column (TE-102)
11. At the venturi input to compensate for temperature (TE-101)

Liquid flow meter:

It was decided to place the liquid flow meter just after the pump before the control valve and bypass pipe line. Since the pump and liquid flow meter have to be shared between the tray column and a packed column (for another project) and due to space restrictions, this was the optimum place. In the case of control valve failure, the liquid flow rate through the bypass line can also be measured.

Venturi flow meter:

It was decided to place the venturi between the gas outlet of the column and the surge tank. Due to the limited space available, this was the best position. The venturi was estimated to weigh approximately 73 kg. At the selected placing an overhead crane was able to move and transport the venturi.

3.3.11 Sensor sizing and selection

Differential pressure transmitters:

From tray pressure drop calculations and suggestions made by Koch-Glitsch all the differential pressure transmitters that were placed across the different column sections was scaled to measure a range of 0 – 4kPa. This range could be converted by the PLC analog card to give a 0 – 4000 digital range, meaning 1000 digital points per 1kPa pressure drop. The same range was chosen for the weeping and entrainment hold-up tanks based on their height of 0.4m.

According to Eq. 8.3 a pressure drop of 4kPa across the venturi would equal a superficial gas (based on air) velocity of 7.9 m/s. Excessive entrainment was achieved at superficial velocities of 5.5 m/s. All the differential pressure transmitters have a turndown ratio of 15:1. It was therefore decided to purchase differential pressure transmitters that can measure a maximum pressure drop of 10 kPa. Detail specifications of the transmitters used are shown in Table 8.5.

Absolute pressure transmitters:

The absolute system pressure is close to atmospheric pressure. The transmitter which would be able to measure this small range has a range of 0-200kPa (abs). To further increase the accuracy and resolution of the measurement the sensors were scaled so that 80kPa equals 4mA (the minimum value) and 120kPa equals 20mA (the maximum value). By reducing the sensor output range the resolution of the measurement increases. Detail specifications of the transmitters used are shown in Table 8.6.

Temperature sensors:

Since accuracy is preferred over measuring range and response time, it was decided to use PT-100 (Platinum Resistance Thermometers) temperature probes instead of thermocouple type sensors.

Liquid flow meter:

The only flow meter that can accurately measure the flow rate for the range of liquids shown in Table 3.3, is a positive displacement flow meter. An oval gear type flow meter that measures a flow rate from 1.8 - 27 m^3/h was purchased and installed. Detail specifications of the flow meter used are shown in Table 8.7.

Gas flow meter:

To verify the accuracy of the venturi meter for other gasses, a CO_2 mass flow meter (FE-102)[1] was purchased and placed in the gas line. Detail specifications of the flow meter used are shown in Table 8.8.

3.3.12 HAZOP, Safety interlocks and control philosophy

In order to develop the control philosophy and strategy a hazard and operability study (HAZOP) was conducted in section 8.3 of Appendix A. Based on the HAZOP study a safety interlock strategy was developed to reduce the probability of equipment (pump, blower, heaters) failure when operating close to limiting design conditions.

The following are the control objectives:

1. Column temperature, by controlling the liquid temperature
2. Liquid flow rate
3. Gas flow rate
4. Sampling the entrainment and weeping rate.
5. Control hot water bath temperature

Table 8.11 is a summary of the control philosophy based on the HAZOP study and the control objectives. The control philosophy was used as an aid to program the control system.

3.3.13 Control system design

The control system can be divided between the control panel with the controllers and switch gear, the human machine interface (HMI) that enable communication between the user and the control panel, and the software with the automation and control loops.

[1] See Figure 3.8

Control panel hardware:

The function of the control panel hardware is to;

1. Convert the analog signals form the different sensors to digital values without losing accuracy. The analog to digital conversion cards has a 12bit resolution meaning it can measure the 0 – 20mA range with a 5µA resolution.
2. Convert digital set points to analog signals for the different valve controllers and actuators.
3. Use the digital values for comparative control.
4. Switch relays and contactors that activate motors and pneumatic valves.
5. Provide safety interlocking by monitoring device operating parameters.
6. Provide the pump and blower with motor rotational speed control through frequency inverters
7. Power all the instruments and sensors
8. Control temperatures, flow rates and pressures

It was therefore decided to use Programmable Logic Controllers (PLCs) with temperature controllers, analog to digital conversion cards, digital to analog conversion cards, and frequency inverters to control the pilot plant operation.

The human machine interface (HMI):

The function of the human machine interface is to:

1. Link the operator with the control system
2. Provide the operator with visual information regarding the system parameters
3. Allow the operator to change set points and make the required selections.

It was therefore decided to use a touch panel as HMI. The touch panel can be used for data logging and was found to be user friendly and inexpensive compared to computer systems. Since the amount of data registers that had to be logged exceeded the number of columns provided in the touch panel data tables, alternative methods were found and will be discussed in section 3.3.14.

The software:

The software was programmed to:

1. Execute comparative control
2. Allocate data registers
3. Convert the digital values from the analog cards, using math and scaling, to flow rates, temperatures, pressures, vibrations, motor load current, and valve positions.

4. Create communication between the PLC, HMI, temperature controllers and frequency inverters.

The PLC and HIM has their own unique software that was programmed to execute the control and automation requirements.

3.3.14 Data recording

Special software was purchased to record the data. The software is computer based and required communication between the computer and the PLC. The software will then monitor the appointed data registers, every 300ms, and log the data every 2 seconds into a .CSV file which can be accessed using Microsoft Excel.

3.3.15 Piping and instrumentation diagram

Based on the detail design requirements and control objectives the P&IDs were constructed as shown in Figure 3.8 and Figure 3.9.

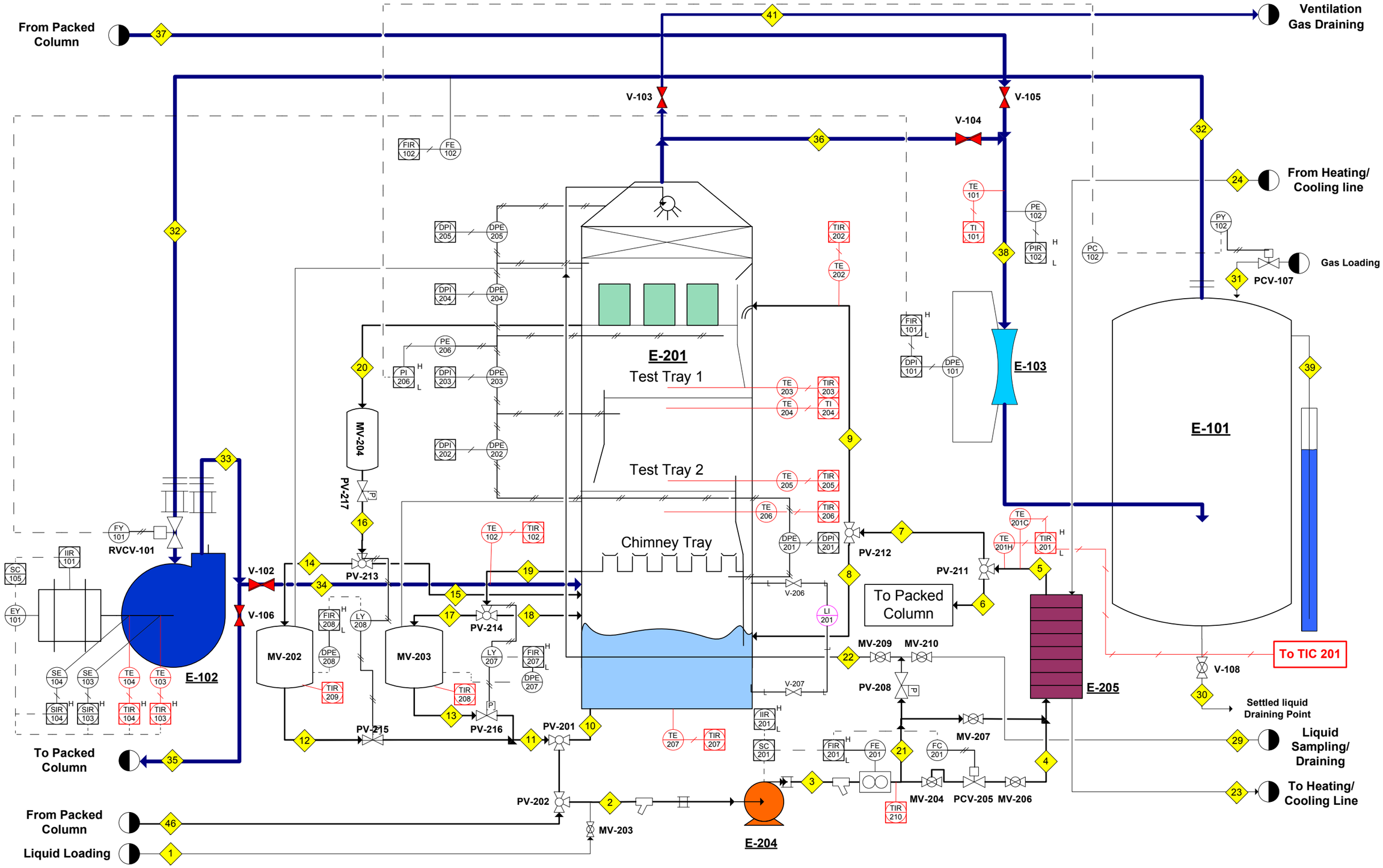

Figure 3.8 The Piping and Instrumentation Diagram of the experimental setup.

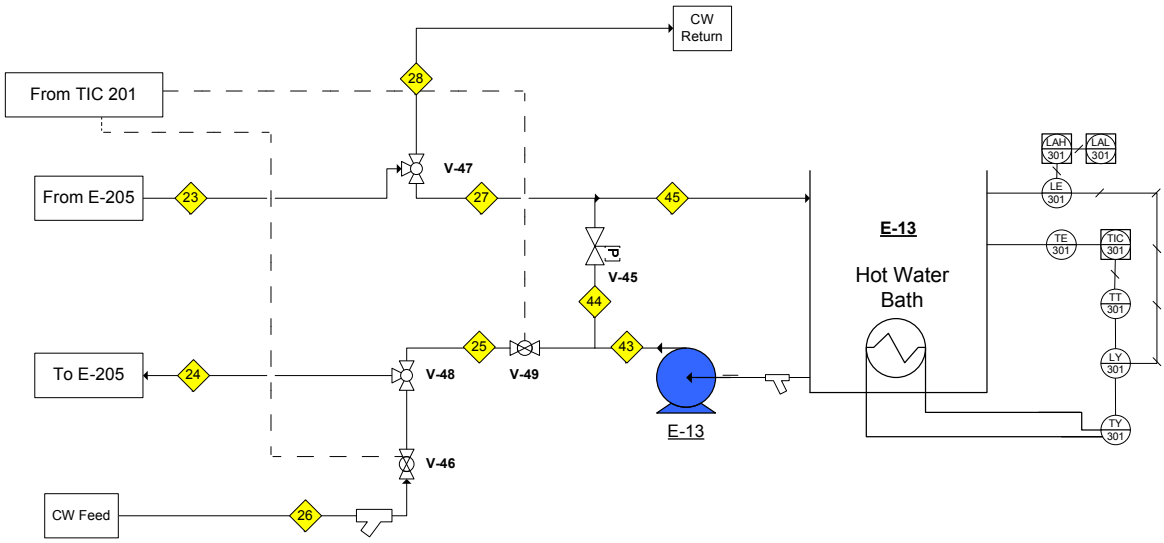

Figure 3.9 The Piping and Instrumentation Diagram of the hot-and-cold water supply section.

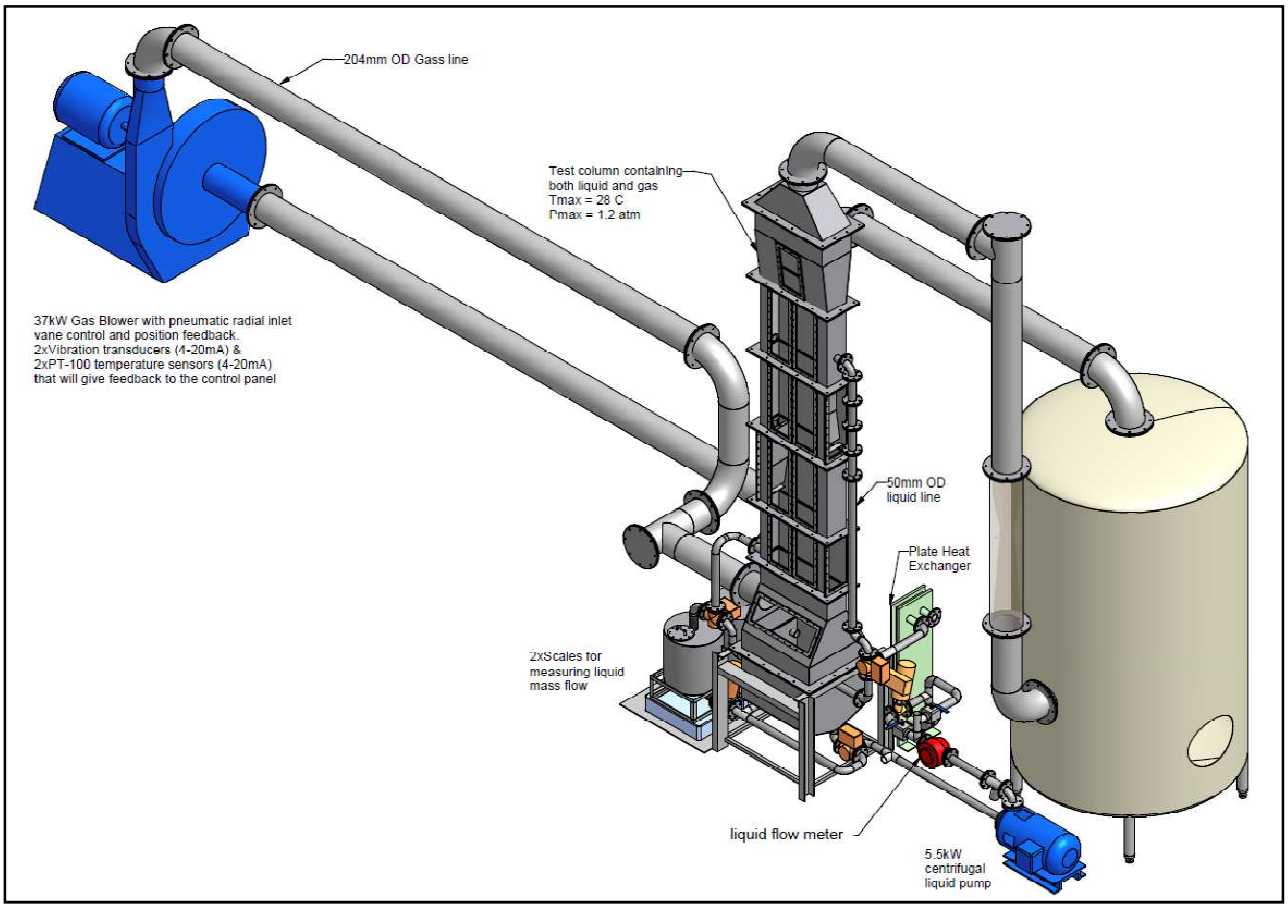

Figure 3.10 Detailed drawing of some of the components of the experimental setup.

3.4 Experimental procedure

The experimental procedure will be explained chronologically from the start-up of the experimental setup until sampling of the data. In order to follow the explanations please refer to Figure 3.8.

Experimental start-up procedure:

1. Start the blower (E-102) with an inverter output frequency setting of around 28Hz. As soon as the blower finishes the start-up cycle the radial vane control valve (RVCV-101) is opened to 30%. At this setting small fluctuations in the valve position will not affect the gas flow rate as much as when the valve position is below 25%.
2. Enter a liquid flow rate set value (10 – 20m^3/h) on the touch panel. Wait approximately 30 seconds for the liquid flow rate control valve (PCV-205) to open, and then start the liquid pump (E-204).
3. After the pump (E-204) has finished the start-up cycle, switch the three way ball valve PV-212 so that the liquid flow through the column (line 9) and not the bypass (line 8) leading to the sump.
4. Switch the cooling water system on and enter 24.8 °C as the liquid temperature set point, which will ensure an average column temperature of approximately 25°C.
5. Monitor the liquid level in the de-entrainment section to prevent the de-entrainment devices from flooding or malfunctioning (when liquid starts to exit the gas-liquid separating devices in the de-entrainment section, flooding occurs). The liquid level in the de-entrainment section should not exceed 70mm. If the de-entrainment section flooded the blower rotational speed must be reduced by reducing the inverter output frequency.
6. The liquid separated by the de-entrainment section exits through a pipeline (line 16), flush with the tray deck, through entrainment hold-up tank (MV-204) to either the entrainment hold-up tank (MV-202) or the sump (line 15). For small entrained liquid rates (L' < 0.07 kg/s) MV-204 must be used to measure entrainment.
7. The liquid captured by the weeping collection (chimney) tray exits through a pipeline (line 19), flush with the tray deck, to either the weeping hold-up tank (MV-203) or the sump (line 18).
8. Before commencing with experiments the entrainment and weeping hold-up tanks should be flushed with liquid (by simulating entrainment and weeping) to ensure the vessel temperatures are simular to the column temperatures.

Experimental procedure:

1. Set the liquid flow rate. To ensure a constant liquid flow rate the control valve will be fully opened by selecting a liquid flow rate set value of 20m^3/h. The pump rotational speed should then be increased or decreased, by changing the inverter output frequency (15 - 50Hz), until the liquid flow rate is approximately 0.5 m^3/h above the required flow rate. Enter the required liquid flow rate set point so that the control valve (PCV-205) can control the liquid flow rate continuously.
2. Change the gas flow rate (by changing the blower rotational speed) until there is a 10 and 70mm visible liquid level in the de-entrainment section.
3. 5 minutes after the column temperature, the differential pressure of each section, gas flow rate, and liquid flow rate has stabilized a sample should be taken. To determine if the system is stable temperature, pressure, and gas and liquid flow rate graphs are plotted on the HMI. Approximately 5 minutes after all the graphs show zero change (gradient of zero) the system is defined as stable.
    a. Automated sequence for small liquid entrainment rates (L' < 0.07 kg/s):
        i. The liquid exiting the de-entrainment section will fill MV-204 by closing PV-217.
        ii. The mass of the liquid inside the tank (MV-204) is logged against time until the sample volume is reached whereafter PV-217 will open to drain the liquid to the sump.
    b. Automated sequence for larger liquid entrainment rates (L' > 0.07 kg/s):
        i. The liquid exiting the de-entrainment section will fill the hold-up tank (MV-202) by switching PV-213. The mass of the liquid in the tank is logged against time. As soon as the sample volume (which is pre-selected) is reached PV-213 will switch back so that the de-entrained liquid can flow to the sump.
        ii. PV-215 will then open followed by PV-201 so that the pump can empty the tank. Just before the liquid level in the tank reaches the bottom (5-7 litres remaining) PV-215 and PV-201 will switch back so that the pump is fed from the column sump.
4. This procedure should be repeated 3-4 times for each liquid and gas flow rate setting to ensure accurate results and to determine if the system was stable. Change the gas flow rate (increase or decrease in random order) to measure a different entrainment rate. Four to five gas flow rates should be used to measure the entrainment rate per liquid flow rate.
5. Change the liquid flow rate (increased or decreased in random order) and follow the same procedure as described in steps 1 – 6.
6. To test the system repeatability experimental conditions (flow rates) should be repeated on different dates and compared as shown in Figure 8.5.

7. For liquid flow rates below 7m^3/h (40m^3/(h.m)) the downcomer escape area should reduced to prevent gas from bypassing through the downcomer (due to an insufficient down comer seal which will occur at liquid velocities below 2.3 m/s). A sensitivity analysis, see Figure 4.1 to Figure 4.3, was conducted to test the influence of the change in downcomer escape area on entrainment for certain liquid rates.

3.5 Factors affecting measurement accuracy

To ensure that the measurements are accurate, all the sensors were calibrated and their measurements verified. A detail summary of the calibration and verification procedures is given in section 8.4 of Appendix A which involved:

1. Calibration of the control system.
2. Calibrating the entrainment and weeping hold-up tanks (MV-202/3/4).
3. Testing for gas and liquid leakages.
4. Verification of sensor measurements.
5. Testing the system with air and water.
6. Verification of system repeatability.

All the sensors purchased were calibrated prior to delivery and their calibration certificates can be found in the in the attached CD at the back of the thesis (or on special request to the author).

To ensure each sample is representative of the amount of entrainment in the system the following is of utmost importance when tanking a sample:

1. The pressure drop across each tray should be stable (zero gradient on HMI graph). The pressure drop represents the liquid hold-up on the tray which affects the amount of entrainment.
2. The gas and liquid flow rates should be stable since they both directly affect entrainment.
3. Gas and liquid temperatures and pressure should be stable since these operating conditions will determine the gas and liquid physical properties which in turn will affect the amount of entrainment.

3.6 Data processing

The raw data was processed using MATLAB and the graphs fitted in Excel. A detailed description of the data processing methods can be found in Appendix A, section 8.6.

4 Experimental results & discussion

Tests were conducted with an air/water system. The results will be presented and compared with entrainment predictive trends from the literature. Since most of the correlations in the literature define entrainment as the mass of liquid entrained over the mass of rising gas, a conversion was made to compare the entrainment as mass of liquid entrained over mass of liquid entering the tray. Only some of the authors reviewed in the literature review section (section 2.1) published entrainment prediction correlations as shown in Table 2.17. In this work equations 2.2, 2.12, 2.38, 2.41, 2.43, 2.57 and 2.58 were used to compare the experimental data with the published entrainment trends. Final conclusions will be made in chapter 5.

4.1 Gas and liquid flow rates

Kister and Haas (1988) and Bennett *et al.* (1995) proposed entrainment prediction correlations (from various data sources) for a liquid flow rate range of 4 – 130 m^3/(h.m). It was therefore decided to test between 17.2 – 112.9 m^3/(h.m) which was the capacity range for the experimental setup. Most of the authors tested for a gas superficial velocity range of 0.9 – 3.7 m/s. Since one of the aims of this investigation is to investigate excessive entrainment it was decided to test for a gas superficial velocity range of 3.4 – 4.6 m/s. This velocity range resulted in a 5 – 20% entrainment range. The overlapping of gas velocity test ranges with the application ranges of the entrainment prediction curves will also show what happens when these entrainment prediction correlations are extrapolated beyond their respective ranges. Table 4.1 is a summary of the gas and liquid flow rates that were used during testing:

Table 4.1 Gas and liquid flow rate ranges used during testing.

	Minimum	Maximum
Q_L [m^3/(h.m)]	17.2	112.9
u_s [m/s]	3.4	4.6

4.2 Experimental results

Since the liquid velocity increases as the downcomer escape area decreases for a constant volumetric flow rate, the momentum of the liquid increases which might influence the entrainment rate (Zuiderweg 1982 based hydrodynamic characterisation on liquid velocity). The first step was therefore to test if the escape area under the downcomer, therefore the liquid velocity, has an influence on the percentage entrainment. It was also necessary to characterise the point where gas start to bypass through the downcomer. Gas that bypasses through the downcomer will have a negative effect on entrainment since only some of the measured gas will pass through the liquid on the tray. The influence of gas velocity on entrainment for a given liquid flow rate was then recorded to characterise and correlate (Figure 8.6 and Figure 8.7) the dependency of entrainment on gas velocity. The final step was to compare the generated entrainment results with the entrainment prediction correlations proposed by the authors mentioned in Table 2.17.

4.2.1 Sensitivity analysis of the downcomer escape area on entrainment

In order to determine the point where gas bypass through the downcomer starts, three different downcomer escape areas were used for the lower (28.6 and 40 $m^3/(h.m)$) liquid flow rates and two downcomer escape areas for the higher liquid flow rates. It was observed visually, and confirmed experimentally in Figure 4.1, that at liquid flow rates of 30 $m^3/(h.m)$ and smaller there was not sufficient downcomer backup (liquid level in the downcomer too low) to seal the downcomer escape area for the largest setting (A_{esc} = 8.575×10^{-3} m^2). The gas therefore bypassed through the downcomer and the measured amount of entrainment was less than for the other two smaller downcomer area of escape settings. This was confirmed in the results as shown in Figure 4.1 , below. There was however no difference in the measured entrainment rates between the smaller two downcomer escape area settings for the low liquid flow rate of 28.6 $m^3/(h.m)$.

At a higher liquid flow rate of 40 $m^3/(h.m)$ the downcomer escape area, perfectly sealed, had no effect on the measured entrainment as shown in Figure 4.2 below. Therefore the only effect the downcomer escape area has on entrainment is when the escape area is large enough for gas to bypass through the downcomer due to insufficient liquid backup in the downcomer. It was decided to use the liquid velocity as a guideline to ensure operation with a positive downcomer seal. Table 4.2 was constructed to assist in determining the liquid flow rates for each downcomer area of escape setting. From Table 4.2 it is clear that the liquid velocity through the downcomer escape area should be above 0.23m/s to ensure a sufficient downcomer seal. This corresponded with the liquid velocity range of 0.3 – 0.6m/s

proposed by Koch-Glitsch the tray manufacturer. Therefore, if the liquid velocity is too high the liquid level in the downcomer will be too high causing the downcomer to flood, whereas a low liquid velocity will result in gas bypass through the downcomer.

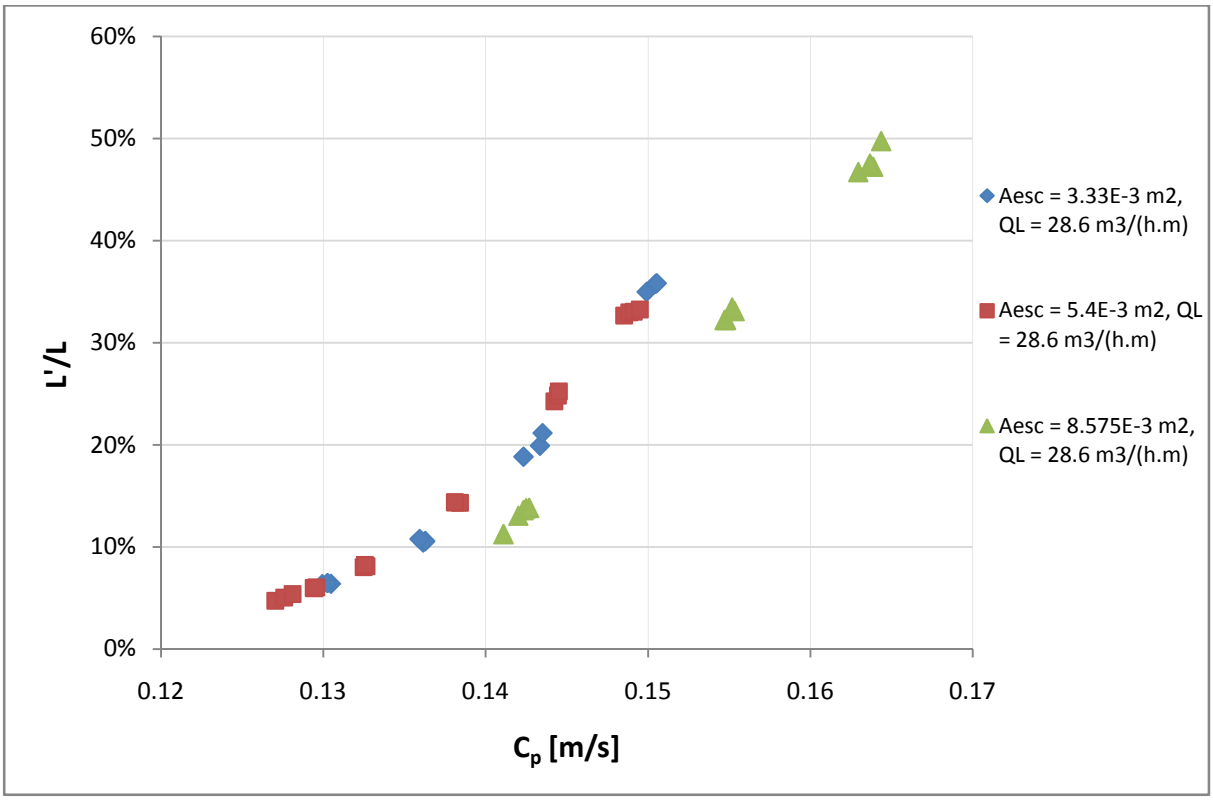

Figure 4.1 The influence of the downcomer escape area on entrainment as a function of the capacity factor $C_p = u_p\sqrt{\rho_g/(\rho_L-\rho_g)}$ for a liquid flow rate of 28.6 m^3/(h.m).

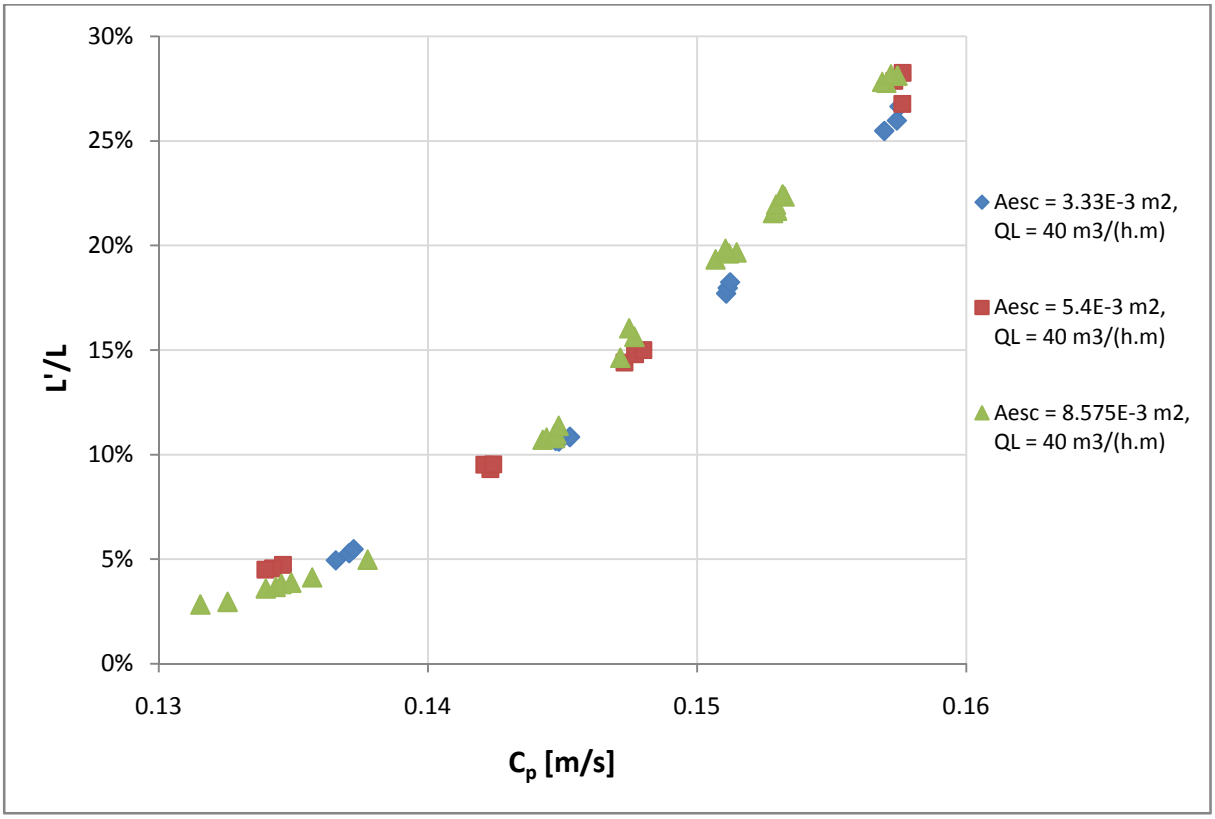

Figure 4.2 The influence of the downcomer escape area on entrainment as a function of the capacity factor $C_p = u_p\sqrt{\rho_g/(\rho_L-\rho_g)}$ for a liquid flow rate of 40 m^3/(h.m).

To test the hypothesis that the downcomer escape area does not have any influence on entrainment, another comparison was made between two downcomer escape area settings for a liquid flow rate of 57.2m^3/(h.m), as shown in Figure 4.3.

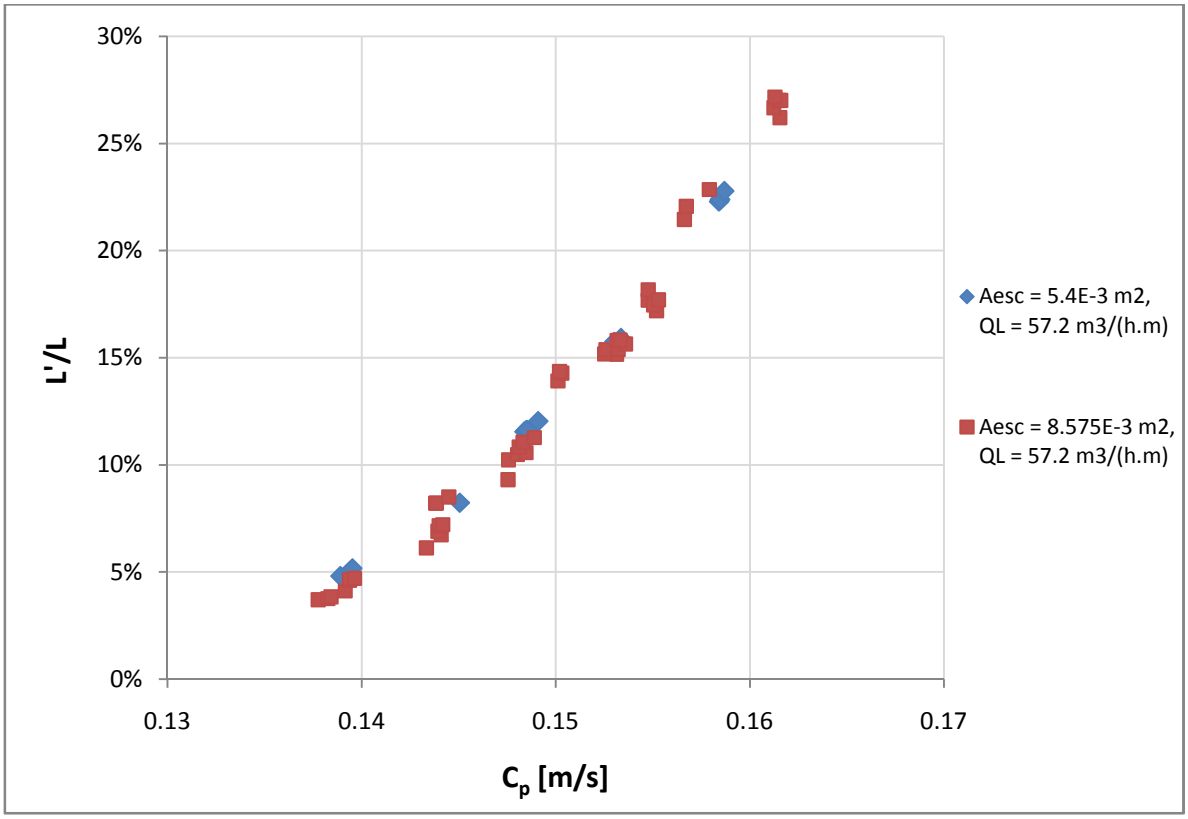

Figure 4.3 The influence of the downcomer escape area on entrainment as a function of the capacity factor $C_p = u_p\sqrt{\rho_g/(\rho_L-\rho_g)}$ for a liquid flow rate of 57.2 m^3/(h.m).

Table 4.2 Liquid velocity for each liquid flow rate against the downcomer escape area

Q_L [m^3/(h.m)]	u_L [m/s] for A_{esc} of 3.33×10^{-3} m^2	u_L [m/s] for A_{esc} of 5.4×10^{-3} m^2	u_L [m/s] for A_{esc} of 8.575×10^{-3} m^2
28.6	0.41	0.26	0.16 ← Gas Bypass
40	0.58	0.36	0.23
57.2	-	0.51	0.32
112.9	-	-	0.64

4.2.2 Entrainment data

In order to generate entrainment data for the air/water system, with physical properties as shown in Table 4.3, it was decided to systematically vary the gas velocity for each liquid flow rate setting. The reason for this was that it is easier to control the liquid flow rate than the gas flow rate. At low liquid flow rates the downcomer escape area had to be changed discarding the option of maintaining a constant gas flow rate and changing the liquid flow rate.

The liquid flow rate was systematically chosen depending on the downcomer area of escape setting and the criteria given in Table 4.2. The gas flow rate was then changed until a liquid level was visible on the de-entrainment tray. Three to four entrainment measurements were taken at each gas/liquid flow rate setting after which the gas velocity was either increased or decreased. The three to four measurements were used directly to generate the entrainment trends and none of the data points were averaged. The raw data can be found in Appendix A, section 8.5. Figure 4.4 and Figure 4.5 shows that by increasing the capacity factor, C_p, and hence the gas velocity for a given liquid rate, an increase in entrainment results. The rate at which the gas velocity increases entrainment differs between the liquid flow rates.

Table 4.3 Air/Water system physical properties used during experimental runs.

ρ_L [kg/m^3]	ρ_G [kg/m^3]	σ [mN.s]	μ [mPa.s]
1020 - 1040	1.16 - 1.19	66 - 68	0.8 – 0.9

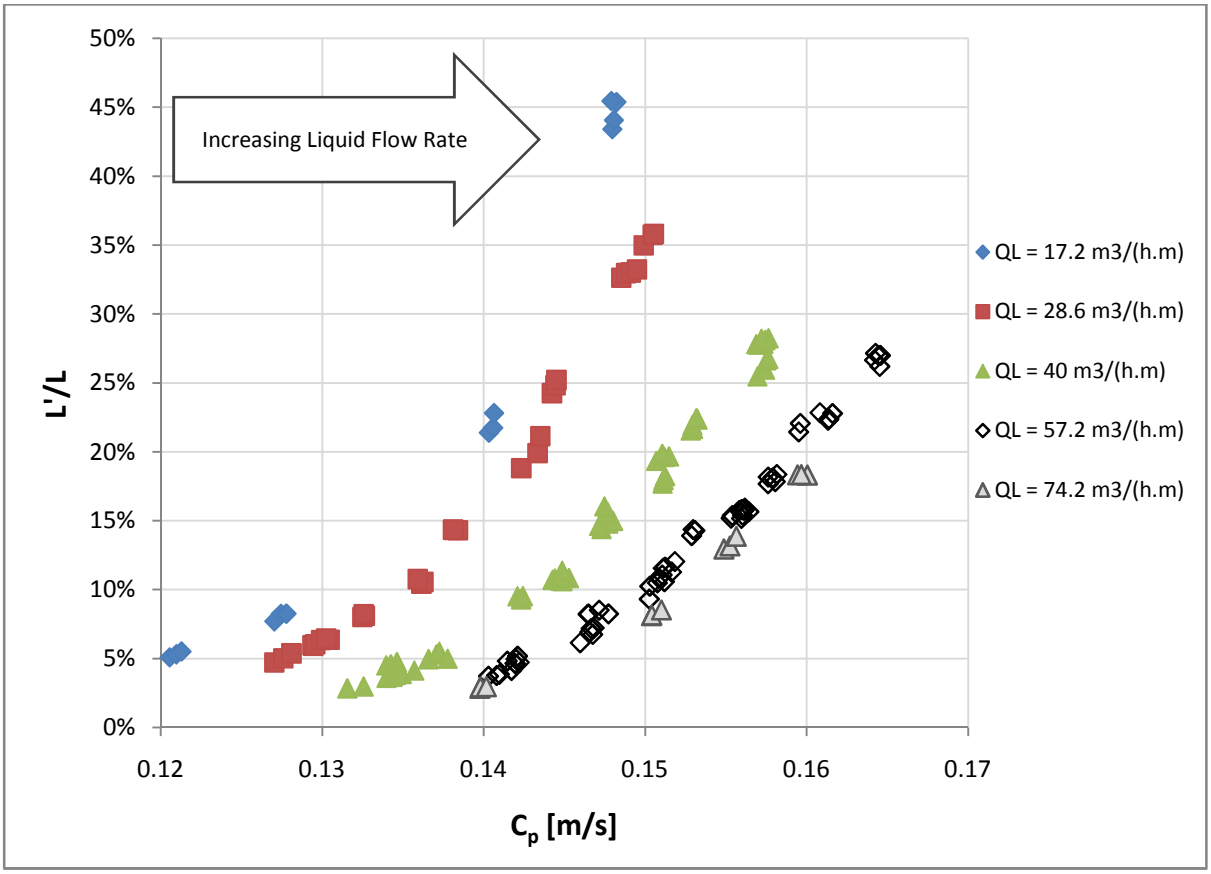

Figure 4.4 The influence of the capacity factor (gas velocity) on entrainment for individual liquid flow rate settings from 17.2 – 74.2 m^3/(h.m).

Figure 4.4 shows that as the liquid flow rate increases from 17.2 – 74.2 m^3/(h.m), the gas velocity has to be increased to maintain a certain percentage entrainment. As the liquid flow rate is increased from 79.9 – 112.9 m^3/(h.m), Figure 4.5, the gas velocity has to be reduced to maintain the percentage entrainment.

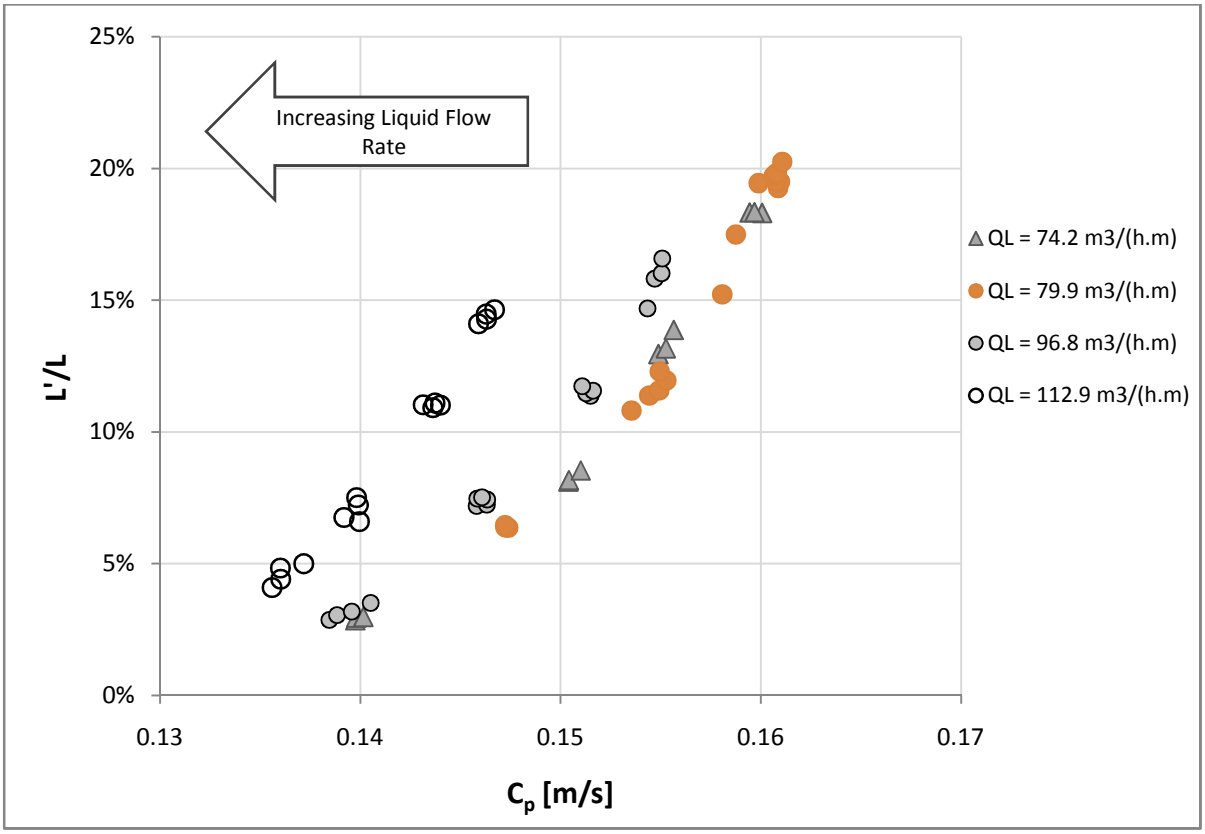

Figure 4.5 The influence of the capacity factor (gas velocity) on entrainment for individual liquid flow rate settings from 79.9 –112.9 m^3/(h.m).

In order to show the effect of the capacity factor and liquid flow rate on the entrainment rate, Figure 4.6 was constructed. This was achieved by manipulating the capacity factor so that a constant entrainment rate was achieved. Figure 4.6 shows that for a liquid range from 17.2 – 74.2 m^3/(h.m) the gas velocity (capacity factor) had to be increased to maintain the percentage entrainment. As the liquid flow rate is increased from 79.9 – 112.9 m^3/(h.m) the gas velocity had to be reduced to maintain the percentage entrainment. There are two main possible reasons for this behaviour. The first possibility is explained by Kister and Haas (1981, 1988) as a change between the flow regimes. They suggest that in the spray regime the gas velocity has to increase with increasing liquid flow rate, since the momentum effects of the cross flowing liquid will suppress jetting at the sieve tray holes and therefore reduce entrainment. As the liquid flow rate increase the liquid hold-up increases to the point where the froth layer is much closer to the tray above, which is commonly found in the froth regime. The droplets ejecting from the froth layer in the froth regime will then have a shorter distance to travel in order to reach the tray above. Consequently, entrainment is favoured by the larger liquid hold-up and the gas velocity has to be reduced to reduce the ejection velocity of the liquid droplets projecting from the froth layer. Colwell (1981) also showed that by reducing the gas velocity the froth height will be reduced resulting in less entrainment.

Figure 4.7 shows that, when entrainment is measured as L'/G, the result is a more complex trend with a possible change in flow regime at low liquid (<30m^3/(h.m)) flow rates. A more simple comparison between the two different methods for measuring entrainment and the influence of the liquid flow rate was done in Figure 2.10.

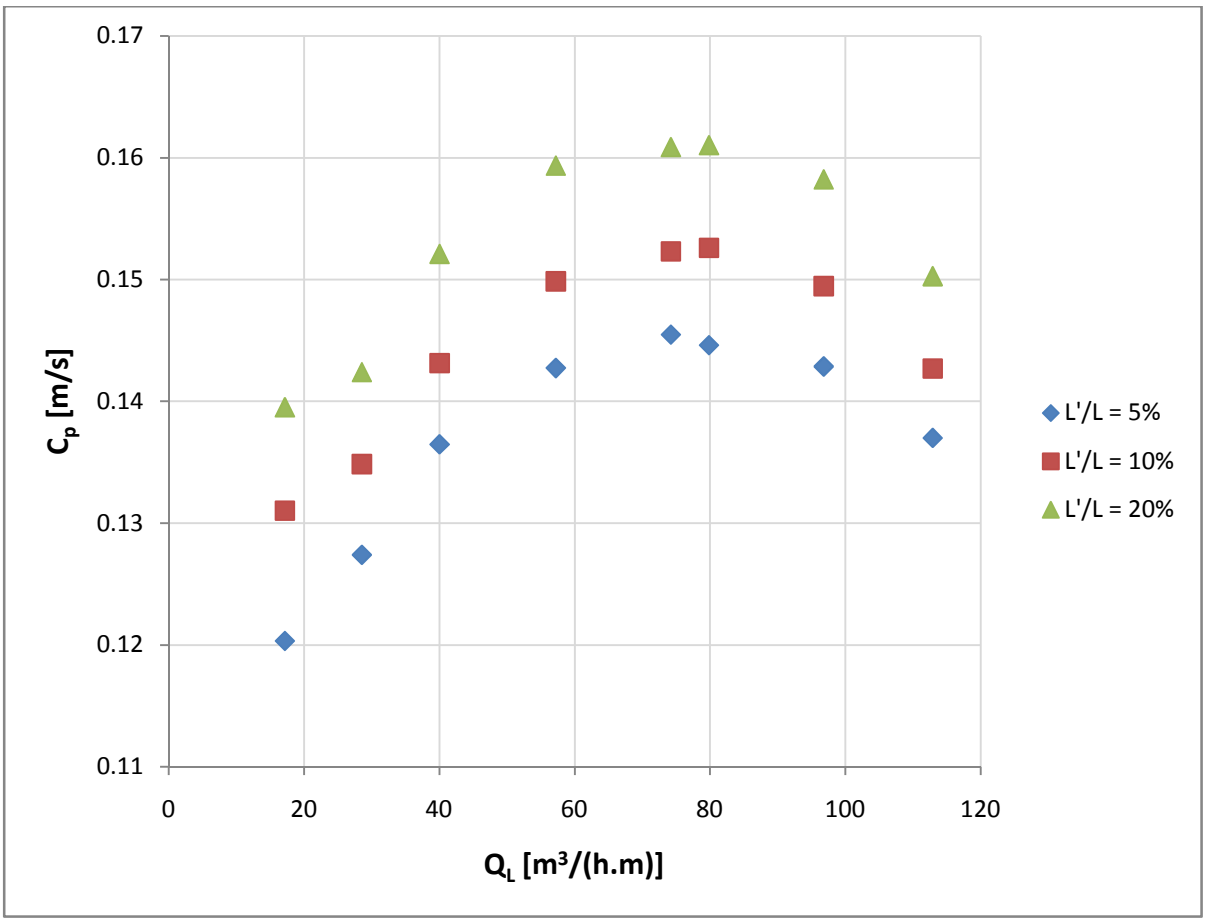

Figure 4.6 Influence of gas and liquid rates on entrainment where entrainment is measured as mass liquid entrained per mass of liquid entering the tray.

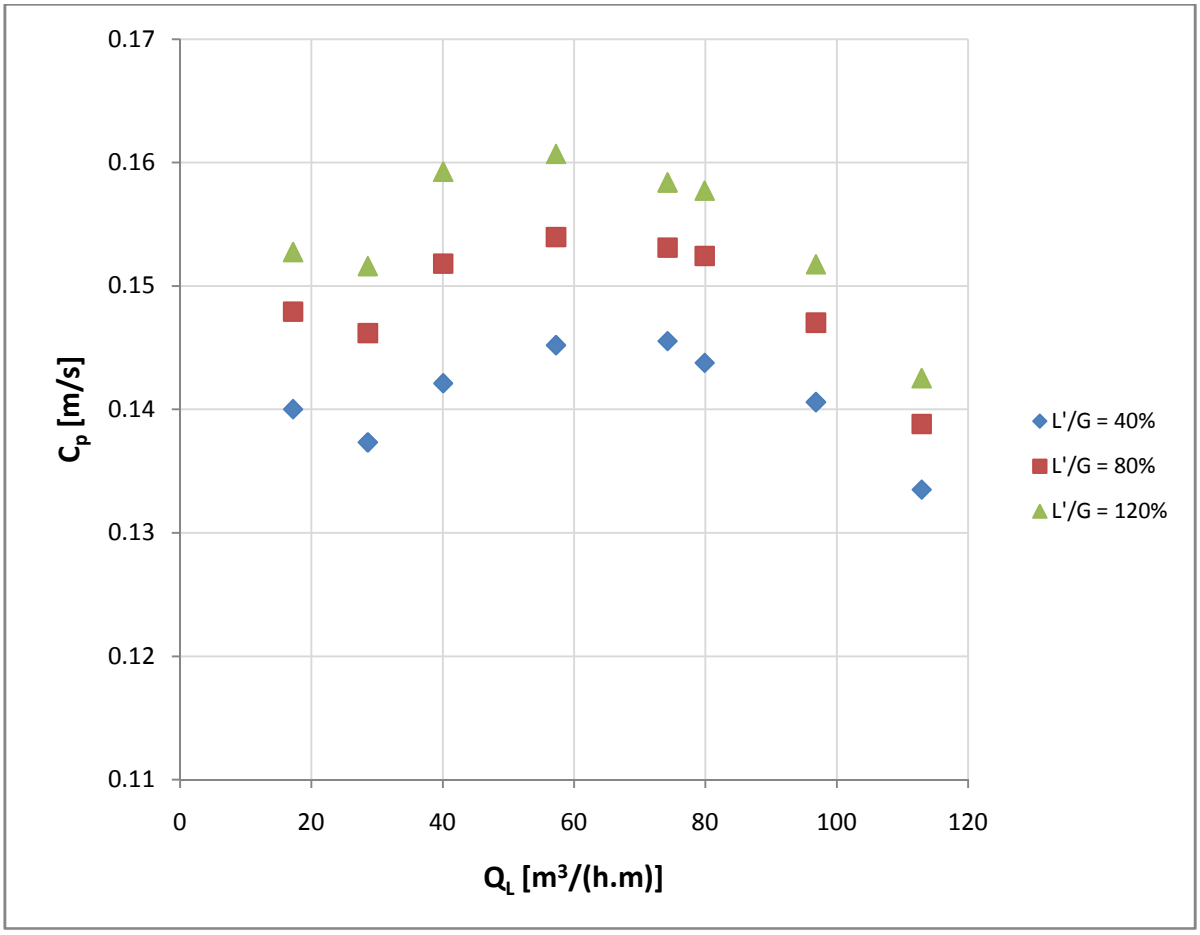

Figure 4.7 Influence of gas and liquid rates on entrainment where entrainment is measured as mass liquid entrained per mass of rising vapour.

The second reason for the change in gas velocity for a given percentage entrainment follows on the increasing liquid hold-up theory proposed by Kister *et al.* (1981) and Kister and Haas (1988). As the liquid flow rate is increased the time or distance required for the froth to develop changes due to the increased horizontal momentum of the cross flowing liquid. As the liquid flow rate increases the momentum of the horizontal flowing liquid increases. Therefore in order to develop a uniform froth a longer flow path is needed at higher liquid flow rates. Since the liquid flow path length of the column used in this work was constant at only 455mm the froth is not fully developed for liquid flow rates higher than 74.2 $m^3/(h.m)$. This observation was also made visually when it was noticed that the froth was pushed up against the opposite wall of the column above the downcomer, see Figure 4.8.

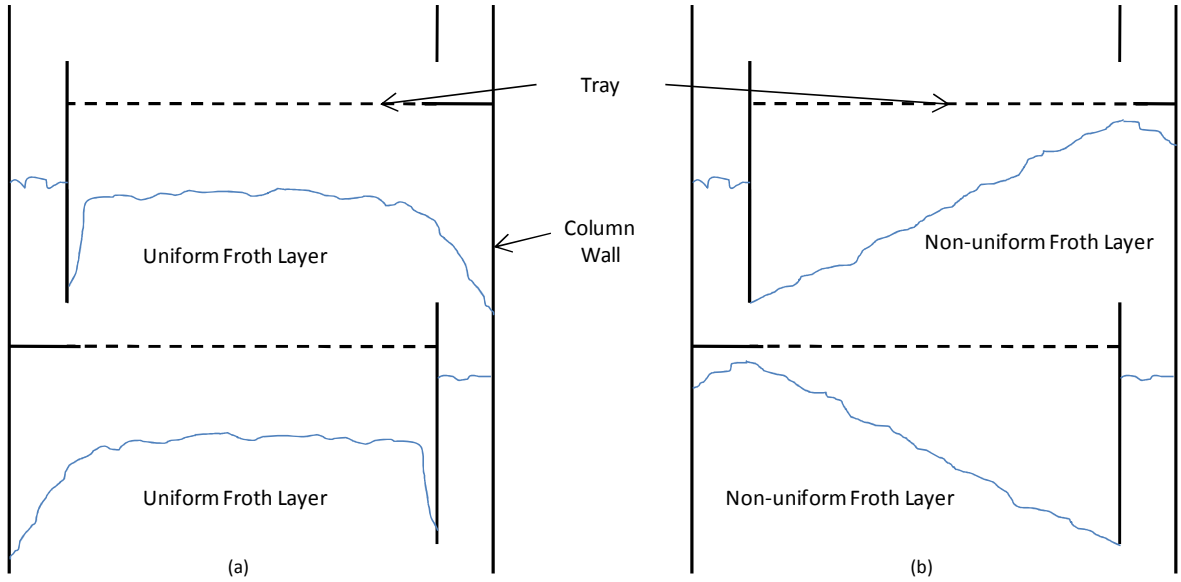

Figure 4.8 (a) Uniform developed froth. (b) Non-uniform developed froth.

As the froth layer pushed up against the column wall the froth layer happens to be much closer to the tray above. This caused most of the droplets ejecting from the froth layer to reach the tray above and increase the percentage entrainment and the gas velocity (C_p) had to be reduced to maintain constant entrainment. According to the flow regime criteria proposed by Kister and Haas (1988) (the largest value between Eq. 2.38, 2.41 and 2.43), and Bennett *et al.* (1995) (Eq. 2.63), the operating regime proposed by this work is the froth regime and never changes. The reason for the increasing entrainment is therefore caused by the increasing liquid flow rate which resulted in the formation of a non-uniform froth layer positioned closer to the tray above. No correlation regarding froth development as a function of the flow path length was found during the literature survey. Hunt *et al.* (1955) mentioned that they chose to use no liquid cross flow in their 152mm round column due to "the unreliability of the performance of liquid overflow weirs in a 152mm diameter column". It was impossible to correlate the effect of flow path length and liquid flow rate on entrainment since this requires the construction of various columns with similar tray geometry.

Kister and Haas (1988) and others suggests that the amount of liquid entrained per mass of gas flowing will increase as the liquid flow rate is increased past the regime transition. This was found to be true as will be shown in Figure 4.9. When the different ways of measuring entrainment are compared (see Figure 4.9) it can be seen that while the entrainment over gas relationship increases the entrainment per liquid load stayed constant. This confirms the findings by Kister and Haas (1988) that an increase in liquid flow rate will increase entrainment (L'/G) in the froth regime, however, if entrainment is related to the amount of liquid on the tray the gas velocity has to be increased to maintain a constant entrainment (L'/L) rate as shown in Figure 4.10. Figure 4.10 was constructed from 5% experimental

entrainment (L'/L) data. To show the difference between the two methods of measuring entrainment the same 5% (L'/L) data is presented as mass liquid entrained per mass rising gas (L'/G) in Figure 4.9.

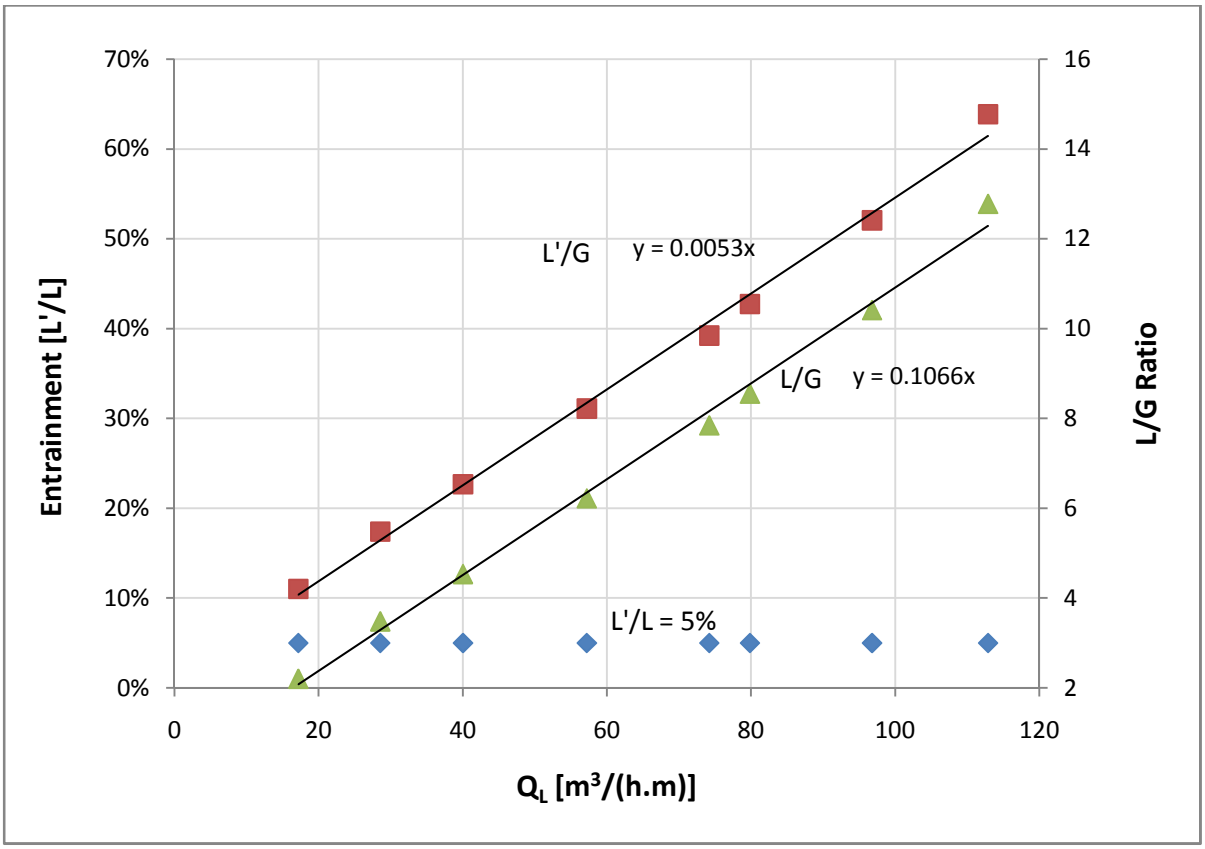

Figure 4.9 Comparing the different methods of measuring the entrainment rate.

Therefore, an increase in entrainment (L'/G) does not necessarily mean that the fraction of liquid on the tray that is entrained (L'/L) increased as well. This method is just another perspective on the influence of liquid flow rate on entrainment.

4.3 Comparing results with predictive trends

The generated results are compared with the entrainment predictive trends (see Table 2.17) in Figure 4.10 for the conditions used in this work (see Table 4.1 and Table 3.4).

By using the flow regime criteria developed by Kister and Haas (1988) and Bennet *et al.* (1995) is was established that the operating regime is the froth regime for liquid flow rates above 40 m^3/(h.m). For liquid flow rates below 40 m^3/(h.m) Kister and Haas (1988) suggests spray regime conditions while Bennett *et al.* (1995) suggests a froth regime. Hunt *et al.*

(1955) and Thomas and Ogboja (1978) did not develop any regime defining correlations. The correlation by Thomas and Ogboja (1978) failed under the conditions required to obtain 5% L'/L entrainment and 40% L'/G entrainment since they measured much lower entrainment rates. Their correlation could therefore not be compared with the experimental data. In Figure 4.10 the 5% entrainment predictive curves are plotted as a function of the capacity factor (based on the gas velocity) and liquid flow rate and compared with the experimentally generated results.

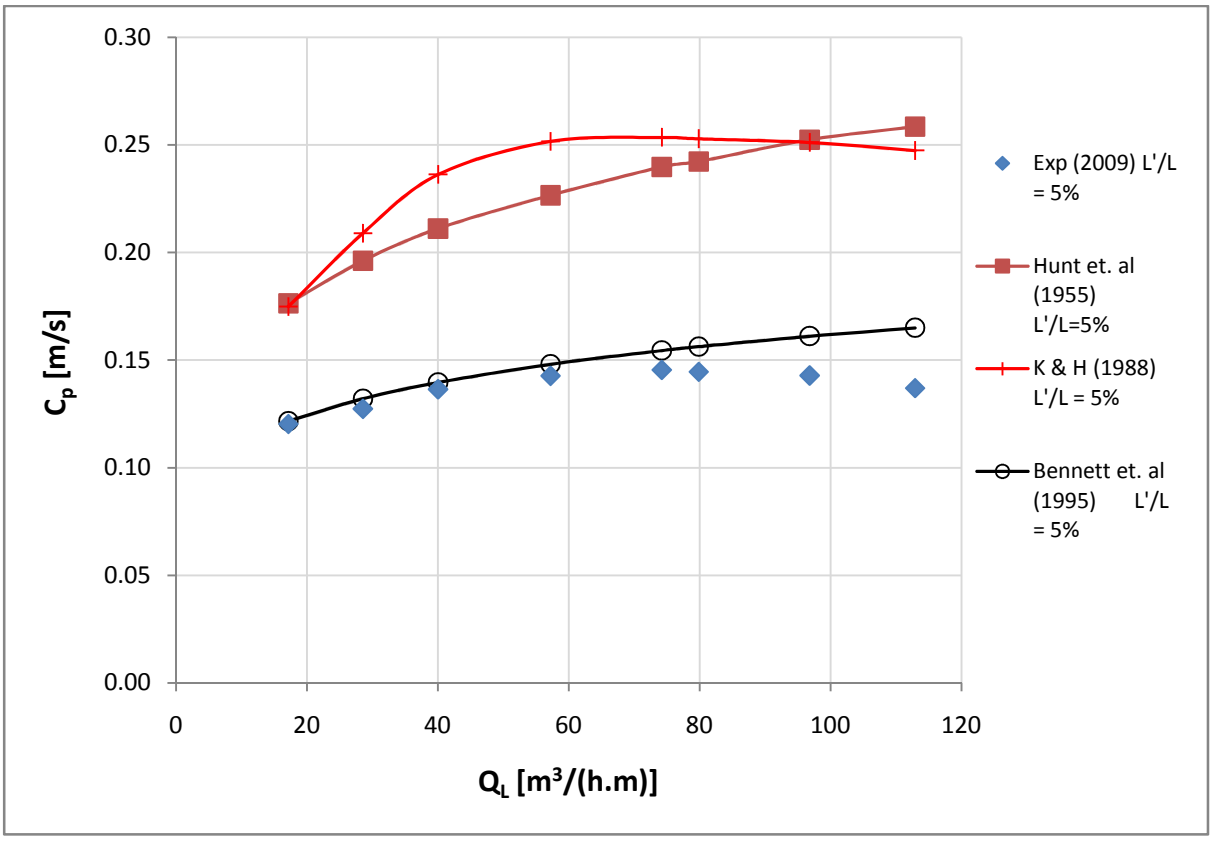

Figure 4.10 Comparing entrainment predictive trends with experimentally generated entrainment data with entrainment measured as L'/L.

To show how the correlations compared with the experimental data when entrainment is measured as L'/G Figure 4.11 was constructed. The sudden inflexion in the correlation by Kister and Haas (1988) in both Figure 4.10 and Figure 4.11 at low liquid rates is due to their anticipation of a change in flow regime from spray to froth regime. It is expected that the correlation of Kister and Haas (1988) would follow the correlation developed by Hunt *et al.* (1955) since Kister and Haas based their froth regime correlation on that of Hunt *et al.* with an empirical hole diameter dependence and a correction term for non-uniformity of the froth at low clear liquid heights.

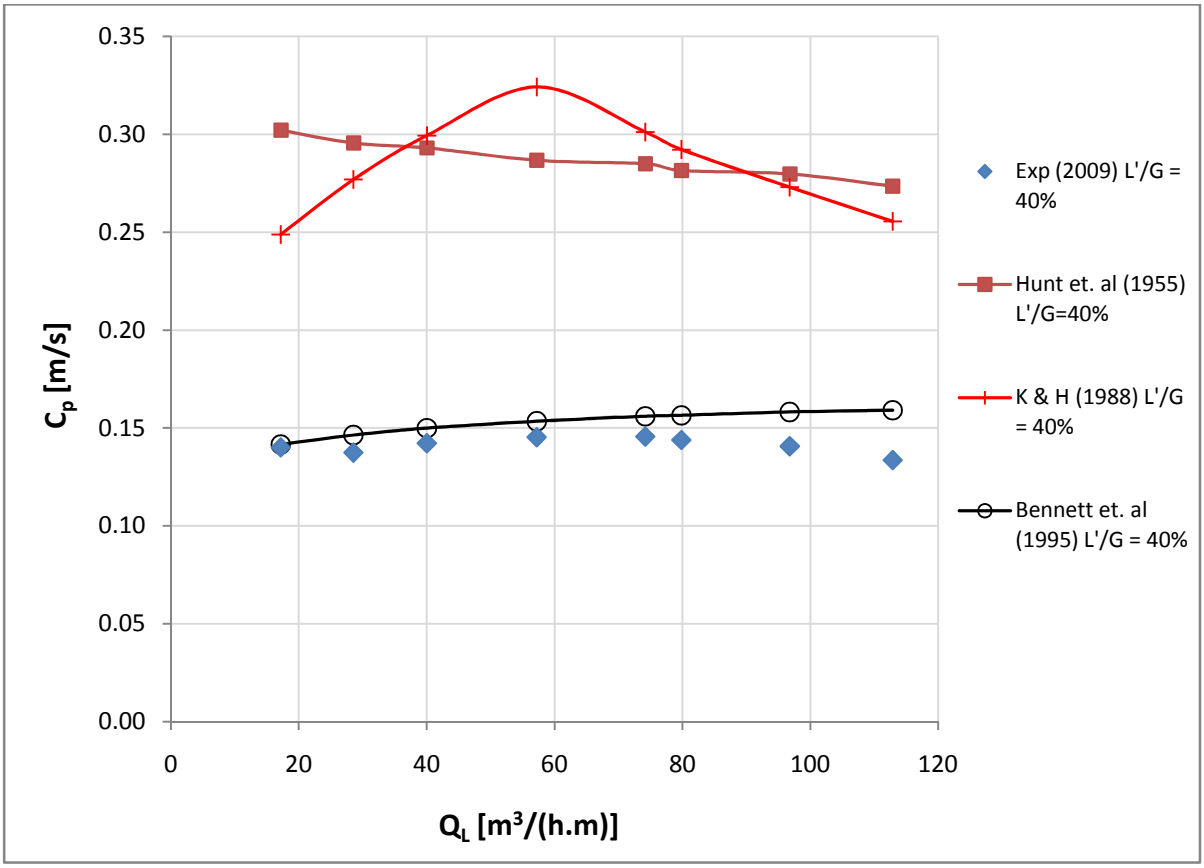

Figure 4.11 Comparing entrainment predictive trends with experimentally generated entrainment data where entrainment is measured as L'/G.

Figure 4.10 shows that the shape of the generated entrainment trends between Hunt *et al.* (1955), Bennett *et al.* (1995), and the experimental data from this work have a similar curvature. The prediction made by the correlation from Kister and Haas (1988) does not follow the same trend as the propositions made by the other authors and the generated data. The differences between the generated data and each one of the predictive trends will be discussed in detail below starting with Hunt *et al.* (1955) and ending with the experimental data.

Since no clear height data was generated in this work, the correlation by Colwell (1981) (Eq. 2.23) was used to calculate the clear liquid heights which were needed for the entrainment prediction correlation developed by Hunt *et al.* (1955). Kister and Haas (1988) also used Colwell's correlation to determine froth heights for entrainment data sets lacking froth height and clear liquid height data. Hunt *et al.* (1955) assumed a constant froth density throughout their gas and liquid flow rate range. Colwell (1981) showed that the froth density is a function of the gas velocity, gas and liquid densities, fractional hole area and clear liquid height. The assumption by Hunt *et al.* (1955) that a uniform froth density exists is therefore an oversimplification. Hunt *et al.* (1955) tested with no liquid cross flow but their correlation is a function of the clear liquid height which is a function of the liquid flow

rate. At high liquid rates the liquid hold-up will increase so that the froth layer is closer to the tray above. Ejecting droplets therefore reaches the tray above much easier and gas velocity has to be reduced. They therefore predicted higher gas velocities which can only apply to no liquid cross-flow applications with lower liquid hold-up than applications with liquid cross flow.

Kister and Haas (1988) used data from various sources in order to pursue a better understanding of the influences of gas and liquid flow rates, and column and tray geometry on entrainment. Even though they specified that their correlation can be used for large range of liquid flow rates (2 – 130 m^3/(h.m)) they do not have data which compares directly to the geometrical parameters and gas and liquid flow rates presented in this work. The high liquid flow rate (49 – 134 m^3/(h.m)) data used to develop their correlation were obtained from Lemieux and Scotti (1969) (presenting 5 trends in their work with only 24 data points which included 3 different tray geometries) who used large hole diameter (12.7 – 25.4 mm) trays with intermediate tray spacing (457 mm), low fractional hole area (0.069 – 0.094), low weir height (25.4 mm) and intermediate gas velocities (Fs = 1.7 – 2.2 $(kg/m)^{1/2}$/s). Most of the data used by Kister and Haas were developed with data obtained from low to intermediate liquid flow rates (4 - 30 m^3/(h.m)) and low to intermediate superficial gas velocities (0.37 – 3 m/s). It is therefore understandable that even though the test ranges of this work falls within most of the application ranges proposed by Kister and Haas (1988), their correlation is extrapolated beyond an accurate range of application and deviations from the experimental data generated in this work is expected.

The gas velocity range (3.3 – 4.0 m/s) used in this work, for the 5% entrainment curve, is much higher than the application range (0.45 – 2.31 m/s) proposed for the correlation developed by Bennett *et al.* (1995). It is, however, surprising how well their correlation follows the data even though it is extrapolated beyond their proposed range of application. The only significant deviation between the predictive correlation developed by Bennett *et al.* and the experimental data were found at the 20% entrainment trends, shown in Figure 4.12. According to the correlation proposed by Bennett *et al.* a gas superficial velocity range of 3.9 – 5.0 m/s is required to maintain 20% entrainment throughout the liquid range. This is much higher than the velocity range, 3.9 – 4.5, covered during the experimental runs.

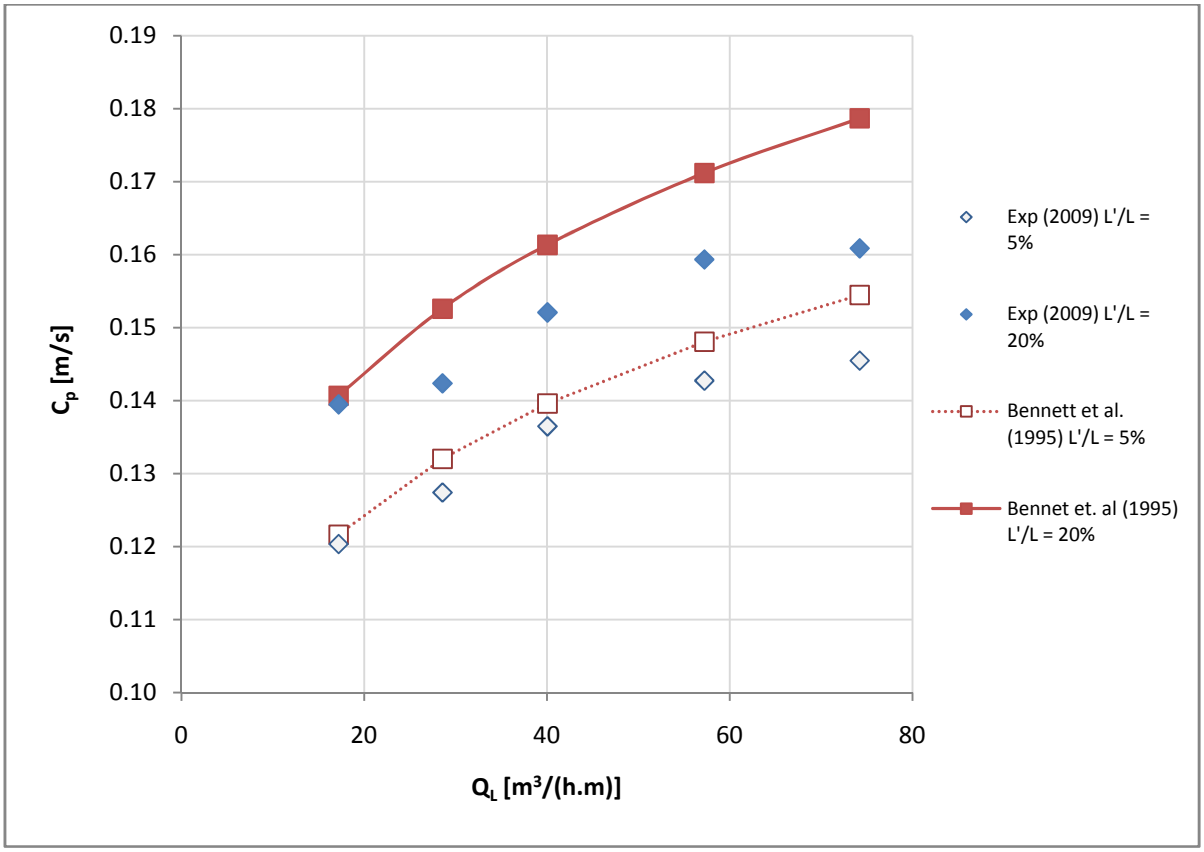

Figure 4.12 Comparison between the experimental data and that of Bennett *et al.* (1995) for 5 and 20% entrainment.

The model developed by Bennett *et al.* (1995) assumed that for small, superficial gas velocities (0.45 − 2.31 m/s), small Weber numbers (0.015 − 1.81) and a relatively large range of Froude numbers (0.134 − 9.29) the effect of droplet drag can be neglected. Droplet drag should only be considered at high superficial gas velocities and high Weber numbers. For the 20% entrainment conditions in Figure 4.12 the superficial gas velocity (3.9 – 4.5 m/s), Weber numbers (1.0 – 2.9) and Froude numbers (6.9 – 12.4) are much higher than the ranges on which Bennett *et al.* (1995) based their correlations. For these high superficial gas velocities the liquid droplet will be carried higher into the space above the froth than when the effect of drag is neglected, resulting in more entrainment than predicted. The correlation developed by Bennett *et al.* (1995) therefore under-predicts entrainment in high superficial gas velocities and the error increases with increasing gas velocity as shown in Figure 4.12.

4.3.1 Deviation between experimental data and predictive trend by Bennett *et al.* (1995)

The deviation between the experimental data and the trend predicted by Bennett *et al.* (1995) increases as the liquid flow rate exceeds 60 m^3/(h.m). This is due to the undeveloped froth (see Figure 4.8) which occurred during the experimental runs for large liquid flow rates. Colwell (1981) showed that the froth height will increases with increasing gas velocity. By increasing the gas velocity the velocity of the droplets ejecting from the froth layer is also higher and more droplets will therefore reach the tray above. At liquid flow rates below 60 m^3/(h.m) and for gas velocities above 3.5 m/s the correlation by Bennett *et al.* (1995) under-predicts entrainment as previously discussed.

4.3.2 Comparison between experimental data and predictive trend by Bennett *et al.* (1995) for a non-air/water (NAW) system

Bennett *et al.* (1995) acknowledges that their non-air/water entrainment prediction correlation, Eq. 2.64, was developed from limited non-air/water data. Since the aim of future work is to investigate the influence of gas and liquid physical properties in entrainment, it was decided to test their prediction correlation for a non-air/water system against the air/water entrainment data generated in this work.

Figure 4.13 shows that there is a significant difference between the entrainment prediction trends developed by Bennett *et al.* for the air/water and non-air/water systems. It is clear that more work is required to investigate the influence of gas and liquid physical properties on entrainment in order to predict entrainment for non-air/water systems with higher accuracy. Bennet *et al.* (1995) suggested that more non-air/water entrainment, froth height and froth density data is required to develop an accurate entrainment prediction correlation.

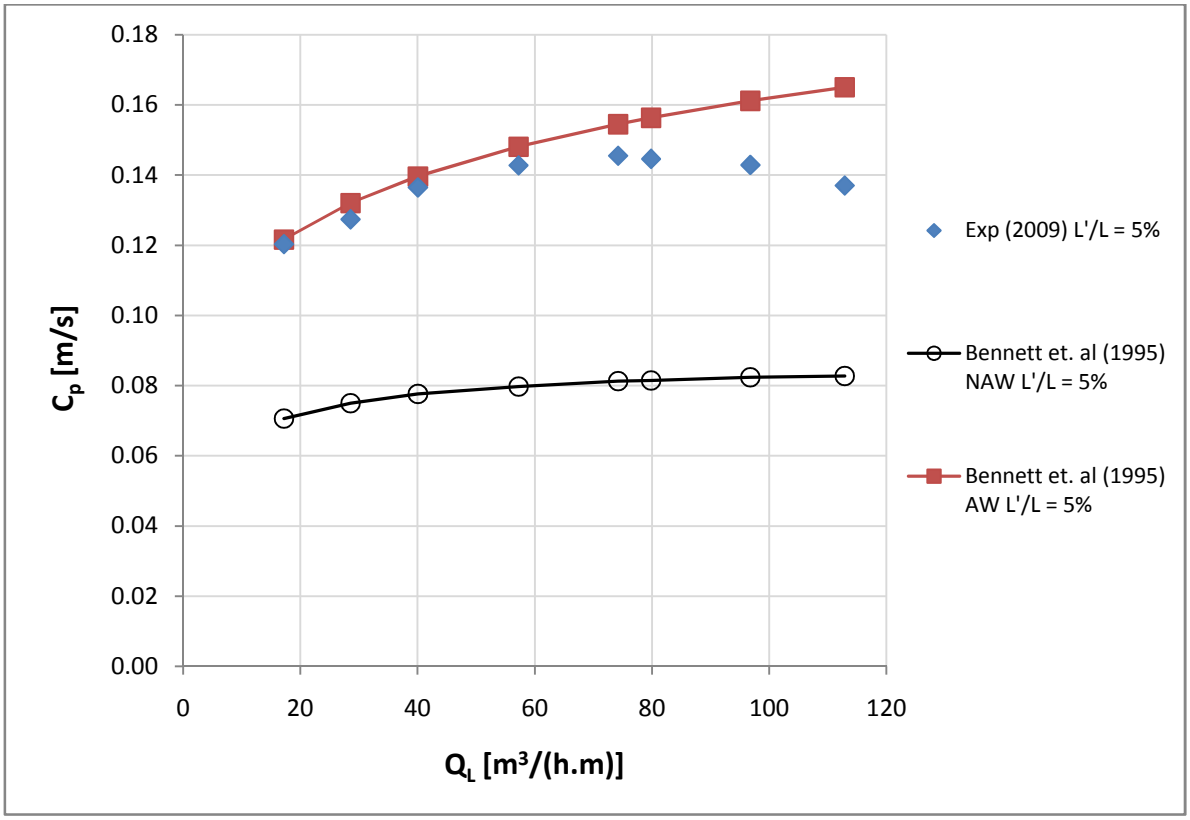

Figure 4.13 Comparison between the experimental data and that of Bennett *et al.* (1995) for 5% non-air/water (NAW) and air/water (AW) entrainment prediction.

5 Conclusions

One of the objectives of this study was to conduct a literature survey to gain insight into the hydrodynamic behaviour inside sieve tray columns that constitutes entrainment. The following conclusions are made based on the findings in the literature:

1. Tray and column geometry, gas and liquid flow rates, and gas and liquid physical properties all have a significant influence on entrainment in both the froth and spray regimes.
2. Most of the work done in the literature is based on air/water system data, which does not account for the influence of gas and liquid physical properties found in commercial distillation, absorption and stripping applications.
3. Bennett *et al.* (1995) proposed an entrainment prediction correlation for non-air/water systems based on very little data. They acknowledge that the database is limited and more entrainment, froth height and froth density data is required for non-air/water systems to improve their correlation.
4. The entrainment prediction correlations developed by Kister and Haas (1988) and Bennett *et al.* (1995) are based on data obtained from various sources with different tray and column geometries and different sampling methods. In order to understand the influence of gas and liquid physical properties and to eliminate the effect of different tray and column geometries, a single column has to be used for all testing.
5. Van Sinderen *et al.* (2003) showed that entrainment is related to the amount of liquid hold-up by using a constant liquid rate and varying weir heights. Kister and Haas (1988) showed that an increase in liquid flow rate will also increase the liquid hold-up. The question is therefore, what is the true influence of liquid flow rate on entrainment other than changing the liquid hold-up and how does the horizontal momentum of the flowing liquid influence the froth behaviour?
6. In the literature entrainment is measured as the mass of liquid entrained over the mass of rising vapour. This measurement does not account for the amount of liquid on the tray and it was decided to measure entrainment as the mass of liquid entrained over the mass of liquid entering the tray. This measurement relates the percentage entrainment to the liquid inventory on the tray and can therefore be used to directly link entrainment with the mass transfer separation efficiency.
7. Most of the entrainment and hydrodynamic data mentioned and used in the literature were generated between 1955 and 1981. There is therefore a need to test new technology trays and to test the methods of old.

Based on the shortcomings found in the literature an experimental setup was designed, constructed and commissioned which can:

1. Measure entrainment with high repeatability for a range of:

   a. Gas and liquid systems (see Table 3.3 and 3.4)
   b. Different tray spacings (315, 415, 515 and 615 mm)
   c. Range of gas (0 – 5 m/s) and liquid flow rates (17.2 – 112.9 m^3/(h.m))
   d. Different downcomer area of escape settings
2. Measure weeping for future testing.

Tests were conducted with an air/water system, without changing column or tray geometry, to compare the experimental results with predictive trends from the literature. Based on the results the following conclusions are made:

1. The downcomer escape area should be sized so that the liquid escaping the downcomer should always exceed a velocity of 0.23 m/s in order to create a sufficient liquid seal in the downcomer. In the case were the liquid velocity was 0.16 m/s, the liquid level in the downcomer was too low and the gas bypassed through the downcomer, resulting in less entrainment. For all the liquid velocities between 0.23 and 0.6 m/s the area of escape did not have an effect on the percentage entrainment.
2. Entrainment increases with increasing gas velocity for a given liquid flow rate. The rate at which entrainment increases as the gas velocity increase depends on the liquid flow rate.
3. As the liquid flow rate exceeds 74 m^3/(h.m) (for air/water) a significant increase in entrainment was noted and the gas velocity had to be reduced to maintain the percentage entrainment. This can be explained by the fact that the increasing horizontal momentum of the cross flowing liquid needs a longer flow path length for the liquid and gas to interact and the froth to fully develop. The undeveloped froth, caused by the short (455 mm) flow path, then creates a non-uniform froth that is pushed up against the column wall above the downcomer (see Figure 4.8). Consequently the froth layer is closer to the tray above resulting in most of the droplets ejecting from the froth to reach the tray above and entrainment is increased. By reducing the gas velocity the froth height and ejection droplet velocity is reduced resulting in a decrease in entrainment. Alternatively the tray spacing could also be increased to reduce entrainment. This, however, is not an operating parameter and should be decided during the design phase of a column. The maximum liquid capacity (for an air/water system) of the column used in this work is therefore approximately 74 m^3/(h.m).
4. The entrainment prediction correlation developed by Hunt *et al.* (1955) does not consider the effect of cross flowing liquid and a variable froth density. Their correlation consequently under-predicts entrainment when compared to the experimental data and the entrainment trend predicted by Bennett *et al.* (1995).

5. Thomas and Ogboja (1978) tested for lower tray spacings, lower liquid flow rates, and smaller fractional hole area trays than presented in this work. The sampling methods used by Thomas and Ogboja (1978) were questioned in section 2.4 of this thesis under the critical evaluation section. Their correlation consequently under predicts entrainment when compared the entrainment predictive trends of Hunt *et al.* (1955), Kister and Haas (1988) and Bennett *et al.* (1995) (see Figure 2.9 to Figure 2.11).
6. Although the proposed application range of the correlation developed by Kister and Haas (1988) overlaps the test range of this work it was found that their correlation was extrapolated beyond an accurate range of application. Their correlation followed a different trend than the predictive trends proposed by other authors and the experimental data and under predicted entrainment.
7. Bennett *et al.* (1995) specified that the application range of their entrainment prediction correlation is limited to a gas superficial velocity range of 0.45 – 2.31 m/s. The superficial velocity range covered in the 5% experimental entrainment tests ranged from 3.3 – 4.0 m/s. Even though their correlation was used at elevated gas velocities, the entrainment prediction trend followed the results obtained during the experimental runs very well. It was however noted that as the gas velocity is increased further to 4.5 m/s the deviation between the experimental runs and their prediction increased. They acknowledged that at high gas velocities and low surface tension liquids a loss in accuracy is expected due to the fact that they don't account for the effects of droplet drag on entrainment. Their correlation therefore under predicts entrainment at high gas velocities.
8. The non-air/water entrainment prediction correlation developed by Bennett *et al.* (1995) was also tested against the experimentally obtained air/water results and a significant difference was noted. More work is required to understand why there is such a large difference but, Bennett *et al.* (1995) acknowledged that deviations are expected due to the limited non-air/water data that was available during the development of their correlation. They recommend that more entrainment, froth height and froth density data is required.

6 Recommendations for future work

Based on the findings discussed in the conclusions, the following recommendations are made:

1. Further testing is required to relate froth development with the flow path length. In order to achieve this the flow path length should be increased while maintaining constant tray fractional hole area, tray hole diameter, weir height and tray spacing. By modelling entrainment data for three to four different column flow path lengths, a better understanding of the influence of flow path length on froth development will be achieved. The influence of flow path length is of great importance in multi-pass trays where the flow path length available for froth development is much shorter than on a single pass tray.
2. Large deviations were found with the non-air/water entrainment correlation proposed by Bennett *et al.* (1995) and they acknowledged that more non-air/water entrainment, froth height and froth density data is required to develop a more accurate correlation. Further testing should therefore be conducted using systems other than air/water to fully understand the influence of gas and liquid physical properties on entrainment.
3. Using non-air/water, together with air/water entrainment data, the influence of gas and liquid physical properties on entrainment should be correlated by modelling the influence of gas and liquid density, liquid viscosity, and liquid surface tension on entrainment. In order to develop a 'physical property model' dimensionless grouping (most probably a combination of dimensionless groupings) of the physical properties will be required.
4. The entrainment prediction correlations developed by Kister and Haas (1988) and Bennett *et al.* (1995) are based on limited gas velocity and liquid flow rate data. The influence of gas velocity on entrainment beyond their recommended ranges is therefore unknown. Tests should be conducted over a broad range of gas and liquid flow rates and the dependency of entrainment on gas and liquid flow rates should be correlated to gain a better understanding of the influence of these parameters on entrainment.
5. Bennett *et al.* (1995) stipulated that there is a shortage of entrainment, froth density and froth height data for non-air/water systems. In order to generate froth density and froth height data, gamma ray scans or light transmission equipment is required which is expensive. It is therefore suggested that the liquid hold-up on the tray should be measured by mounting a differential pressure transmitter flush with the tray deck and the other leg protruding into the vapour space above the tray as done by Payne and Prince (1977). The dependence of entrainment on the liquid hold-up should be investigated and correlated since this is a much simpler method to

observe froth behaviour. Using liquid hold-up data together with the gas and liquid physical properties and flow rates a model relating these parameters to entrainment can be developed. If a correlation between liquid hold-up and entrainment can be found, it can be extended to commercial applications. The current experimental setup can only measure tray pressure drop. An additional differential pressure transmitter is therefore required to measure the dynamic pressure drop (one leg of the pressure transmitter inserted flush with the tray deck while the other leg is placed in the vapour space above the froth and below the top tray)

6. Based on the work done by Van Sinderen *et al.* (2003), who tested the influence of liquid hold-up at constant liquid flow rates, it is recommended that the influence of liquid flow rate on froth development and entrainment should be investigated. Tests should be conducted at fixed liquid hold-up conditions so that the momentum effect of the horizontal flowing liquid can be quantified and the influence thereof on entrainment correlated.

7 References

Arnold, D.S., Plank, C.A. and Schoeborn, E.M., (1952) *Chem. Eng. Prog.*, 48, 633

Bennett, D.L., Kao, A.S. and Wong, L.W., (1995) *AIChE Journal,* 41, 2067-2066

Bolles, W.L. and Smith, D.B. "*Design of Equilibrium Stage Processes*" McGraw-Hill: New York, 1963

Colwell, C.J., (1981) *Ind. Eng. Chem. Process Des. Dev.*, 20, 298-307.

Crowe, C.T., Elger, D.F. and Robertson, J.A. "*Engineering Fluid Mechanics"*, 7th Edition, John Wiley & Sons, Inc.

De Goederen, C.W.J., (1965) *Chem. Eng. Sci.,* 20, 1115 – 1124

Fair, J.R. (1961). *Pet Chem. Eng*. 211-218

Friend, L., Lemieux, E.J. and Schreiner, W.C., (1960) *Chem. Eng.,* 67, 101

Hofhuis, P.A.M. and Zuiderweg, F.J., (1979) *Inst. Chem. Eng. Symp. Ser.* No 56 "Distillation 1979", 2.2/1

Hunt, C.d'A., Hanson, D.N. and Wilke, C.R., (1955) *AIChE Journal,* 1, 441 - 451

Jaćimović, B.M. and Genić, S.B. (2000) *Chem. Eng. Tech.*, 23, 171 – 176.

Jeronimo, M.A. and Sawistowski, H., (1973) *Trans. Inst. Chem. Eng.,* 51, 265.

Jeronimo, M.A. and Sawistowski, H., (1979) *Inst. Chem. Eng. Symp. Ser.* No. 56 "Distillation 1979", 2.2/41

Kister, H.Z., Pinczewski, W.V. and Fell, C.J.D., (1981) *Ind. Eng. Chem. Process Des. Dev.*, 20, 528-532.

Kister and Haas (1987) *Inst. Chem. Eng. Symp. Ser.,*104, p. A483, Inst. Chem. Engrs. (London)

Kister, H.Z. and Haas, J.R., (1988) *Ind. Eng. Chem. Res.*, 27, 2331-2341.

Kister, H.Z., Haas, J.R. and Braun, C.E., (1990) *Chem. Eng. Progr*., 63 – 69.

Kister, H.Z., (1992) "*Distillation Design"*, p.421-519. McGraw-Hill. New York.

Lemieux, E.H. and Scotti, L.H., (1969) *Chem. Eng. Prog.,* 65, 52

Lockett, M.J., Spiller, G.T. and Porter, K.E., (1976) *Trans. Instn Chem. Engrs.,* 54, 202 – 205

Lockett, M.J., (1981) *Trans. Instn Chem. Engrs* (Trans IChemE), 59, 26 – 34

Lockett, M.J. and Banik, S., (1986) *Ind. Eng. Chem. Process Des. Dev.*, 25, 561

Mayfield, F.D., Church, W.L., Green, A.C., Lee, D.C. and Rasmussen, R.W. (1952) *Ind. Eng. Chem.,* 44, 2238

Nutter, D.E., (1979) Inst. Chem. Eng. Symp. Ser. No 56 "Distillation 1979", 3.2/47

Payne, G.J. and Prince, R.G.H, (1975) *Trans. Instn Chem. Engrs.,* 53, 209 – 223

Payne, G.J. and Prince, R.G.H, (1977) *Trans. Instn Chem. Engrs.,* 55, 266 – 273

Pinczewski, W.V. and Fell, C.J.D., (1982) *Ind. Eng. Chem. Process Des. Dev.*, 21, 774 – 776

Pinczewski, W.V., Benke, N.D. and Fell, C.J.D., (1975) *AIChE Journal,* 21, 1210

Prince, R.G.H., Jones, A.P. and Panic, R.J., (1979) *Inst. Chem. Eng. Symp. Ser. No 56 "Distillation 1979"*, 2.2/27

Porter, K.E. and Wong, P.F.Y., (1969) *Inst. Chem. Eng. Symp. Ser. No. 32* "Distillation 1969", 2:22

Porter, K.E. and Jenkins, J.D., (1979) *Inst. Chem. Eng. Symp. Ser. No. 56* "Distillation 1979", 5.1/1

Pupich, P. and Goedecke, R., (1987) *Chem. Eng. Tech.,* 10, 224

Sakata, M. and Yanagi, T., (1979) *Inst. Chem. Eng. Symp. Ser. No 56* "Distillation 1979", 3.2/21

Sakata, M. and Yanagi, T., (1982) *Ind. Eng. Chem. Process Des. Dev.*, 21, 712 - 717

Seader, J.D. and Henley, E.J., (1998) *Separation Process Principles,* John Wiley & Sons, Inc.

Silvey, F.C. and Keller, G.J., (1966) *Chem. Eng. Progr.,* 62 (1), 68 – 74.

Sinnott, R.K. "*Coulson and Richardson's Chemical Engineering Design*", 3rd Edition, Volume 6, (1999).

Souders, M and Brown, G.G., (1934) *Ind. Eng. Chem*, 26, 98 – 103.

Thomas, W.J. and Haq, A.M., (1976) *Ind. Eng. Chem. Process Des. Dev.*, 15, 509.

Thomas, W.J. and Ogboja, O. (1978) *Ind. Eng. Chem. Process Des. Dev.*, 17, 429 – 443

Van Sinderen, A.H., Wijn, E.F. and Zanting, R.W.J. (2003), *Inst. Chem. Engrs.* (Trans IChemE), 81, part A, 94 -106.

Zuiderweg, F.J., (1982) *Chem. Eng. Sci.,* 37, 1441-1464.

8 Appendix A

8.1 Equipment design specifications

Table 8.1 Blower Design Specifications

Gasses to be used	Flow rate [m^3/h]	Delivery Pressure [kPa]
Air	5600	12
CO_2	2100	15
SF_6	900	16
System pressure (max)	1.2	atm
Design Specifications		
Operating temp. range		5 – 80 ºC
Inlet and Exit Pipe diameter		203mm
Motor should be spark proof		
Radial vane control valve at inlet to control gas flow rate		
Blower must be gas tight		
Supply with safety sensors (vibration, bearing temperature)		

Table 8.2 Design specifications for the liquid pump.

Liquids to be used	Flow rate [m3/h]	Delivery Pressure [kPa]
Water	20	±300
Ethylene Glycol	20	±300
Silicone Oil	20	±300

n-Butanol	20	±300
Isopar G	20	±300
Methanol for cleaning	-	-
Design Specifications		
Operating temp. range	5 - 80	ºC
Inlet and Exit Pipe diameter	2"	
Motor should be spark proof		

8.1.1 Surge Tank Design

The surge tank design details will be elaborated upon in this section.

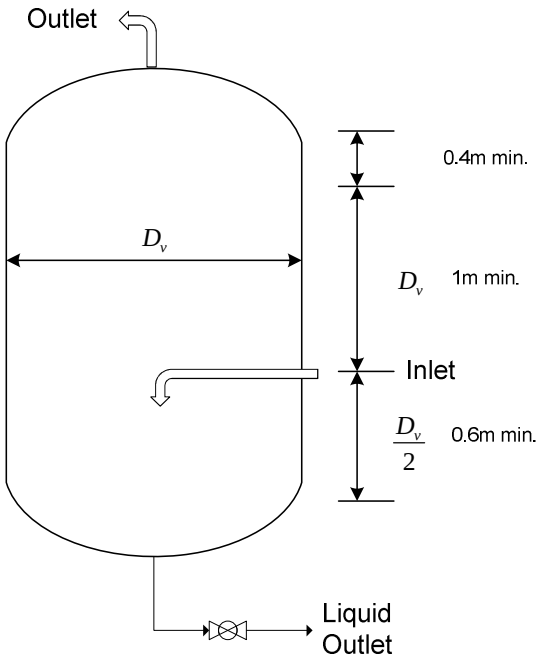

Figure 8.1 Vertical liquid-vapour Separator.

The vessel diameter, D_v, is calculated with Eq. 8.1;

$$D_v = \sqrt{\frac{4Q_v}{\pi u_t}} \tag{8.1}$$

The terminal velocity is a function of the gas and liquid densities;

$$u_t = 0.07\sqrt{\left(\frac{\rho_L - \rho_g}{\rho_g}\right)} \tag{8.2}$$

Using Eq. 8.1, the gas and liquid densities, and the gas volumetric flow rate the geometry of the surge tank was determined as shown in Table 8.3.

Table 8.3 Surge Tank Geometry.

	Description	Values	Units
D_v	Vessel Diameter	1.6	m
	Height	2.8	m
	Volume	5	m^3
$D_v/2$	Inlet Height	0.8	m

8.1.2 Heat exchanger design specifications

The design specifications for the plate heat exchanger are shown in Table 8.4.

Table 8.4 Heat Exchanger Design Specifications.

Description	Inlet Temperature [°C]	Outlet Temperature [°C]	Flow [kg/s]	Flow [m^3/h]
Liquid Side (Based on Water)	25.7	25	5.5	20
Cooling Water Side	20	22	2.1	8
Design Conditions				
Heat Exchanger Type			Plate	
Operating temperature range		20 - 85	ºC	
Inlet and Outlet Pipe diameters		2	in.	
Maximum Pressure Drop		2	bar gauge	
Maximum Pressure		6/7.5	bar gauge	
Materials of Construction		Stainless Steel 316 with compatible seals		
Liquids that will flow through the "liquid" side		See Table 3.3		

8.2 Sensor design specifications

8.2.1 Venturi design

The correlation in Eq. 8.3, which measures the gas mass flow, was derived from the Euler equation for compressible flow assuming isothermal conditions (see Eq. 8.4, for the derivation). This correlation was programmed into the PLC and the output recorded. An absolute pressure transmitter (PE-102)[2] was used to measure P_1, and a differential pressure transmitter (DPE-101) to measure P_2. The differential pressure transmitter was used since it has a higher resolution, sensitivity and accuracy than using another absolute pressure

[2] See Figure 3.8

transmitter. The advantage of this correlation is that by entering the specific gas constant, the mass flow is calculated for that specific gas based on the gas temperature (in Kelvin) and the pressure drop across the venturi.

$$G = C_D A_2 P_2 \sqrt{\frac{2 \ln \frac{P_1}{P_2}}{RT}} \qquad 8.3$$

The physical design of the venturi was obtained from the British Standards Institution (BSI) section 1.1 (1981) for fluid flow in closed conduits. The sizing, as shown in Figure 8.2, was done based on the C_D (discharge coefficient) curve of the venturi. It was decided to size the venturi so that the value for C_D would equal close to one (0.995) where the C_D curve is almost linear. This, according to the BSI, occurs at a Reynolds number range between $2x10^5$ and $1x10^6$. According to Crowe *et al.* (2001) (Engineering Fluid Mechanics 7th edition) the C_D value will range between 1 – 1.02 for this range of Reynolds numbers. The measurements made by the venturi will be validated in a later section of this dissertation.

Constructing the venturi had its own challenges. To ensure that the surface is smooth and uniform it had to be machined from solid mild steel grade EN8. Since the lathe in the department's workshop can only cut tapered sections shorter than 250mm the venturi had to be made in sections that were press fitted together. This required and depended on the skill of the machinist, who executed the task to perfection. The venturi was then electro-galvanized to protect the surface against corrosion.

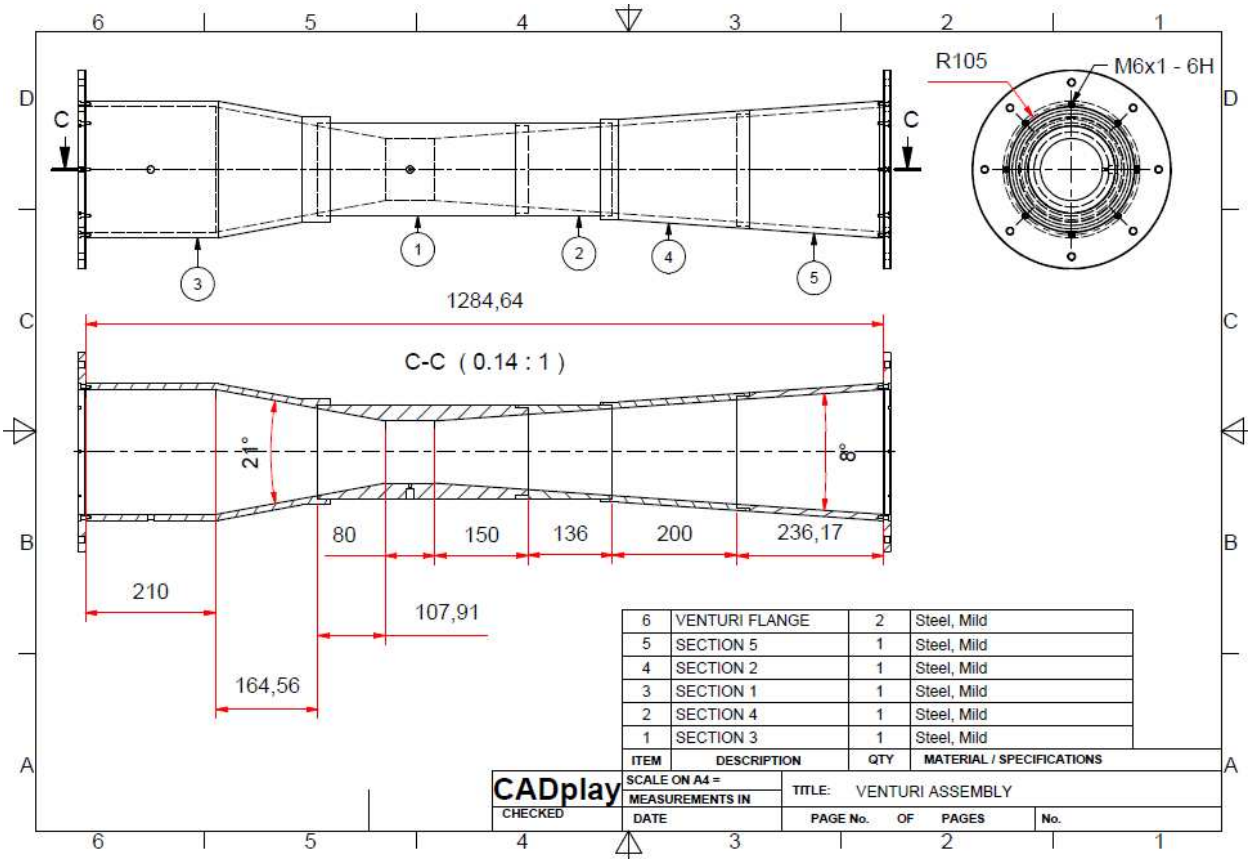

Figure 8.2 Physical dimensions of the Venturi.

Since the fluid is gas it is compressible and is assumed to be isothermal across the venturi. The Euler conservation of mass equation will be used to derive the gas mass flow correlation through a venturi:

$$vdP + udu = 0$$

$$\int_1^2 vdP + \frac{u_2^2}{2} + \frac{u_1^2}{2} = 0$$

$$v = \frac{RT}{P}$$

$$u_1 = \frac{\rho_2 u_2 A_2}{\rho_1 A_1} = \frac{P_2 u_2 A_2}{P_1 A_1}$$

$$RT \ln \frac{P_2}{P_1} + \frac{u_2^2}{2}\left[1 - \left(\frac{P_2 A_2}{P_1 A_1}\right)^2\right] = 0$$

$$u_2 = \sqrt{\frac{2RT \ln \frac{P_1}{P_2}}{1 - \left(\frac{P_2 A_2}{P_1 A_1}\right)^2}}$$

$$C_D = \frac{1}{\sqrt{1 - \left(\frac{P_2 A_2}{P_1 A_1}\right)^2}}$$

$$G = \rho_2 u_2 A_2 = C_D \sqrt{2RT \ln \frac{P_1}{P_2}} \rho_2 A_2$$

$$G = \frac{C_D A_2 P_2}{RT} \sqrt{2RT \ln \frac{P_1}{P_2}}$$

$$G = C_D A_2 P_2 \sqrt{\frac{2 \ln \frac{P_1}{P_2}}{RT}} \qquad 8.4$$

8.2.2 Sensor specification tables

Table 8.5 Digital differential pressure transmitter specifications.

Sensor Specifications	
Make	Endress + Hauser
Measuring Range	0 – 10kPa
Turn Down Ratio	15:1
Measuring Accuracy	±0.05%
Maximum Linearity Error	±0.075%
Special Classification	ATEX II 2G EEx d IIC T6
Membrane Material	316L
Seal	Viton
Output	0 – 20mA

Table 8.6 Digital absolute pressure transmitters.

Sensor Specifications	
Make	Endress + Hauser
Measuring Range	0 – 200kPa abs
Turn Down Ratio	15:1
Measuring Accuracy	±0.05%
Maximum Linearity Error	±0.075%
Special Classification	ATEX II 2G EEx d IIC T6
Membrane Material	316L

Sensor Specifications	
Fill Fluid	Silicone Oil
Output	0 – 20mA

Table 8.7 Liquid flow meter specifications summary.

Sensor Specifications	
Make	Flomec
Measuring Range	1.8 – 27 m^3/h
Zero & Span	Adjustable
Analog Output	4 – 20mA
Analog Output Accuracy	±0.25% Full Scale
Special Classification	IECEX & ATEX approved, Intrinsically safe RT 12

Table 8.8 Gas mass flow meter specifications summary.

Sensor Specifications	
Make	Sierra
Type	Hot Wire Anemometer
Measuring Range	200 – 2100 kg/h
Analog Output	4 – 20mA
Repeatability	±0.2% Full Scale

8.3 HAZOP, Safety interlocks and control philosophy

In order to design the control system with the required safety interlocks, a hazard and operability study was conducted as shown in Table 8.9.

Table 8.9 Hazard and operability table.

Equipment	Gas Blower (E-102)
Intention	Supply column (E-201) with gas at required pressure (100-105kPa) and flow (500 - 3000 m3/h, based on Air)
Line No.	33, 34, 35, 36, 38, 42, 32
Intention	transfer gas to column (E-201)

Guide Word	Deviation	Cause	Consequences	Action
No	Flow	RVCV-101 stuck closed	No flow through column - weeping	Trigger (FAL-101), Stop Blower, inspect RVCV-101 air supply, actuator to valve connection, actuator feedback
		Blower motor failure, Bearing Temp High, Excessive Vibration interlocks	No flow through column - weeping	Shut system down, inspect control loop, Blower bearing temps and vibration level (Trigger Alarms), blower motor

		Duty exceeds blower motor size (gas density high)	No flow through column - weeping	Close RCVC - 101
Less	Flow	RVCV-101 stuck	Less flow through column - weeping	Stop Blower, inspect RVCV-101 air supply, actuator to valve connection, actuator feedback
	Fow	Blower Inverter communication failure	Less flow through column - weeping	Restart Inverter, check inverter error messages
More	Flow	Demister blocked/flooded	Column Pressure build-up	Trigger Column Pressure Alarm High (PAH-206). Shut system down, run cleaning process through spray ball if needed
	Flow	RVCV-101 stuck	Excessive flow - entrainment	Stop Blower, inspect RVCV-101 air supply, actuator to valve connection, actuator feedback

Equipment	Distillation Characterization Tray Column (E-201)
Intention	Simulating distillation hydrodynamic conditions using an inert gas-liquid system at atmospheric conditions and 25 degrees C
Line No.	34, 36
Intention	Simulate distillation hydrodynamics

Guide Word	Deviation	Cause	Consequences	Action
No	Gas Flow	V-102 shut close and/or V-104 shut closed	No flow-weeping	Open V-102 and/or V-104
Less	Gas Pressure	V-102 shut close and V-104 open	No flow-weeping	Trigger (PAL-206), Open valve
More	Gas Pressure	V-102 open and V-104 shut closed	No flow-weeping, glass in window sections will crack	Trigger (PAH-206), stop blower
Equipment	Surge/Settling Tank (E-101)			
Intention	Damp gas pressure fluctuations and settling of liquid droplets			
Line No.	30, 31			
Intention	Load system with gas and maintain system pressure			
No	Pressure	PCV - 102 stuck closed	Drop in system pressure gas leak into the system which could cause fire and or explosion	Trigger System pressure alarm Low (PAL-102) Close regulator on gas bottle, inspect PCV-102 air supply, actuator to valve connection, actuator feedback
	Pressure	Feed Bottle empty	Drop in system pressure in case of gas leak, insufficient system loading	close bottle pressure regulator valve
	Pressure	MV-108 open	Drop is system pressure, gas leakage into environment, fire hazard	Close MV-108, ventilate are

More	Pressure	PCV-102 stuck open	Rise in system pressure	Trigger (PAH -102) close PCV-102 and bottle pressure regulator valve, inspect control valve

Equipment	Liquid Pump (E-204)
Intention	Circulating liquid @ 2-20m3/h & 4-6 bar via heat exchanger (E-205) through column (E-201)
Line No.	2
Intention	Transfer liquid to pump

Guide Word	Deviation	Cause	Consequences	Action
No	Flow	Pump stoped, valves switched to closed lines, low liquid level in sump	No Flow, possible pump cavitation and rise in liquid temp	Trigger FAL-201, stop pump (E-204), re-fill liquid sump
Less	Flow	Strainer blocked, low liquid level in sump		Trigger FAL-201, stop pump (E-204), clean strainer, re-fill liquid sump

Line No.	3
Intention	transfer liquid to heat exchanger (E-205)

Guide Word	Deviation	Cause	Consequences	Action
No	Flow	Strainer blocked, or PCV-205 stuck close, or manual valves closed	Liquid temp & pressure build-up in pump	Trigger FAL-201, stop pump (E-204), clean strainer
		Flow meter (FE-201) rotor failure	Liquid temp & pressure build-up in pump	Trigger FAL-201, stop pump (E-204), open flow meter, inspect strainer

		Pump (P-201) failure	-	Trigger FAL-201, stop pump (E-204), inspect control loop and pump.
Line No.	4			
Intention	Transfer liquid to heat exchanger (E-205)			
Guide Word	**Deviation**	**Cause**	**Consequences**	**Action**
No	Flow	PCV-205 stuck closed	Liquid temp & pressure build-up in pump	Trigger FAL-201, stop pump (E-204), use bypass line 21, inspect valve
More	Flow	PCV-205 stuck open	Flooding of column	Trigger FAH-201, reduce inverter frequency, inspect valve
Equipment	Liquid Heat Exchanger (E-205)			
Intention	Control liquid temperature			
Line No.	23, 24			
Intention	Supply heating or cooling water to heat exchanger			
Guide Word	**Deviation**	**Cause**	**Consequences**	**Action**
Less	Flow	cooling water flow too low due to, cooling tower operation failed, or blocked strainer, or control valve failure	Liquid temp build-up	Trigger TAH-201, stop pump (E-204), inspect strainer, cooling tower outlet temp, cooling line control valve

8.3.1 Safety interlocks

The following safety interlocks, see Table 8.10, were made based on the HAZOP study and equipment failure protection;

Table 8.10 Control system interlocks.

Equipment	Monitor	If	Action
Blower (E-102)	Bearing temp	> 70°C	Stop Motor
[37kW motor]	Axle Vibration	> 7 mm/s	Stop Motor
	Motor Current	> 64 Amps	Close RVCV-101, Stop Motor, Trigger alarm
Pump (E-204)	Motor Load	too high	Stop Pump
[5.5kW motor]	liquid flow rate	< 2m^3/h	Stop Pump
Column (E-201)	Pressure	> 110kPa	Close PCV-107,
		>115kPa	stop blower
		< 98kPa	Open PCV-107
		<95kPa	Stop blower
Surge Tank (E-101)	Pressure	< 96kPa	Open PCV-107
		<93kPa	Stop blower
Hot Water Bath (E-301)	Level	too low	Disable heating elements

8.3.2 Control philosophy

Table 8.11 Pilot plant control philosophy.

Controlled Variable	Manipulative Variable	Type of Control
TI-201	CV-301 (Heating)	Continuous PID
(Column Temperature)	CV-302 (Cooling)	Continuous PID
	PV-303 (Select between heating & cooling lines)	Switch, comparative control
TI-301	Heating Elements (TY-301)	Continuous PID
FI-201	PCV-205	Continuous
(Liquid Flow Rate)		PID
	SC-201 (Motor Frequency)	Set point
FIR-101	RVCV-101	Fixed Setting
(Gas Flow Rate)	SC-105 (Motor Frequency)	Set Point
FIR-207 (Weeping Sampling)	PV-214	Comparative Automation
	PV-216	
	PV-201	
FIR-208 (Entrainment Sampling)	PV-213	Comparative Automation
	PV-215	
	PV-201	

8.4 Verification of the experimental setup

8.4.1 Calibrating and commissioning of the control system

After construction and installation of the control panel was completed the following steps were taken to commission the control system:

1. The analog channels of the PLC were calibrated
2. Automation sequences were tested
3. The interlocks were tested
4. Testing equipment operation

8.4.1.1 *Calibrating the analog channels*

The function of the analog channels is to convert the analog signals from the sensors to digital values and visa versa. To calibrate each channel the channel gain and offset was changed so that the converted digital value represented the sensor measurement value. CALOG – PRO and the CALOG – TEMP calibrators were used to verify the accuracy of the analog to digital, and digital to analog conversions. Table 8.12 and Table 8.13 provide more information regarding the measuring and sourcing specifications of the two calibrators.

Table 8.12 The CALOG – PRO specifications.

Measuring	Analog Input Ranges	Accuracy [%]	Resolution
	0 – 24mA	0.01	1µA
	0 – 32V	0.005	1mV
	-10 – 100mV	0.005	1µV
	0.5 – 100Hz	0.001	0.1Hz
	1 – 20 000Hz	0.001	1Hz

Sourcing	Analog Output Ranges	Accuracy [%]	Resolution
	0 – 24mA	0.01	1µA
	0 – 12V	0.01	1mV

Table 8.13 The CALOG – TEMP specifications.

Measuring	Analog Input Ranges	Accuracy [%]	Resolution
	0 – 24mA	0.02 FS	1µA
	-10 – 100mV	0.01 FS	1µV
	RTD Type Pt 100	0.05 FS	0.01°C
Sourcing	**Analog Output Ranges**	**Accuracy [%]**	**Resolution**
	0 – 24mA	0.02 FS	1µA
	-10 – 100mV	0.01 FS	1µV
	RTD Type Pt 100	0.05 FS	0.01°C

8.4.1.2 *Testing automation sequences*

There are only two automation sequences namely the measurement of the entrainment and weeping rates. The automation sequence was first tested by simulating the measuring procedure. Artificial values were entered into the algorithm to test and adjust the functionality. After all the equipment and utilities were tested a water run was completed to fully test the automation sequence.

8.4.1.3 *Testing interlocks*

All the safety interlocks in the software were tested with artificial values, which represented the system parameters, and by simulating failure conditions. To simulate failure conditions

the sensors that monitored the operation of a specific device would be manually placed in an environment representing a “failure condition” to test the interlock. For example to test the blower bearing temperature interlock one of the temperature sensors was disengaged and placed in boiling water, the interlock was engaged and the blower switched off immediately.

The main interlock is the emergency stops that are placed at four different locations across the plant. If any one of the stops were engaged or activated all plant operation would stop.

8.4.1.4 *Testing the equipment*

After the control panel was tested the equipment was connected. Each individual element or device was then switched on and closely monitored. Since the pump (E-204) and heating elements of the hot water bath (E-301) could not be tested with a dry run, the system was first filled with water.

8.4.2 Calibrating entrainment and weeping hold-up tanks

The weeping and entrainment hold-up tanks were calibrated by determining the cross sectional area of vessel. The area is needed so that the mass can be calculated by Eq. 3.2. The following procedure was followed to determine the vessel cross sectional area:

1. Enter the geometrically calculated value for the vessel area into the correlation provided by Eq. 3.2.
2. The vessel was then filled with water up to the adjustable minimum level, see Figure 3.6, which was the zero reference point.
3. For MV-202/3[3] the following procedures were conducted:
    a. A 20 litre bucket was flushed with water, emptied without towel drying, and placed on a previously calibrated electronic balance which was then zeroed.
    b. A bucket was filled to weigh 15.00 kg. The content was then emptied into the hold-up vessel through an access hole at the top.
    c. The value for the area in Eq. 3.2 was then changed so that the output equalled 15.00 kg.
    d. More water was added in 15.00 kg increments and the area verified.
    e. This procedure was repeated a second time.

[3] See **Figure 3.8**

f. The final verification was done by adding 3 volumes of 15.00 kg into the hold-up vessels (MV-202/3)

4. For the smaller entrainment hold-up vessel (MV-204):
    a. A 5 litre bucket was flushed with water, emptied without towel drying, and placed on a previously calibrated electronic balance which was then zeroed.
    b. The bucket was then filled to weigh 4.00 kg. The content was emptied into the hold-up vessel through an access hole at the top.
    c. The value for the area in Eq. 3.2 was then changed so that the output equalled 4.00 kg.
    d. This procedure was repeated a three times.
    e. To test and verify the linearity of the vessel area a water mass of 2.00 kg was added and it was found that the area required stayed constant.

Table 8.14 and Table 8.13 show the measuring accuracy of the hold-up vessels. From Table 8.14 it can be seen that the measurement accuracy for MV-202/3 is approximately 0.2% excluding the 0.5% accuracy of the PLC analog to digital conversion chart. The measurement accuracy for MV-204 is approximately 0.5% excluding the accuracy of the PLC conversion which is another 0.5%.

Table 8.14 Calibration results for the hold-up vessels (MV-202/3).

Description	Actual	Deviation
Mass Added	15.00 kg	±0.03 kg
Mass Added	30.00 kg	±0.03 kg
Mass Added	45.00 kg	±0.03 kg

Table 8.15 Calibration results for the hold-up vessel (MV-204).

Description	Actual	Deviation
Mass Added	2.00 kg	±0.01 kg
Mass Added	4.00 kg	±0.01 kg
Mass Added	4.00 kg	±0.01 kg

Table 8.16 Calibrated area results for the hold-up vessels (MV-202/3/4).

Description	Area [mm²]
MV-202	123200
MV-203	123300
MV-204	12300

8.4.3 Testing system for leakages

To test the system for leakages compressed air was fed to the system through PCV-107 (the gas pressure control valve) and soap water was sprayed on all the surfaces and joints. Main leakages were found at the blower shaft seal and the window sections. After most of the leakages were sealed the system was then placed under a maximum pressure of 10kPa gage. Modifications were made to the blower shaft seal and gas leakage was drastically reduced. It was impossible to find a shaft seal for the blower that would be able to maintain a complete seal. It was therefore decided to operate the system just above, +5kPa, atmospheric pressure when using gasses other than air.

8.4.4 Verification of sensor measurements

The aim of this part of the work was to verify if the sensor measurements were realistic and the methods used for verification provided approximate “ball park” values.

8.4.4.1 *Calibrating the venturi flow meter*

The venturi measurements were verified using a Pitot tube. Velocity profiles, using Eq. 3.2 and the pressure drop across the Pitot tube, were developed for four different air mass flow rates on the method shown in Figure 8.3.

$$V = \sqrt{\frac{2\Delta P}{\rho}} \qquad 8.5$$

The velocity profiles were determined by moving the Pitot tube in 6 increments from the pipe wall to the pipe centre. The air density was determined using a calibrated digital absolute pressure transmitter measuring the absolute air pressure 1m behind the Pitot tube.

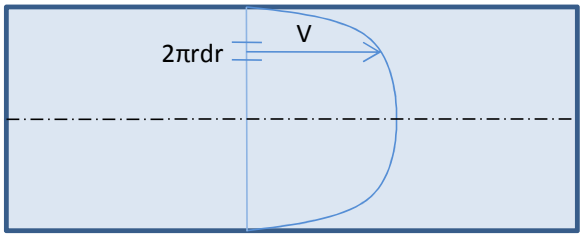

Figure 8.3 Velocity profile across a pipe section.

The velocity profiles were then used to develop Figure 8.4. The area under the graph is used to determine the average air volumetric and mass flow rates based on Eq. 8.6;

$$\dot{m} = \int \rho V 2\pi r.dr \qquad 8.6$$

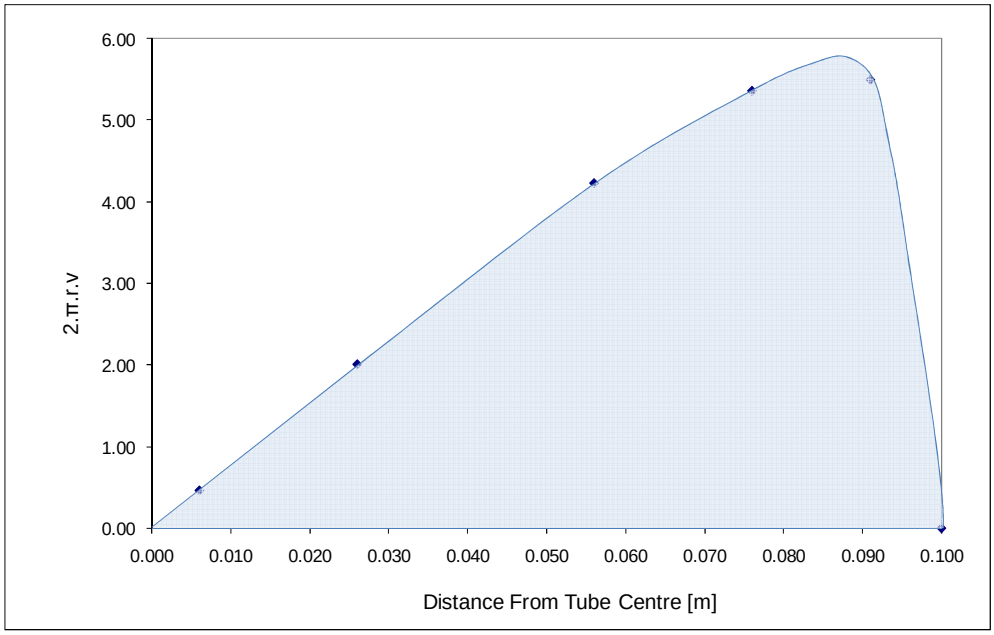

Figure 8.4 The area under the graph method was used to determine the average volumetric flow rate across the gas pipeline for each volumetric flow rate.

Table 8.17 shows the comparative results for the venturi with a C_D value of one with that of the Pitot tube:

Table 8.17 Verification of venturi measurements.

Pitot Tube [kg/h]	Venturi [kg/h]	Pitot Tube over Venturi
831	848	0.98
1118	1130	0.99
1393	1430	0.97
2010	2010	1.00

The measurements made with the Pitot tube was only used as verification of the venturi flow rates.

8.4.4.2 *Liquid flow meter*

The liquid flow meter measurement was verified by measuring a change in the sump volume over time. To do this the sump level was monitored through a level indicator (sight glass) while the water was pumped into the draining system. Since the sump cross sectional area and change in liquid level could be measured the sampling volume was determined. A stop watch was used to measure the sampling time.

Table 8.18 Liquid flow meter measurement verification.

Sample Volume [litres]	Sampling Time	Calculated flow measurement [m^3/h]	Flow meter measurement [m^3/h]
99.1	65.0	5.49	5.48
99.1	23.1	15.44	15.70

Some difficulty was experienced determining the high flow rate since the liquid level in the sump oscillated. The result however confirmed that the liquid flow meter measurements were accurate to an order of magnitude.

8.4.4.3 *Differential pressure transmitters*

The digital differential pressure transmitter measurements were verified without any pressure drop by opening both pressure tapings to the atmosphere to determine the zero point. The max pressure drop of 4kPa was verified by filling a flexible tube with water and elevating it so that the water level is approximately 408 mm above the centre line of the device.

The height was determined with a tape measure and is therefore only an approximation.

8.4.4.4 *Temperature sensors*

The temperature sensor measurements were verified by using the Calog calibrator over a range of 20 - 90°C. The temperature measurements were found to be ±1°C accurate.

8.4.5 Testing the system with Air and Water

After the all the sensor measurements and functionality was verified the system was filled with water and the first runs were conducted. The experimental method and the method the data was acquired will be covered in more detail in a later section of this dissertation.

8.4.5.1 *Verify system repeatability*

Table 8.19 will give an indication of the expected measurement accuracies of the various parameters. The gas mass flow measurement accuracy is calculated in Table 8.20.

Table 8.19 Calculated measurement accuracies.

Parameter	Measurement Accuracy	Maximum Deviation
Entrained Liquid L'	±0.5% MV-202/4 + ±0.5% PLC	0.01×30kg= 0.3kg
Liquid Flow Rate L	±0.25% MV-202/4 + ±0.5% PLC	0.0075×20m^3/h = 0.15m^3/h
Gas Mass Flow Rate [kg/h] see Table 8.20	-0.25% P1&P2, -0.2 [C_D], -1℃ [T]	(2044-2002)/2044 = 2%
C_p [m/s]	±2% From Venturi	0.02×4m/s = 0.08m/s

The gas mass flow accuracy was calculated entering the maximum deviated value for each of the parameters required to calculate the mass flow into Eq. 8.3. The maximum expected deviation was then calculated by comparing the result that does not consider deviation with the result that does as shown in Table 8.19.

Table 8.20 Calculating maximum deviation expected from venturi mass flow meter using Eq. 8.3.

Parameter	Value	Deviation	Value with maximum deviation
C_D [-]	1.02	-0.02	1
P_1 [Pa]	101440	-0.25%	101186
P_2 [Pa]	99250	-0.25%	99002
T [K]	298.2	-1°C	297.2
G [kg/h]	2044		2002

To verify the system repeatability, data was generated on four different days at the same liquid flow rate. Figure 8.5 shows that the data generated at four different dates follow the same trend for the percentage liquid entrained against the capacity factor (based on the perforation area).

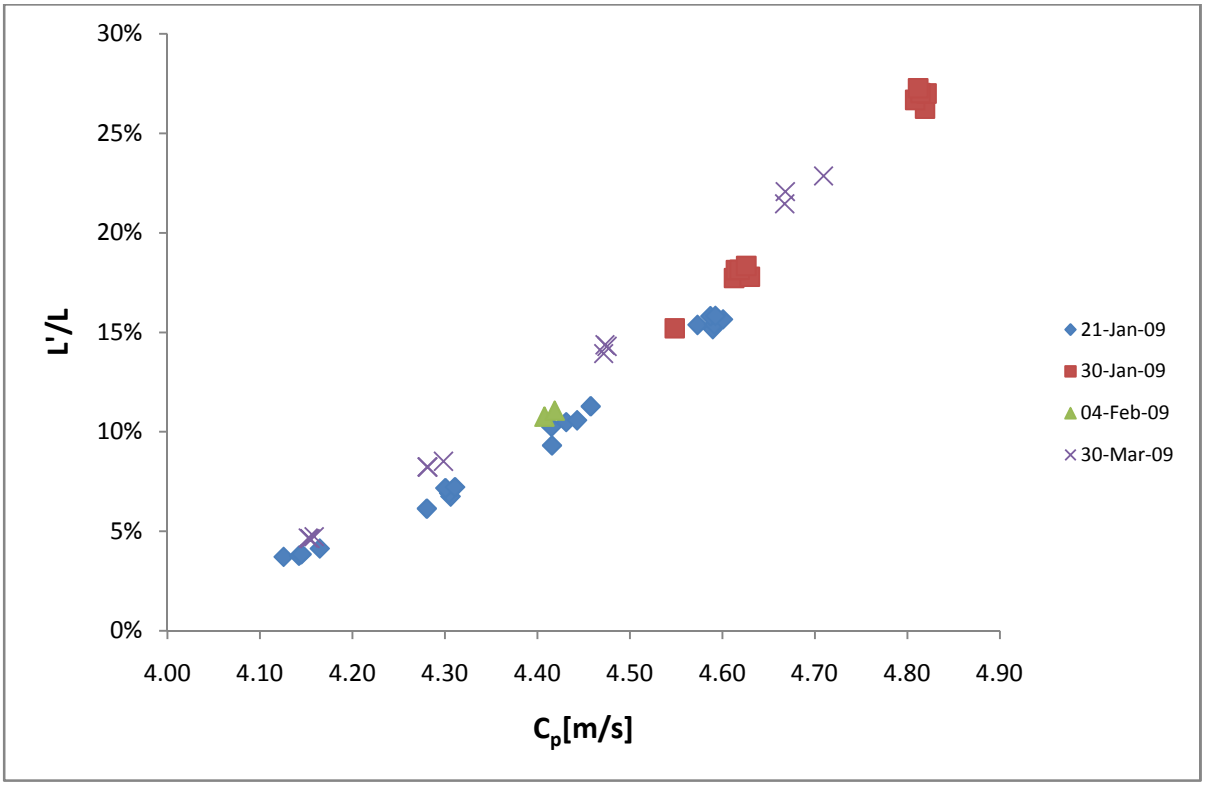

Figure 8.5 Entrainment data collected at four different dates for a liquid flow rate of 57.3 m^3/(h.m).

To prove that the entrainment data sampling order does not affect the generated results data was recorded systematically (see Figure 8.5) for different gas superficial velocities.

8.5 Experimental data for air water at 25°C

The raw experimental data will be presented in the tables (Table 8.21 to Table 8.28) to follow:

Table 8.21 Experimental entrainment data for 17.2 $m^3/(h.m)$ setting and $A_{esc} = 3.33\times10^{-3}$ m^2.

ρ_l [kg/m^3]	ρ_v [kg/m^3]	A_n [m^2]	A_{esc} [m^2]	Liquid Flow [m^3/h]	u_L [m/s]	Q_L [$m^3/h.m$]	Gas Flow [kg/h]	u_s [m/s]	L [kg/s]	L' [kg/s]	L'/L [%]	L'/G [%]	Cp [m/s]
997	1.18	9.538E-02	3.330E-03	2.97	0.248	16.99	1364.05	3.38	0.82	0.04	5.10%	11.09%	0.121
997	1.18	9.538E-02	3.330E-03	2.99	0.249	17.07	1369.19	3.39	0.83	0.04	5.32%	11.58%	0.121
997	1.18	9.538E-02	3.330E-03	2.97	0.248	16.96	1373.22	3.40	0.82	0.05	5.52%	11.90%	0.121
997	1.18	9.538E-02	3.330E-03	2.98	0.249	17.05	1439.82	3.56	0.83	0.06	7.72%	15.94%	0.127
997	1.18	9.538E-02	3.330E-03	2.98	0.249	17.05	1445.09	3.57	0.83	0.07	8.25%	16.98%	0.127
997	1.18	9.538E-02	3.330E-03	2.98	0.249	17.04	1449.56	3.57	0.83	0.07	8.27%	16.96%	0.128
997	1.17	9.538E-02	3.330E-03	3.04	0.254	17.37	1585.85	3.94	0.84	0.18	21.40%	40.91%	0.140
997	1.17	9.538E-02	3.330E-03	3.02	0.252	17.29	1589.13	3.95	0.84	0.18	21.76%	41.29%	0.141
997	1.17	9.538E-02	3.330E-03	3.00	0.250	17.15	1590.43	3.95	0.83	0.19	22.81%	42.93%	0.141
997	1.17	9.538E-02	3.330E-03	3.05	0.254	17.43	1672.36	4.15	0.84	0.37	43.42%	78.96%	0.148
997	1.17	9.538E-02	3.330E-03	3.04	0.253	17.36	1673.36	4.16	0.84	0.37	44.07%	79.79%	0.148
997	1.17	9.538E-02	3.330E-03	3.04	0.254	17.37	1675.70	4.16	0.84	0.38	45.38%	82.10%	0.148
997	1.17	9.538E-02	3.330E-03	3.05	0.254	17.41	1672.24	4.15	0.84	0.38	45.46%	82.59%	0.148

Table 8.22 Experimental entrainment data for 28.6 $m^3/(h.m)$ setting and A_{esc} = 3.33×10^{-3} m^2, 5.4×10^{-3} m^2 and 8.575×10^{-3} m^2.

ρ_l [kg/m^3]	ρ_v [kg/m^3]	A_n [m^2]	A_{esc} [m^2]	Liquid Flow [m^3/h]	u_L [m/s]	Q_L [m^3/h.m]	Gas Flow [kg/h]	u_s [m/s]	L [kg/s]	L' [kg/s]	L'/L [%]	L'/G [%]	Cp [m/s]
997	1.16	9.538E-02	3.330E-03	4.97	0.414	28.39	1459.10	3.67	1.38	0.09	6.35%	21.54%	0.130
997	1.16	9.538E-02	3.330E-03	4.97	0.415	28.41	1463.61	3.69	1.38	0.09	6.37%	21.57%	0.130
997	1.16	9.538E-02	3.330E-03	4.99	0.416	28.50	1461.91	3.68	1.38	0.09	6.45%	21.94%	0.130
997	1.15	9.538E-02	3.330E-03	5.03	0.419	28.72	1525.75	3.85	1.39	0.15	10.42%	34.23%	0.136
997	1.15	9.538E-02	3.330E-03	5.02	0.419	28.69	1527.17	3.86	1.39	0.15	10.55%	34.59%	0.136
997	1.15	9.538E-02	3.330E-03	4.99	0.417	28.54	1524.15	3.85	1.38	0.15	10.77%	35.17%	0.136
997	1.15	9.538E-02	3.330E-03	4.98	0.416	28.48	1593.21	4.03	1.38	0.26	18.82%	58.68%	0.142
997	1.15	9.538E-02	3.330E-03	5.01	0.418	28.62	1604.33	4.06	1.39	0.28	19.90%	61.94%	0.143
997	1.15	9.538E-02	3.330E-03	5.02	0.419	28.70	1606.15	4.07	1.39	0.29	21.14%	65.93%	0.143
997	1.16	9.538E-02	3.330E-03	4.96	0.414	28.35	1688.29	4.22	1.37	0.48	34.98%	102.47%	0.150
997	1.16	9.538E-02	3.330E-03	4.96	0.414	28.33	1694.67	4.24	1.37	0.49	35.75%	104.26%	0.150
997	1.16	9.538E-02	3.330E-03	4.97	0.414	28.39	1695.18	4.24	1.38	0.49	35.81%	104.65%	0.150
997	1.16	9.538E-02	5.400E-03	5.04	0.259	28.79	1428.40	3.59	1.40	0.07	4.72%	16.59%	0.127
997	1.16	9.538E-02	5.400E-03	5.00	0.257	28.57	1434.42	3.60	1.38	0.07	5.02%	17.45%	0.128
997	1.16	9.538E-02	5.400E-03	5.03	0.259	28.73	1440.06	3.62	1.39	0.07	5.37%	18.70%	0.128
997	1.16	9.538E-02	5.400E-03	5.03	0.259	28.77	1455.69	3.65	1.39	0.08	5.93%	20.43%	0.129
997	1.16	9.538E-02	5.400E-03	5.01	0.258	28.66	1455.45	3.65	1.39	0.08	5.97%	20.51%	0.129
997	1.16	9.538E-02	5.400E-03	5.05	0.260	28.84	1457.88	3.65	1.40	0.08	6.04%	20.85%	0.130
997	1.16	9.538E-02	5.400E-03	5.04	0.259	28.79	1492.02	3.73	1.40	0.11	8.01%	26.97%	0.132
997	1.16	9.538E-02	5.400E-03	5.01	0.258	28.62	1493.10	3.74	1.39	0.11	8.10%	27.10%	0.133
997	1.16	9.538E-02	5.400E-03	5.03	0.259	28.76	1492.17	3.74	1.39	0.11	8.23%	27.66%	0.133
997	1.17	9.538E-02	5.400E-03	5.02	0.258	28.66	1560.61	3.90	1.39	0.20	14.31%	45.86%	0.138
997	1.17	9.538E-02	5.400E-03	4.97	0.256	28.43	1557.70	3.89	1.38	0.20	14.34%	45.66%	0.138
997	1.17	9.538E-02	5.400E-03	5.04	0.259	28.80	1556.43	3.89	1.40	0.20	14.36%	46.36%	0.138
997	1.16	9.538E-02	5.400E-03	4.96	0.255	28.37	1620.34	4.07	1.37	0.33	24.26%	74.11%	0.144

Table 8.22 Experimental entrainment data for 28.6 $m^3/(h.m)$ setting and A_{esc} = 3.33×10^{-3} m^2, 5.4×10^{-3} m^2 and 8.575×10^{-3} m^2.

ρ_l [kg/m^3]	ρ_v [kg/m^3]	A_n [m^2]	A_{esc} [m^2]	Liquid Flow [m^3/h]	u_L [m/s]	Q_L [m^3/h.m]	Gas Flow [kg/h]	u_s [m/s]	L [kg/s]	L' [kg/s]	L'/L [%]	L'/G [%]	Cp [m/s]
997	1.16	9.538E-02	5.400E-03	4.98	0.256	28.43	1622.29	4.08	1.38	0.34	24.83%	75.92%	0.144
997	1.16	9.538E-02	5.400E-03	4.98	0.256	28.47	1623.37	4.08	1.38	0.35	25.21%	77.15%	0.144
997	1.16	9.538E-02	5.400E-03	4.97	0.256	28.42	1671.39	4.19	1.38	0.45	32.64%	96.84%	0.148
997	1.16	9.538E-02	5.400E-03	4.97	0.256	28.42	1674.77	4.20	1.38	0.45	32.97%	97.62%	0.149
997	1.16	9.538E-02	5.400E-03	4.97	0.256	28.41	1677.52	4.21	1.38	0.45	33.02%	97.55%	0.149
997	1.16	9.538E-02	5.400E-03	4.97	0.256	28.41	1681.83	4.22	1.38	0.46	33.24%	97.98%	0.149
997	1.17	9.538E-02	8.575E-03	5.02	0.163	28.69	1591.68	3.97	1.39	0.16	11.26%	35.40%	0.141
997	1.16	9.538E-02	8.575E-03	5.02	0.163	28.71	1599.74	4.00	1.39	0.18	13.07%	40.91%	0.142
997	1.17	9.538E-02	8.575E-03	5.02	0.163	28.70	1606.67	4.00	1.39	0.19	13.62%	42.45%	0.142
997	1.17	9.538E-02	8.575E-03	5.02	0.162	28.66	1605.86	4.01	1.39	0.19	13.81%	42.99%	0.142
997	1.17	9.538E-02	8.575E-03	4.95	0.160	28.27	1611.13	4.01	1.37	0.19	13.82%	42.31%	0.143
997	1.16	9.538E-02	8.575E-03	5.01	0.162	28.65	1742.83	4.36	1.39	0.45	32.23%	92.43%	0.155
997	1.16	9.538E-02	8.575E-03	5.02	0.163	28.69	1742.72	4.36	1.39	0.45	32.24%	92.59%	0.155
997	1.16	9.538E-02	8.575E-03	5.03	0.163	28.73	1748.93	4.38	1.39	0.46	33.09%	94.86%	0.155
997	1.17	9.538E-02	8.575E-03	5.02	0.163	28.67	1748.57	4.37	1.39	0.46	33.45%	95.68%	0.155
997	1.16	9.538E-02	8.575E-03	5.00	0.162	28.59	1835.06	4.59	1.39	0.65	46.72%	127.00%	0.163
997	1.16	9.538E-02	8.575E-03	5.03	0.163	28.73	1844.21	4.62	1.39	0.66	47.23%	128.37%	0.164
997	1.16	9.538E-02	8.575E-03	5.00	0.162	28.58	1842.11	4.61	1.38	0.66	47.53%	128.64%	0.164
997	1.16	9.538E-02	8.575E-03	5.02	0.162	28.66	1848.92	4.64	1.39	0.69	49.74%	134.51%	0.164

Table 8.23 Experimental entrainment data for 40 $m^3/(h.m)$ setting and A_{esc} = 3.33×10^{-3} m^2, 5.4×10^{-3} m^2 and 8.575×10^{-3} m^2.

ρ_l [kg/m^3]	ρ_v [kg/m^3]	A_n [m^2]	A_{esc} [m^2]	Liquid Flow [m^3/h]	u_L [m/s]	Q_L [$m^3/h.m$]	Gas Flow [kg/h]	u_s [m/s]	L [kg/s]	L' [kg/s]	L'/L [%]	L'/G [%]	Cp [m/s]
997	1.18	9.538E-02	3.330E-03	7.01	0.585	40.05	1546.75	3.83	1.94	0.10	4.95%	22.38%	0.137
997	1.18	9.538E-02	3.330E-03	6.98	0.582	39.89	1553.34	3.84	1.93	0.10	5.29%	23.71%	0.137
997	1.18	9.538E-02	3.330E-03	7.01	0.585	40.07	1553.17	3.85	1.94	0.11	5.49%	24.70%	0.137
997	1.17	9.538E-02	3.330E-03	6.99	0.583	39.96	1638.15	4.06	1.94	0.21	10.62%	45.23%	0.145
997	1.17	9.538E-02	3.330E-03	7.04	0.587	40.20	1635.73	4.06	1.95	0.21	10.66%	45.71%	0.145
997	1.17	9.538E-02	3.330E-03	7.03	0.587	40.18	1643.11	4.08	1.95	0.21	10.85%	46.28%	0.145
997	1.17	9.538E-02	3.330E-03	7.02	0.586	40.12	1637.80	4.07	1.94	0.21	10.90%	46.58%	0.145
997	1.17	9.538E-02	3.330E-03	7.03	0.586	40.15	1703.24	4.25	1.95	0.34	17.71%	72.81%	0.151
997	1.17	9.538E-02	3.330E-03	7.02	0.586	40.13	1704.25	4.25	1.95	0.35	17.97%	73.82%	0.151
997	1.17	9.538E-02	3.330E-03	6.99	0.583	39.94	1706.24	4.25	1.94	0.35	18.25%	74.52%	0.151
997	1.17	9.538E-02	3.330E-03	6.99	0.583	39.96	1772.36	4.41	1.94	0.49	25.48%	100.22%	0.157
997	1.17	9.538E-02	3.330E-03	6.99	0.583	39.92	1778.47	4.42	1.93	0.50	25.97%	101.72%	0.157
997	1.17	9.538E-02	3.330E-03	6.98	0.582	39.88	1780.31	4.42	1.93	0.51	26.64%	104.12%	0.157
997	1.18	9.538E-02	5.400E-03	7.01	0.360	40.03	1517.88	3.75	1.94	0.09	4.51%	20.73%	0.134
997	1.18	9.538E-02	5.400E-03	7.01	0.361	40.05	1522.32	3.76	1.94	0.09	4.57%	20.99%	0.134
997	1.18	9.538E-02	5.400E-03	7.00	0.360	40.00	1528.24	3.76	1.94	0.09	4.73%	21.62%	0.135
997	1.16	9.538E-02	5.400E-03	7.05	0.363	40.30	1602.50	4.01	1.95	0.18	9.30%	40.82%	0.142
997	1.16	9.538E-02	5.400E-03	7.03	0.362	40.18	1599.72	4.00	1.95	0.19	9.52%	41.71%	0.142
997	1.16	9.538E-02	5.400E-03	7.02	0.361	40.09	1603.58	4.01	1.94	0.19	9.53%	41.58%	0.142
997	1.17	9.538E-02	5.400E-03	6.95	0.358	39.73	1660.56	4.15	1.93	0.28	14.41%	60.16%	0.147
997	1.17	9.538E-02	5.400E-03	7.03	0.362	40.19	1663.96	4.16	1.95	0.29	14.79%	62.35%	0.148
997	1.17	9.538E-02	5.400E-03	7.02	0.361	40.12	1667.85	4.17	1.94	0.29	14.99%	62.92%	0.148
997	1.16	9.538E-02	5.400E-03	7.03	0.362	40.20	1774.79	4.44	1.95	0.52	26.75%	105.72%	0.158
997	1.17	9.538E-02	5.400E-03	6.98	0.359	39.87	1773.00	4.43	1.93	0.54	27.86%	109.30%	0.157
997	1.16	9.538E-02	5.400E-03	7.01	0.361	40.08	1775.60	4.44	1.94	0.55	28.24%	111.23%	0.158

Table 8.23 Experimental entrainment data for 40 $m^3/(h.m)$ setting and A_{esc} = 3.33×10^{-3} m^2, 5.4×10^{-3} m^2 and 8.575×10^{-3} m^2.

ρ_l [kg/m^3]	ρ_v [kg/m^3]	A_n [m^2]	A_{esc} [m^2]	Liquid Flow [m^3/h]	u_L [m/s]	Q_L [$m^3/h.m$]	Gas Flow [kg/h]	u_s [m/s]	L [kg/s]	L' [kg/s]	L'/L [%]	L'/G [%]	Cp [m/s]
997	1.19	9.538E-02	8.575E-03	7.00	0.227	40.00	1495.15	3.67	1.94	0.05	2.83%	13.22%	0.132
997	1.19	9.538E-02	8.575E-03	7.00	0.227	40.00	1508.54	3.70	1.94	0.06	2.96%	13.70%	0.133
997	1.18	9.538E-02	8.575E-03	7.02	0.227	40.11	1518.01	3.75	1.94	0.07	3.60%	16.61%	0.134
997	1.18	9.538E-02	8.575E-03	7.02	0.227	40.12	1521.50	3.76	1.94	0.07	3.67%	16.90%	0.134
997	1.18	9.538E-02	8.575E-03	6.98	0.226	39.86	1526.12	3.76	1.93	0.07	3.81%	17.37%	0.135
997	1.18	9.538E-02	8.575E-03	7.02	0.227	40.12	1532.12	3.77	1.94	0.08	3.88%	17.72%	0.135
997	1.19	9.538E-02	8.575E-03	7.02	0.227	40.12	1541.88	3.79	1.94	0.08	4.13%	18.74%	0.136
997	1.15	9.538E-02	8.575E-03	6.95	0.225	39.70	1545.25	3.90	1.92	0.10	4.98%	22.33%	0.138
997	1.18	9.538E-02	8.575E-03	7.05	0.228	40.28	1633.29	4.04	1.95	0.21	10.71%	46.08%	0.144
997	1.17	9.538E-02	8.575E-03	7.02	0.227	40.12	1635.32	4.06	1.94	0.21	10.80%	46.21%	0.145
997	1.17	9.538E-02	8.575E-03	7.01	0.227	40.04	1630.48	4.06	1.94	0.21	10.82%	46.36%	0.144
997	1.17	9.538E-02	8.575E-03	7.02	0.227	40.10	1634.12	4.07	1.94	0.21	10.96%	46.93%	0.145
997	1.17	9.538E-02	8.575E-03	7.03	0.228	40.16	1636.38	4.06	1.95	0.21	10.98%	47.00%	0.145
997	1.17	9.538E-02	8.575E-03	7.04	0.228	40.22	1638.50	4.06	1.95	0.22	11.38%	48.73%	0.145
997	1.16	9.538E-02	8.575E-03	7.01	0.227	40.05	1656.29	4.15	1.94	0.28	14.63%	61.72%	0.147
997	1.16	9.538E-02	8.575E-03	7.02	0.227	40.09	1661.61	4.16	1.94	0.30	15.63%	65.82%	0.148
997	1.16	9.538E-02	8.575E-03	6.99	0.226	39.93	1659.79	4.16	1.94	0.31	16.04%	67.34%	0.147
997	1.17	9.538E-02	8.575E-03	6.99	0.227	39.97	1698.81	4.24	1.94	0.37	19.34%	79.39%	0.151
997	1.17	9.538E-02	8.575E-03	7.03	0.228	40.15	1706.06	4.25	1.95	0.38	19.63%	80.59%	0.151
997	1.17	9.538E-02	8.575E-03	7.04	0.228	40.23	1709.36	4.26	1.95	0.38	19.67%	80.79%	0.151
997	1.17	9.538E-02	8.575E-03	7.01	0.227	40.06	1703.70	4.25	1.94	0.39	19.85%	81.43%	0.151
997	1.16	9.538E-02	8.575E-03	6.97	0.226	39.82	1718.55	4.31	1.93	0.42	21.55%	87.12%	0.153
997	1.16	9.538E-02	8.575E-03	6.96	0.225	39.76	1719.88	4.32	1.93	0.42	21.66%	87.38%	0.153
997	1.16	9.538E-02	8.575E-03	7.01	0.227	40.07	1718.73	4.32	1.94	0.43	21.96%	89.31%	0.153
997	1.16	9.538E-02	8.575E-03	6.99	0.226	39.95	1724.55	4.32	1.94	0.43	22.35%	90.33%	0.153

Table 8.23 Experimental entrainment data for 40 $m^3/(h.m)$ setting and A_{esc} = 3.33×10^{-3} m^2, 5.4×10^{-3} m^2 and 8.575×10^{-3} m^2.

ρ_l [kg/m^3]	ρ_v [kg/m^3]	A_n [m^2]	A_{esc} [m^2]	Liquid Flow [m^3/h]	u_L [m/s]	Q_L [$m^3/h.m$]	Gas Flow [kg/h]	u_s [m/s]	L [kg/s]	L' [kg/s]	L'/L [%]	L'/G [%]	Cp [m/s]
997	1.16	9.538E-02	8.575E-03	7.00	0.227	40.01	1723.27	4.32	1.94	0.44	22.44%	90.90%	0.153
997	1.17	9.538E-02	8.575E-03	7.01	0.227	40.05	1769.71	4.42	1.94	0.54	27.78%	109.69%	0.157
997	1.17	9.538E-02	8.575E-03	7.01	0.227	40.08	1767.83	4.42	1.94	0.54	27.82%	110.05%	0.157
997	1.17	9.538E-02	8.575E-03	7.01	0.227	40.07	1775.63	4.43	1.94	0.55	28.12%	110.72%	0.157
997	1.17	9.538E-02	8.575E-03	7.02	0.227	40.11	1772.35	4.42	1.94	0.55	28.19%	111.31%	0.157

Table 8.24 Experimental entrainment data for 57.2 $m^3/(h.m)$ setting and A_{esc} = 5.4×10^{-3} m^2 and 8.575×10^{-3} m^2.

ρ_l [kg/m^3]	ρ_v [kg/m^3]	A_n [m^2]	A_{esc} [m^2]	Liquid Flow [m^3/h]	u_L [m/s]	Q_L [$m^3/h.m$]	Gas Flow [kg/h]	u_s [m/s]	L [kg/s]	L' [kg/s]	L'/L [%]	L'/G [%]	Cp [m/s]
997	1.17	9.538E-02	5.400E-03	9.99	0.514	57.10	1595.77	3.98	2.77	0.13	4.81%	30.05%	0.141
997	1.17	9.538E-02	5.400E-03	9.99	0.514	57.11	1600.64	4.00	2.77	0.14	4.96%	30.86%	0.142
997	1.17	9.538E-02	5.400E-03	10.01	0.515	57.20	1602.25	4.00	2.77	0.14	5.17%	32.19%	0.142
997	1.18	9.538E-02	5.400E-03	9.99	0.514	57.11	1673.07	4.14	2.77	0.23	8.23%	49.04%	0.148
997	1.17	9.538E-02	5.400E-03	9.95	0.512	56.83	1709.93	4.24	2.75	0.32	11.63%	67.43%	0.151
997	1.17	9.538E-02	5.400E-03	10.04	0.516	57.35	1707.34	4.24	2.78	0.32	11.55%	67.71%	0.151
997	1.18	9.538E-02	5.400E-03	9.96	0.513	56.93	1718.96	4.26	2.76	0.33	12.04%	69.56%	0.152
997	1.16	9.538E-02	5.400E-03	10.02	0.515	57.26	1754.06	4.39	2.78	0.44	15.75%	89.68%	0.156
997	1.16	9.538E-02	5.400E-03	10.04	0.516	57.36	1757.50	4.40	2.78	0.44	15.75%	89.68%	0.156
997	1.16	9.538E-02	5.400E-03	10.03	0.516	57.32	1758.61	4.40	2.78	0.44	15.92%	90.50%	0.156
997	1.17	9.538E-02	5.400E-03	9.97	0.513	56.97	1819.14	4.54	2.76	0.62	22.29%	121.80%	0.161
997	1.17	9.538E-02	5.400E-03	10.04	0.516	57.37	1818.79	4.54	2.78	0.62	22.39%	123.22%	0.161
997	1.17	9.538E-02	5.400E-03	9.98	0.514	57.05	1823.44	4.54	2.76	0.63	22.78%	124.35%	0.162

Table 8.24 Experimental entrainment data for 57.2 $m^3/(h.m)$ setting and A_{esc} = 5.4×10^{-3} m^2 and 8.575×10^{-3} m^2.

ρ_l [kg/m^3]	ρ_v [kg/m^3]	A_n [m^2]	A_{esc} [m^2]	Liquid Flow [m^3/h]	u_L [m/s]	Q_L [m^3/h.m]	Gas Flow [kg/h]	u_s [m/s]	L [kg/s]	L' [kg/s]	L'/L [%]	L'/G [%]	Cp [m/s]
997	1.15	9.538E-02	8.575E-03	9.98	0.323	57.03	1571.57	3.97	2.76	0.10	3.71%	23.52%	0.140
997	1.15	9.538E-02	8.575E-03	10.00	0.324	57.12	1576.46	3.99	2.77	0.10	3.77%	23.82%	0.141
997	1.15	9.538E-02	8.575E-03	10.01	0.324	57.19	1579.41	3.99	2.77	0.11	3.85%	24.30%	0.141
997	1.15	9.538E-02	8.575E-03	9.98	0.323	57.02	1588.58	4.01	2.76	0.11	4.13%	25.85%	0.142
997	1.16	9.538E-02	8.575E-03	10.00	0.324	57.12	1597.81	4.00	2.77	0.13	4.63%	28.86%	0.142
997	1.16	9.538E-02	8.575E-03	9.99	0.324	57.09	1598.14	4.00	2.77	0.13	4.65%	28.99%	0.142
997	1.16	9.538E-02	8.575E-03	9.90	0.321	56.56	1601.80	4.01	2.74	0.13	4.72%	29.06%	0.142
997	1.16	9.538E-02	8.575E-03	9.99	0.324	57.10	1639.77	4.12	2.77	0.17	6.14%	37.29%	0.146
997	1.16	9.538E-02	8.575E-03	10.09	0.327	57.65	1647.33	4.15	2.79	0.19	6.75%	41.19%	0.147
997	1.15	9.538E-02	8.575E-03	10.14	0.328	57.93	1643.96	4.15	2.81	0.19	6.91%	42.50%	0.147
997	1.16	9.538E-02	8.575E-03	9.89	0.320	56.53	1647.22	4.14	2.74	0.20	7.17%	42.91%	0.147
997	1.16	9.538E-02	8.575E-03	10.01	0.324	57.22	1647.50	4.15	2.77	0.20	7.22%	43.74%	0.147
997	1.17	9.538E-02	8.575E-03	9.99	0.324	57.09	1650.40	4.12	2.77	0.23	8.22%	49.59%	0.146
997	1.17	9.538E-02	8.575E-03	10.00	0.324	57.14	1651.39	4.12	2.77	0.23	8.22%	49.65%	0.146
997	1.17	9.538E-02	8.575E-03	9.95	0.322	56.88	1659.38	4.14	2.76	0.23	8.51%	50.89%	0.147
997	1.15	9.538E-02	8.575E-03	10.14	0.328	57.95	1684.05	4.25	2.81	0.26	9.31%	55.90%	0.150
997	1.15	9.538E-02	8.575E-03	10.07	0.326	57.53	1684.95	4.25	2.79	0.29	10.24%	61.00%	0.150
997	1.15	9.538E-02	8.575E-03	10.06	0.326	57.51	1689.47	4.27	2.79	0.29	10.49%	62.27%	0.151
997	1.15	9.538E-02	8.575E-03	10.05	0.326	57.43	1694.75	4.28	2.78	0.29	10.58%	62.53%	0.151
997	1.17	9.538E-02	8.575E-03	10.02	0.325	57.27	1700.51	4.25	2.78	0.30	10.83%	63.66%	0.151
997	1.17	9.538E-02	8.575E-03	9.98	0.323	57.05	1703.53	4.25	2.76	0.31	11.06%	64.63%	0.151
997	1.15	9.538E-02	8.575E-03	10.01	0.324	57.17	1699.09	4.29	2.77	0.31	11.28%	66.21%	0.152
997	1.16	9.538E-02	8.575E-03	10.05	0.326	57.43	1721.51	4.31	2.78	0.39	13.92%	81.01%	0.153
997	1.17	9.538E-02	8.575E-03	9.98	0.323	57.04	1724.91	4.31	2.76	0.39	14.28%	82.41%	0.153
997	1.16	9.538E-02	8.575E-03	9.99	0.324	57.09	1723.05	4.31	2.77	0.40	14.36%	83.03%	0.153

Table 8.24 Experimental entrainment data for 57.2 m^3/(h.m) setting and A_{esc} = 5.4×10^{-3} m^2 and 8.575×10^{-3} m^2.

ρ_l [kg/m^3]	ρ_v [kg/m^3]	A_n [m^2]	A_{esc} [m^2]	Liquid Flow [m^3/h]	u_L [m/s]	Q_L [m^3/h.m]	Gas Flow [kg/h]	u_s [m/s]	L [kg/s]	L' [kg/s]	L'/L [%]	L'/G [%]	Cp [m/s]
997	1.16	9.538E-02	8.575E-03	9.99	0.324	57.07	1748.87	4.38	2.77	0.42	15.18%	86.44%	0.155
997	1.15	9.538E-02	8.575E-03	10.10	0.327	57.74	1745.67	4.42	2.80	0.42	15.16%	87.49%	0.156
997	1.15	9.538E-02	8.575E-03	10.09	0.327	57.68	1746.59	4.42	2.80	0.43	15.39%	88.68%	0.156
997	1.15	9.538E-02	8.575E-03	10.09	0.327	57.65	1739.22	4.41	2.79	0.43	15.37%	88.89%	0.155
997	1.15	9.538E-02	8.575E-03	10.04	0.325	57.36	1751.74	4.43	2.78	0.43	15.65%	89.39%	0.156
997	1.15	9.538E-02	8.575E-03	10.04	0.325	57.36	1746.95	4.42	2.78	0.44	15.81%	90.58%	0.156
997	1.15	9.538E-02	8.575E-03	10.13	0.328	57.88	1748.46	4.42	2.81	0.44	15.82%	91.40%	0.156
997	1.16	9.538E-02	8.575E-03	10.01	0.324	57.19	1772.95	4.45	2.77	0.49	17.68%	99.50%	0.158
997	1.16	9.538E-02	8.575E-03	9.99	0.324	57.11	1779.02	4.46	2.77	0.49	17.83%	99.90%	0.158
997	1.16	9.538E-02	8.575E-03	10.00	0.324	57.14	1777.88	4.45	2.77	0.50	18.11%	101.57%	0.158
997	1.16	9.538E-02	8.575E-03	10.03	0.325	57.31	1773.49	4.44	2.78	0.50	18.17%	102.46%	0.158
997	1.16	9.538E-02	8.575E-03	10.02	0.324	57.23	1780.45	4.46	2.77	0.51	18.36%	102.96%	0.158
997	1.16	9.538E-02	8.575E-03	10.00	0.324	57.16	1795.49	4.50	2.77	0.59	21.45%	119.13%	0.159
997	1.16	9.538E-02	8.575E-03	9.98	0.323	57.01	1797.49	4.50	2.76	0.61	22.06%	122.10%	0.160
997	1.16	9.538E-02	8.575E-03	9.99	0.324	57.09	1808.88	4.54	2.77	0.63	22.84%	125.79%	0.161
997	1.16	9.538E-02	8.575E-03	10.02	0.325	57.28	1851.61	4.64	2.78	0.73	26.20%	141.39%	0.164
997	1.16	9.538E-02	8.575E-03	10.00	0.324	57.16	1847.61	4.63	2.77	0.74	26.66%	143.90%	0.164
997	1.16	9.538E-02	8.575E-03	10.02	0.325	57.28	1850.88	4.64	2.78	0.75	27.00%	145.78%	0.165
997	1.16	9.538E-02	8.575E-03	9.97	0.323	56.99	1848.77	4.63	2.76	0.75	27.15%	146.03%	0.164
997	1.16	9.538E-02	8.575E-03	10.04	0.325	57.34	1849.57	4.64	2.78	0.75	27.00%	146.04%	0.164

Table 8.25 Experimental entrainment data for 74.2 m^3/(h.m) setting and A_{esc} = 5.4×10^{-3} m^2 and 8.575×10^{-3} m^2.

ρ_l [kg/m^3]	ρ_v [kg/m^3]	A_n [m^2]	A_{esc} [m^2]	Liquid Flow [m^3/h]	u_L [m/s]	Q_L [m^3/h.m]	Gas Flow [kg/h]	u_s [m/s]	L [kg/s]	L' [kg/s]	L'/L [%]	L'/G [%]	Cp [m/s]
997	1.17	9.538E-02	5.400E-03	12.99	0.668	74.23	1580.38	3.92	3.60	0.10	2.85%	23.34%	0.140
997	1.19	9.538E-02	5.400E-03	12.95	0.666	74.02	1712.94	4.19	3.59	0.29	8.12%	61.19%	0.150
997	1.19	9.538E-02	5.400E-03	12.97	0.667	74.13	1711.61	4.19	3.59	0.29	8.17%	61.74%	0.150
997	1.19	9.538E-02	5.400E-03	12.99	0.668	74.25	1717.31	4.21	3.60	0.31	8.53%	64.38%	0.151
997	1.18	9.538E-02	5.400E-03	12.96	0.667	74.07	1756.44	4.33	3.59	0.47	12.96%	95.34%	0.155
997	1.18	9.538E-02	5.400E-03	12.98	0.668	74.18	1762.01	4.36	3.60	0.50	13.87%	101.91%	0.156
997	1.19	9.538E-02	5.400E-03	12.93	0.665	73.87	1819.85	4.47	3.58	0.66	18.32%	129.76%	0.160

Table 8.26 Experimental entrainment data for 79.9 m^3/(h.m) setting and A_{esc} = 8.575×10^{-3} m^2.

ρ_l [kg/m^3]	ρ_v [kg/m^3]	A_n [m^2]	A_{esc} [m^2]	Liquid Flow [m^3/h]	u_L [m/s]	Q_L [m^3/h.m]	Gas Flow [kg/h]	u_s [m/s]	L [kg/s]	L' [kg/s]	L'/L [%]	L'/G [%]	Cp [m/s]
997	1.16	9.538E-02	8.575E-03	13.96	0.452	79.80	1654.25	4.17	3.87	0.25	6.37%	53.59%	0.147
997	1.16	9.538E-02	8.575E-03	13.98	0.453	79.90	1653.40	4.16	3.87	0.25	6.39%	53.84%	0.147
997	1.16	9.538E-02	8.575E-03	13.98	0.453	79.91	1653.03	4.16	3.87	0.25	6.39%	53.86%	0.147
997	1.16	9.538E-02	8.575E-03	14.00	0.453	79.98	1652.52	4.16	3.88	0.25	6.47%	54.60%	0.147
997	1.18	9.538E-02	8.575E-03	13.97	0.452	79.81	1739.56	4.30	3.87	0.42	10.81%	86.57%	0.153
997	1.17	9.538E-02	8.575E-03	13.99	0.453	79.96	1746.48	4.33	3.88	0.44	11.38%	90.93%	0.154
997	1.18	9.538E-02	8.575E-03	13.96	0.452	79.75	1753.46	4.34	3.87	0.45	11.58%	91.87%	0.155
997	1.17	9.538E-02	8.575E-03	13.98	0.453	79.88	1754.17	4.36	3.87	0.46	11.95%	94.96%	0.155

Table 8.26 Experimental entrainment data for 79.9 $m^3/(h.m)$ setting and $A_{esc} = 8.575 \times 10^{-3}$ m^2.

ρ_l [kg/m^3]	ρ_v [kg/m^3]	A_n [m^2]	A_{esc} [m^2]	Liquid Flow [m^3/h]	u_L [m/s]	Q_L [$m^3/h.m$]	Gas Flow [kg/h]	u_s [m/s]	L [kg/s]	L' [kg/s]	L'/L [%]	L'/G [%]	Cp [m/s]
997	1.17	9.538E-02	8.575E-03	13.95	0.452	79.70	1751.22	4.35	3.86	0.47	12.30%	97.63%	0.155
997	1.17	9.538E-02	8.575E-03	13.95	0.452	79.72	1783.52	4.45	3.86	0.59	15.22%	118.70%	0.158
997	1.17	9.538E-02	8.575E-03	13.93	0.451	79.60	1792.27	4.46	3.86	0.67	17.50%	135.56%	0.159
997	1.17	9.538E-02	8.575E-03	13.99	0.453	79.93	1814.15	4.53	3.87	0.75	19.26%	148.03%	0.161
997	1.16	9.538E-02	8.575E-03	14.00	0.454	80.02	1799.59	4.51	3.88	0.75	19.44%	150.83%	0.160
997	1.17	9.538E-02	8.575E-03	13.97	0.452	79.81	1816.23	4.53	3.87	0.75	19.50%	149.51%	0.161
997	1.16	9.538E-02	8.575E-03	13.99	0.453	79.92	1809.78	4.53	3.87	0.76	19.52%	150.40%	0.161
997	1.16	9.538E-02	8.575E-03	13.98	0.453	79.90	1807.68	4.53	3.87	0.76	19.71%	152.03%	0.161
997	1.17	9.538E-02	8.575E-03	14.02	0.454	80.11	1812.28	4.53	3.88	0.77	19.76%	152.43%	0.161
997	1.17	9.538E-02	8.575E-03	13.97	0.452	79.82	1812.63	4.53	3.87	0.77	19.83%	152.34%	0.161
997	1.16	9.538E-02	8.575E-03	13.97	0.452	79.81	1813.05	4.54	3.87	0.78	20.25%	155.53%	0.161

Table 8.27 Experimental entrainment data for 96.8 $m^3/(h.m)$ setting and $A_{esc} = 8.575 \times 10^{-3}$ m^2.

ρ_l [kg/m^3]	ρ_v [kg/m^3]	A_n [m^2]	A_{esc} [m^2]	Liquid Flow [m^3/h]	u_L [m/s]	Q_L [$m^3/h.m$]	Gas Flow [kg/h]	u_s [m/s]	L [kg/s]	L' [kg/s]	L'/L [%]	L'/G [%]	Cp [m/s]
997	1.19	9.538E-02	8.575E-03	16.94	0.549	96.79	1574.99	3.86	4.69	0.13	2.86%	30.71%	0.138
997	1.19	9.538E-02	8.575E-03	16.94	0.549	96.78	1580.80	3.87	4.69	0.14	3.05%	32.60%	0.139
997	1.19	9.538E-02	8.575E-03	16.95	0.549	96.85	1590.92	3.89	4.69	0.15	3.18%	33.73%	0.140
997	1.20	9.538E-02	8.575E-03	16.89	0.547	96.53	1604.59	3.90	4.68	0.16	3.51%	36.85%	0.140
997	1.18	9.538E-02	8.575E-03	16.95	0.549	96.87	1650.96	4.09	4.70	0.34	7.20%	73.68%	0.146
997	1.18	9.538E-02	8.575E-03	16.95	0.549	96.83	1658.12	4.10	4.69	0.34	7.24%	73.77%	0.146

Table 8.27 Experimental entrainment data for 96.8 $m^3/(h.m)$ setting and $A_{esc} = 8.575 \times 10^{-3}$ m^2.

ρ_l [kg/m^3]	ρ_v [kg/m^3]	A_n [m^2]	A_{esc} [m^2]	Liquid Flow [m^3/h]	u_L [m/s]	Q_L [$m^3/h.m$]	Gas Flow [kg/h]	u_s [m/s]	L [kg/s]	L' [kg/s]	L'/L [%]	L'/G [%]	Cp [m/s]
997	1.18	9.538E-02	8.575E-03	16.94	0.549	96.83	1659.17	4.10	4.69	0.35	7.44%	75.72%	0.146
997	1.18	9.538E-02	8.575E-03	16.95	0.549	96.88	1651.60	4.09	4.70	0.35	7.48%	76.52%	0.146
997	1.18	9.538E-02	8.575E-03	16.97	0.550	96.96	1657.91	4.08	4.70	0.35	7.52%	76.75%	0.146
997	1.19	9.538E-02	8.575E-03	16.96	0.549	96.91	1721.79	4.23	4.70	0.53	11.38%	111.71%	0.151
997	1.18	9.538E-02	8.575E-03	16.93	0.548	96.73	1716.84	4.23	4.69	0.54	11.47%	112.75%	0.151
997	1.19	9.538E-02	8.575E-03	16.92	0.548	96.71	1724.63	4.23	4.69	0.54	11.57%	113.18%	0.152
997	1.18	9.538E-02	8.575E-03	16.98	0.550	97.00	1716.25	4.22	4.70	0.55	11.74%	115.77%	0.151
997	1.18	9.538E-02	8.575E-03	16.95	0.549	96.88	1750.97	4.32	4.70	0.69	14.69%	141.85%	0.154
997	1.18	9.538E-02	8.575E-03	16.93	0.548	96.72	1754.52	4.33	4.69	0.74	15.82%	152.15%	0.155
997	1.18	9.538E-02	8.575E-03	16.93	0.548	96.72	1757.74	4.34	4.69	0.75	16.03%	153.86%	0.155
997	1.18	9.538E-02	8.575E-03	16.93	0.548	96.75	1757.67	4.34	4.69	0.78	16.59%	159.30%	0.155

Table 8.28 Experimental entrainment data for 112.9 m^3/(h.m) setting and A_{esc} = 8.575×10^{-3} m^2.

ρ_l [kg/m^3]	ρ_v [kg/m^3]	A_n [m^2]	A_{esc} [m^2]	Liquid Flow [m^3/h]	u_L [m/s]	Q_L [m^3/h.m]	Gas Flow [kg/h]	u_s [m/s]	L [kg/s]	L' [kg/s]	L'/L [%]	L'/G [%]	Cp [m/s]
997	1.15	9.538E-02	8.575E-03	19.71	0.638	112.61	1433.05	3.64	5.46	0.08	1.48%	20.32%	0.128
997	1.15	9.538E-02	8.575E-03	19.74	0.639	112.78	1438.99	3.66	5.47	0.08	1.53%	20.89%	0.129
997	1.14	9.538E-02	8.575E-03	19.78	0.641	113.05	1445.02	3.68	5.48	0.08	1.54%	21.00%	0.129
997	1.14	9.538E-02	8.575E-03	19.79	0.641	113.09	1438.66	3.66	5.48	0.09	1.62%	22.15%	0.129
997	1.14	9.538E-02	8.575E-03	19.78	0.641	113.02	1445.19	3.68	5.48	0.10	1.79%	24.38%	0.129
997	1.16	9.538E-02	8.575E-03	19.74	0.640	112.81	1526.91	3.82	5.47	0.22	4.09%	52.71%	0.136
997	1.16	9.538E-02	8.575E-03	19.73	0.639	112.72	1531.57	3.83	5.46	0.24	4.41%	56.57%	0.136
997	1.16	9.538E-02	8.575E-03	19.78	0.641	113.03	1531.64	3.83	5.48	0.26	4.83%	62.12%	0.136
997	1.16	9.538E-02	8.575E-03	19.75	0.640	112.86	1545.34	3.86	5.47	0.27	4.99%	63.63%	0.137
997	1.17	9.538E-02	8.575E-03	19.77	0.640	112.97	1581.95	3.93	5.48	0.36	6.59%	82.10%	0.140
997	1.17	9.538E-02	8.575E-03	19.74	0.640	112.83	1573.67	3.91	5.47	0.37	6.75%	84.42%	0.139
997	1.17	9.538E-02	8.575E-03	19.81	0.642	113.20	1580.96	3.93	5.49	0.40	7.23%	90.27%	0.140
997	1.17	9.538E-02	8.575E-03	19.77	0.640	112.95	1579.44	3.93	5.47	0.41	7.51%	93.65%	0.140
997	1.17	9.538E-02	8.575E-03	19.76	0.640	112.93	1621.61	4.04	5.47	0.60	10.92%	132.64%	0.144
997	1.17	9.538E-02	8.575E-03	19.77	0.641	112.98	1625.75	4.05	5.48	0.60	11.02%	133.58%	0.144
997	1.17	9.538E-02	8.575E-03	19.75	0.640	112.83	1614.90	4.03	5.47	0.60	11.03%	134.41%	0.143
997	1.17	9.538E-02	8.575E-03	19.70	0.638	112.56	1623.35	4.04	5.46	0.61	11.09%	134.22%	0.144
997	1.17	9.538E-02	8.575E-03	19.77	0.641	113.00	1645.63	4.10	5.48	0.77	14.11%	169.00%	0.146
997	1.17	9.538E-02	8.575E-03	19.75	0.640	112.87	1650.02	4.12	5.47	0.78	14.28%	170.39%	0.146
997	1.17	9.538E-02	8.575E-03	19.78	0.641	113.05	1650.93	4.11	5.48	0.79	14.47%	172.91%	0.146
997	1.17	9.538E-02	8.575E-03	19.75	0.640	112.87	1655.96	4.12	5.47	0.80	14.63%	174.04%	0.147

8.6 Data processing

Entrainment data was generated by logging the mass (in kilograms) in MV-202/4 (see **Figure 3.8**) every two seconds. During the sample the data was labelled (marked) so that MATLAB (the mathematical software used for data processing) can find the groups of entrainment data in the database (data was continuously logged during the experimental runs). A typical sample will consist of 30 – 70 data points. MATLAB was then used to fit a linear model to the data using linear regression, and data points that deviated with more than 2 standard deviations were identified as outliers and subsequently removed. This ensured that all the data was within the 95% confidence intervals. A final regression was then performed on the data without the outliers and the gradient would be the entrained liquid flow rate measured in kg/s.

Entrainment data for a given flow rate was then plotted as a function of the capacity factor ($C_p = u_p\sqrt{\rho_g/(\rho_L - \rho_g)}$) and trendlines were fitted as shown in Figure 8.6 and Figure 8.7. To verify that the trendlines are accurate the measured data was compared with the fitted data in Figure 8.8. The solver function in Microsoft Excel was used to generate the entrainment trends in Figure 4.6, Figure 4.7 and Figure 4.9 - Figure 4.13 which was within the measuring range. None of the fitted experimental entrainment trends exceeded the measuring range to insure interpolation and accuracy.

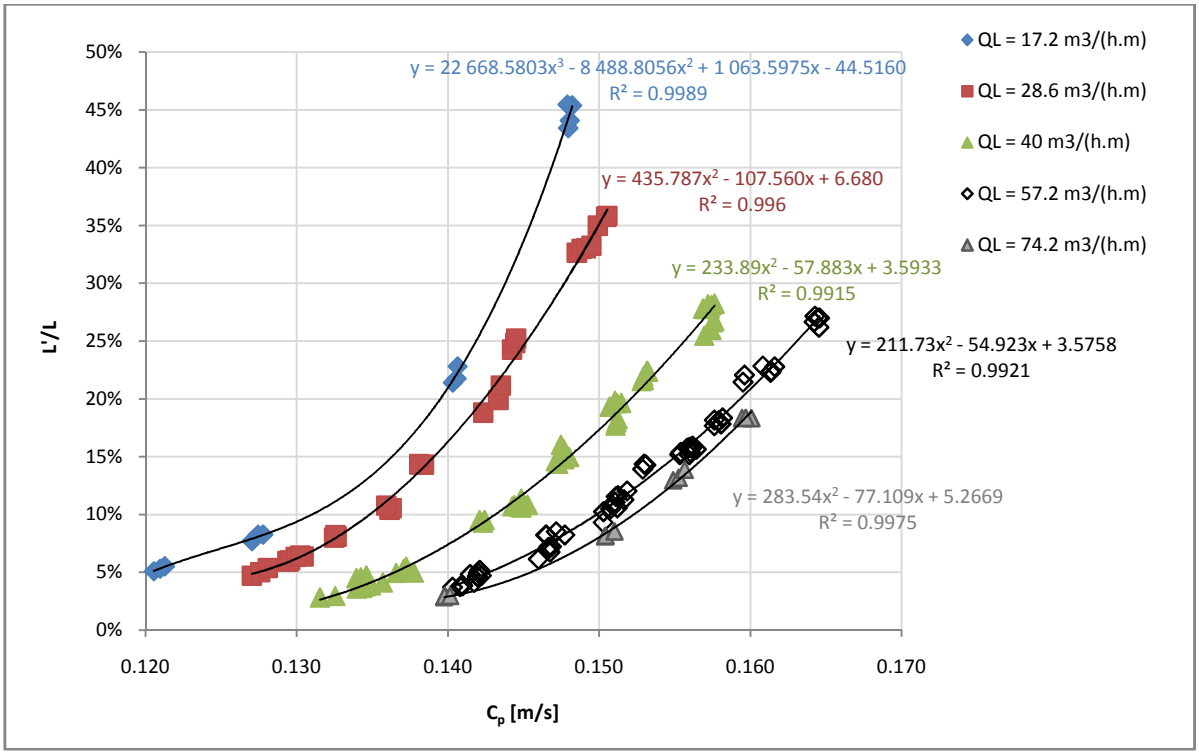

Figure 8.6 Fitting trendlines to entrainment data for each liquid flow rate [17.2 – 74.2 m^3/(h.m)] as a function of entrainment.

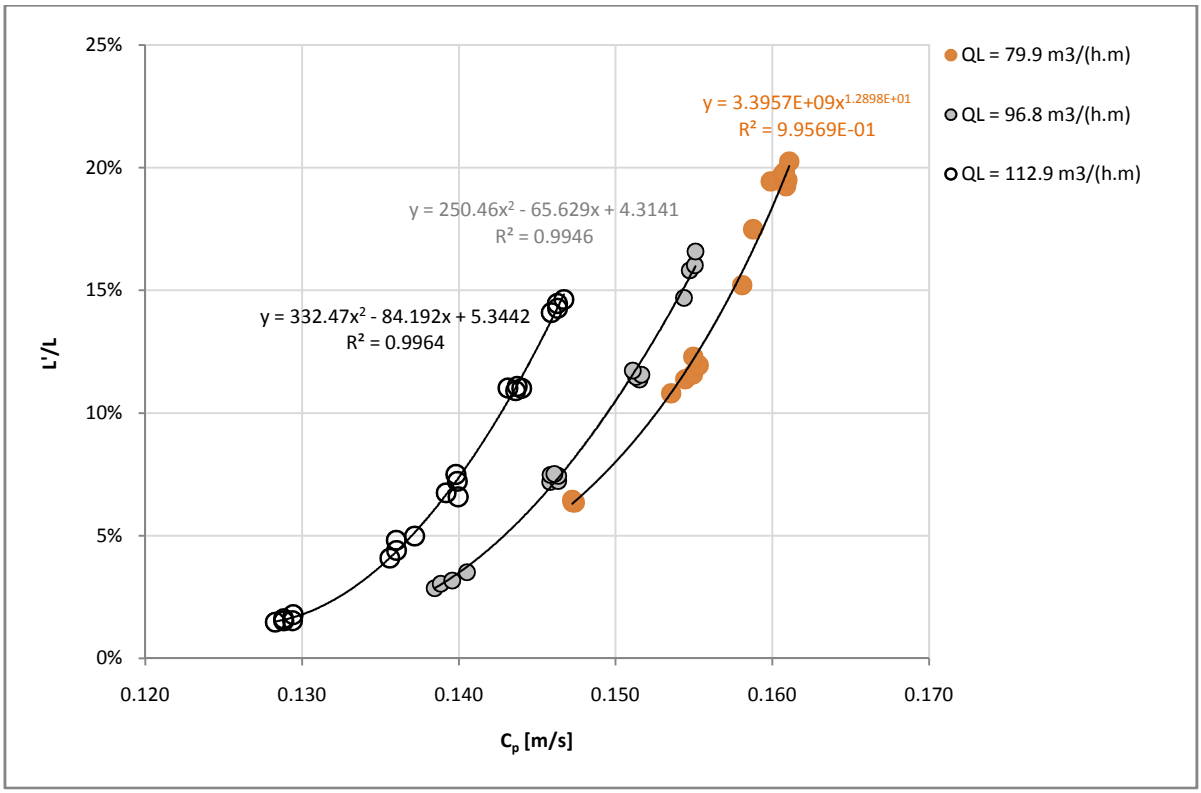

Figure 8.7 Fitting trendlines to entrainment data for each liquid flow rate [79.9 – 112.9 m^3/(h.m)] as a function of entrainment.

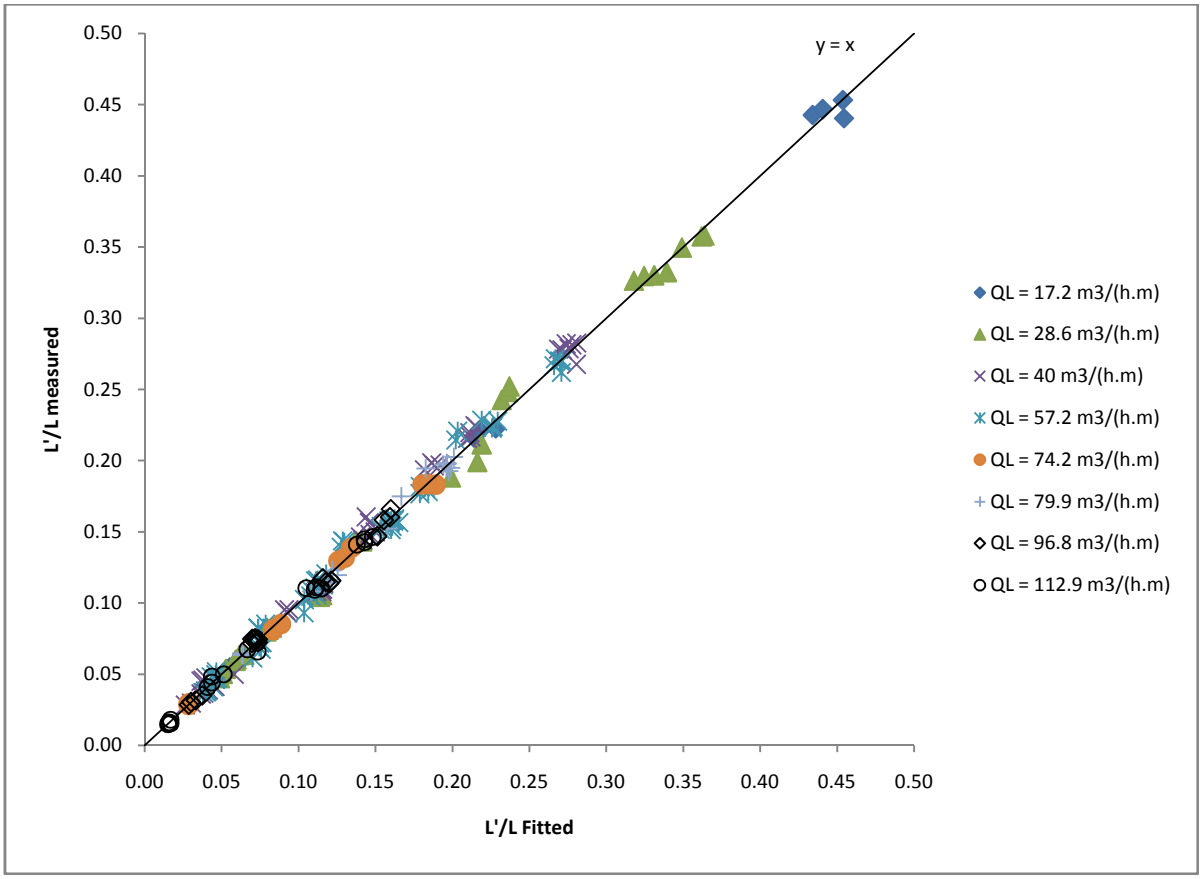

Figure 8.8 Verification of the fitted correlation for entrainment against the data.